

Profile Synthesis Of Planar Variable Joints

Brian James Slaboch
Marquette University

Recommended Citation

Slaboch, Brian James, "Profile Synthesis Of Planar Variable Joints" (2013). *Dissertations (2009 -)*. Paper 283.
http://epublications.marquette.edu/dissertations_mu/283

PROFILE SYNTHESIS OF PLANAR VARIABLE JOINTS

by

Brian J. Slaboch, B.S., M.S.

A Dissertation Submitted to the Faculty of the Graduate School,
Marquette University,
in Partial Fulfillment of the Requirements for
the Degree of Doctor of Philosophy

Milwaukee, Wisconsin

August 2013

ABSTRACT
PROFILE SYNTHESIS OF PLANAR VARIABLE JOINTS

Brian J. Slaboch, B.S., M.S.

Marquette University, 2013

Reconfigurable mechanisms provide quick changeover and reduced costs for low volume manufacturing applications. In addition, these mechanisms provide added flexibility in the context of a constrained environment. A subset of planar reconfigurable mechanisms use variable joints to provide this added adaptability.

In this dissertation, the profile synthesis of planar variable joints that change from a rotational motion to a translational motion was investigated. A method was developed to perform automated profile synthesis. It was shown that combinations of higher variable joints can be used to create kinematically equivalent variable joints that are geometrically different.

The results were used to create two new reconfigurable mechanisms that utilize the synthesized variable joints. The first reconfigurable mechanism is a four-bar mechanism that performs a rigid body guidance task not possible using conventional four-bar theory. The second mechanism uses variable joints in a 3-RPR parallel mechanism for singularity avoidance without adding redundant actuation.

ACKNOWLEDGEMENTS

Brian J. Slaboch, B.S., M.S.

I could not have done this without the help and support from many people. First, I would like to thank Dr. Philip Voglewede for his guidance throughout this process. I would also like to thank my family and friends for their love and encouragement. Mom and Dad, you have been with me from the beginning, and I couldn't have done this without you. In addition, I would like to thank the guys in the lab with special thanks to Jinming for being a great friend for so many years. My committee also played an important role, and I thank them for pushing me to do my best work. Finally, I would like to thank Kate for being there for me when I needed her the most.

TABLE OF CONTENTS

ACKNOWLEDGEMENTS	i
TABLE OF CONTENTS	ii
LIST OF FIGURES	vii
CHAPTER 1 Introduction	1
1.1 Introduction	1
1.2 Research Purpose	2
1.3 Joint Profile Synthesis	3
1.4 Profile Synthesis of an Example Variable Joint	4
1.5 Organization of the Dissertation	5
CHAPTER 2 Motivation and Literature Review	6
2.1 A Brief History of Kinematics	6
2.2 Reconfigurable Mechanisms	8
2.3 Types of Reconfigurable Mechanisms	10
2.3.1 Kinematotropic Mechanisms	11
2.3.2 Metamorphic Mechanisms	12
2.3.3 Mechanisms with Variable Topology	13
2.4 Summary of Reconfigurable Mechanisms	15
2.5 Joints	15
2.5.1 Lower Pairs	16
2.5.2 Higher Pairs	16
2.5.3 Variable Joints	17

TABLE OF CONTENTS — *Continued*

2.5.4	Practical Considerations for Variable Joints	18
2.6	Summary	19
CHAPTER 3 Higher Variable Joints		21
3.1	Overview of Higher Variable Joints	21
3.1.1	Motivation for Higher Variable Joints	22
3.1.2	Mobility of Bodies in Contact	24
3.1.3	Configuration Space Terminology	25
3.2	Type R_u Variable Kinematic Joints	26
3.2.1	Case 1: Type R_1 Higher Variable Joints	27
3.2.2	Case 2: Type R_2 Higher Variable Joints	31
3.2.3	Case 3: Type R_3 Higher Variable Joints	32
3.2.4	Review of Type R_u Higher Variable Joints	33
3.3	Type P_v Higher Variable Joints	33
3.3.1	Case 1: Type P_1 Higher Variable Joints	35
3.3.2	Case 2: Type P_2 Higher Variable Joints	37
3.3.3	Review of Type P_v Higher Variable Joints	39
3.4	Summary	40
CHAPTER 4 Profile Synthesis of R_uP_v Variable Joints		41
4.1	Profile Synthesis of an Example R_1P_1 Variable Joint	41
4.2	Enumeration of Rotational to Translational Variable Joints	42
4.3	Design Configuration Space of Variable Joints	45
4.4	Profile Synthesis Equations for R_uP_v Variable Joints	47
4.4.1	Assumptions	47
4.4.2	Profile of Link 1	48

TABLE OF CONTENTS — *Continued*

4.4.3	Profile of Link 2	50
4.4.4	Constraints for R_uP_v Variable Joints	52
4.5	Adjustable Plier Designs Based on R_uP_v Variable Joints	53
4.5.1	Example R_1P_2 Variable Joint for Adjustable Pliers	55
4.5.2	Alternative Solution	59
4.5.3	Kinematic Redundancies	60
4.5.4	Summary of Adjustable Plier Designs	62
4.6	Constraints on the Direction of Translation	63
4.6.1	External Arc Interference	63
4.6.2	Internal Arc Interference	65
4.6.3	Determining the Separation Angles for an R_1P_v Joint	66
4.7	Summary	68
CHAPTER 5 Four-Bar Mechanism with Variable Topology		70
5.1	Problem Setup	70
5.2	Solution Method using R_uP_v Variable Joints	71
5.3	Four-Bar Mechanism Analysis	73
5.3.1	Overview of Solution Methodology	75
5.3.2	Two Position Rigid Body Guidance for an $RRRR$	76
5.4	Two Position Rigid Body Guidance for an $RRRP$	79
5.5	Determining Transmission Angles for a Reconfigurable Four-Bar	80
5.6	Numerical Example	83
5.7	Joint Design for the Four-Bar Mechanism	85
5.8	Discussion of Alternative Solutions	88
5.9	Summary	90

TABLE OF CONTENTS — *Continued*

CHAPTER 6 Singularity Avoidance in a 3-R<u>P</u>R Parallel Manipulator	91
6.1 Introduction	91
6.2 3R <u>P</u> R Singularities	92
6.3 Problem Setup	97
6.4 Solution Method using $R_u P_v$ Variable Joints	98
6.5 Numerical Example	101
6.6 Joint Design for the 3-R <u>P</u> R	105
6.7 Summary	106
CHAPTER 7 Summary and Conclusions	108
7.1 Higher Variable Joints	108
7.2 Profile Synthesis of $R_u P_v$ Variable Joints	109
7.3 Four Bar Mechanism with Variable Topology	109
7.4 Singularity Avoidance in a 3-R <u>P</u> R Parallel Manipulator	110
7.5 Conclusions	110
7.6 Final Remarks	113
REFERENCES	115
APPENDIX A Analysis of Reconfigurable Mechanisms	121
A.1 Introduction	121
A.2 Current Matrix Representations	122
A.2.1 Adjacency Matrices	122
A.2.2 EU-Matrix Transformations	124
A.2.3 Improved Adjacency Matrix	125
A.2.4 Directionality Topology Matrices	126

TABLE OF CONTENTS — *Continued*

A.3	Mechanism State Matrices	127
A.3.1	Matrix Notation	128
A.3.2	Representative Example	130
A.4	Augmented Mechanism State Matrices	132
A.5	Examples	133
A.5.1	3RRR Mechanism	133
A.5.2	Planar Metamorphic Mechanism	134
A.5.3	2R-2P Mechanism	135
A.6	Review of Mechanism State Matrices	136
APPENDIX B	Lower Pairs	138

LIST OF FIGURES

1.1	General Profile of a Joint	4
1.2	Example Rotational to Translational Variable Joint	4
1.3	Rotational to Translational Variable Joint	4
2.1	One DOF Wren Platform	12
2.2	Two DOF Wren Platform	12
2.3	The Mechanisms Oscillate Between Pins P_1 and P_2	13
2.4	Classification of Mechanisms with Variable Topology	14
2.5	Mechanism Performing Skew-Axial Motion	15
2.6	Mechanism Performing Straight Line Motion	15
2.7	Change in Kinematic Pair	17
2.8	Change in Orientation	17
3.1	Higher Variable Joints	22
3.2	Fixed and Moving Centroides of a Variable Joint	23
3.3	Rotation About the Z-axis is Possible	25
3.4	Immobile Object due to Frictionless Contacts	25
3.5	Different Cases for Revolute Higher Variable Joints	27
3.6	One Constraint Body is Not Sufficient to Constrain Body B to Purely Rotational Motion.	29
3.7	Two Constraint Bodies, A_1 and A_2 are Placed on the Outside of Body B	30
3.8	(A) The C-obstacles Intersect at the Origin. (B) Only Pure Rotation is Possible Along the θ Axis.	31
3.9	(A) The Only Free Motion is Rotation about the Center of body B . (B) Only Pure Rotation is Possible Along the θ axis.	32

LIST OF FIGURES — *Continued*

3.10 (A) The only free motion is rotation about the center of body B . (B) Only pure rotation is possible along the θ axis.	33
3.11 Different Cases for Prismatic Higher Variable Joints	34
3.12 (A) Two Point Contacts are Needed for Translational Motion. (B) Three Point Contacts are Needed for Translational Motion.	35
3.13 Only Translational Motion is Possible due to the C-obstacles	36
3.14 Cross Sections for: (A) $\theta = -10^\circ$. (B) $\theta = 0^\circ$ (C) $\theta = 10^\circ$	36
3.15 Cross Sections for: (A) $\theta = -10^\circ$. (B) $\theta = 0^\circ$ (C) $\theta = 10^\circ$	37
3.16 Only translational motion is possible due to the c-obstacles	38
3.17 Cross Sections for: (A) $\theta = -10^\circ$. (B) $\theta = 0^\circ$ (C) $\theta = 10^\circ$	38
3.18 Cross Sections for: (A) $\theta = -15^\circ$. (B) $\theta = 0^\circ$ (C) $\theta = 15^\circ$	39
4.1 R_1P_1 Variable Joint	43
4.2 $R_1R_2R_3$ Variable Joint	44
4.3 Configuration Space for a R_uP_v Variable Joint	46
4.4 General Joint Profile	48
4.5 A Change of δ_1 in the Radial Direction	52
4.6 The R_uP_v Variable Joints	54
4.7 Design Configuration Space Representation of Adjustable Pliers.	55
4.8 The R_1P_2 Variable Joint for Adjustable Pliers	56
4.9 Different configurations of the R_1P_2 variable joint	57
4.10 Design Configuration Space Representation of Adjustable Pliers.	58
4.11 R_1P_2 Adjustable Plier Design	59
4.12 R_3P_2 Variable Joint	60
4.13 R_3P_2 Adjustable Plier Design	62
4.14 Adjustable Plier Designs	64

LIST OF FIGURES — *Continued*

4.15 Knipex R_2 adjustable plier design	64
4.16 Craftsman R_1 adjustable plier design	64
4.17 External Arc Interference Example.	65
4.18 External Arc Interference	66
4.19 All External Arc Interference Regions	66
4.20 Internal Arc Interference	66
4.21 All Internal Arc Interference Regions	66
4.22 Possible α , β , γ Combinations with $\theta_i = 25^\circ$, $\theta_f = 65^\circ$, $\theta_t = 110^\circ$, $\theta_R = 0^\circ$, and $d = 5$	67
4.23 Unrealistic Joint Design	68
4.24 Separation Angles after Imposing the Constraints from Eq. 4.10	69
5.1 Problem Setup for Manufacturing Application	71
5.2 RRRR Four-Bar Mechanism	71
5.3 RRRP Four-Bar Mechanism	71
5.4 Solution Using a R_uP_v Variable Joint	72
5.5 Graphical Symbol for an R_uP_v Variable Joint	73
5.6 Final Result	74
5.7 Combined RRRR and RRRP Four-Bar Mechanism	74
5.8 Solution Using a R_uP_v Variable Joint	75
5.9 Two Position Rigid Body Guidance: RRRR	77
5.10 Two Position Rigid Body Guidance: RRRP	79
5.11 RRRR Transmission Angle	81
5.12 RRRP Transmission Angle	81
5.13 Resulting Four-Bar Mechanism	83

LIST OF FIGURES — *Continued*

5.14 Design Configuration Space	85
5.15 Calculated R_2P_2 Joint	86
5.16 Mechanism Design with an R_2P_2 Variable Joint	87
5.17 Final Joint Design for the R_2P_2 Variable Joint	87
5.18 Three Position Rigid Body Guidance: RRRR	89
6.1 3-R <u>P</u> R Parallel Mechanism	92
6.2 3-R <u>P</u> R Singular Configuration	94
6.3 Non-Singular Configuration	97
6.4 Singular Configuration	97
6.5 3-R <u>P</u> R with Variable Topology	98
6.6 3-R <u>P</u> R with Variable Topology	99
6.7 Singular Configuration	99
6.8 Structure	99
6.9 Animation Showing the Final Result	101
6.10 3-R <u>P</u> R Mechanism Singular Configuration	102
6.11 3-R <u>P</u> R Reachable Workspace $\phi = 0^\circ$	103
6.12 3-R <u>P</u> R Initial Position	104
6.13 3-R <u>P</u> R Final Position	104
6.14 Singular Configuration with $\phi = 0$	104
6.15 Design Configuration Space	106
6.16 Calculated R_2P_2 Joint	106
6.17 Final Joint Design for the R_2P_2 Variable Joint	107
A.1 (A) The Six-Bar Linkage in State 1 has Three DOF. (B) The Six-bar Linkage becomes a Five-bar Linkage in State 2 with Two DOF.	123

LIST OF FIGURES — *Continued*

A.2	Joint Code of Common Kinematic Pairs	127
A.3	(A) 3RRR Linkage with Three DOF. (B) 3RRR Linkage with Two DOF. (C) 3RRR Linkage with One DOF.	134
A.4	The Mechanism Oscillates Between Pins P_1 and P_2	135
A.5	2R-2P Mechanism with Perpendicular Prismatic Joints	136
A.6	2R-2P Mechanism with Parallel Prismatic Joints	137

CHAPTER 1

Introduction

“You can’t make bricks without straw.”

1.1 Introduction

There is an ever increasing demand for mechanisms that perform a variety of different tasks. One possible technique is to have adaptable mechanisms. A reconfigurable mechanism is a mechanism that changes its topology or degrees of freedom (DOF). Application areas for reconfigurable mechanisms include, but are not limited to, deployable truss structures [1], origami [2], and industrial manufacturing [3].

A subset of reconfigurable mechanisms, Type II Mechanisms with Variable Topology (MVTs), require variable joints. Variable joints are able to change their kinematic pair or representative orientation based on the required mechanism function. Variable joints are found in everyday items such as adjustable pliers or door latches. Conventional mechanisms rely on the classic lower (i.e., revolute and prismatic joints) and higher (i.e., cams, Reuleaux triangle, etc.) pairs to constrain the motion of two links. However, greater adaptability can be gained by using variable joints in a mechanism. Variable joints can help reduce the number of required actuators, which reduce the power supplies, wiring, and coordination of

the DOF.

1.2 Research Purpose

Reconfigurable mechanisms have the potential to revolutionize mechanism design. The ability for a mechanism to seamlessly switch from one mechanism to another is an active area of research with significant upside potential, including reduced weight, cost savings, and added flexibility.

Synthesis of reconfigurable mechanisms is a complicated problem. Most reconfigurable mechanisms are created by either locking a joint with an external force or by passing through a singularity. In both cases, the type of joint does not change. Rather, the joint becomes inactive (or active), due to constraints placed on the mechanism.

MVTs that contain variable joints (Type II MVTs) are distinctly different from reconfigurable mechanisms that change due to locking a joint. For example, by using a planar, variable joint, a four-bar mechanism could seamlessly switch from a RRRR four-bar to a RRRP¹ four-bar. This Type II MVT is in contrast to a reconfigurable four-bar mechanism in which one of the joints is locked by an external force, thereby reducing the mechanism to a structure.

In order to synthesize Type II MVTs, the joint profiles of variable joints must be well understood, and, therefore, the joint profiles are the focus of this dissertation. This dissertation provides a method that can be used to perform automated profile synthesis of planar, variable joints that change from a revolute

¹The notation “RRRR” and “RRRP” denote the order in which revolute and prismatic joints are connected in a four-bar mechanism.

pair to a prismatic pair. The results of this work are subsequently applied to two applications involving industrial manufacturing and singularity avoidance in parallel manipulators.

The proverb that heads this chapter is fitting for the problem solved in this dissertation. Just as you cannot make bricks without straw, you cannot make Type II MVTs without variable joints. Hence, the broader impact of this research is that engineers will have a new tool to create planar, variable joints that change from a revolute pair to a prismatic pair. In addition, the dissertation provides a new way of thinking about the profiles of variable joints, and the methods used in this work have the potential to be expanded to other types of variable joints as well. The potential applications for reconfigurable mechanisms that use these variable joints are limitless.

1.3 Joint Profile Synthesis

An easy way to visualize the variable joint synthesis problem is by example. Figure 1.1 provides a general representation of a joint where link 1 (a hollow rigid body) is assumed fixed, and link 2 (a solid rigid body) moves in the plane relative to link 1. Each link has a distinct profile which constrains the relative motion between the two links. Similarly, each link of the variable joint in Fig. 1.2 has a distinct profile which constrains the relative motion between the two links. However, the joint in Fig. 1.2 provides a more prescribed motion due to its methodical design. The variable joint is able to change from a revolute pair to a prismatic pair due to the geometric profiles of the two links. The goal is to find the

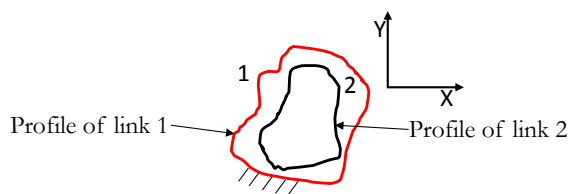


Figure 1.1: General Profile of a Joint

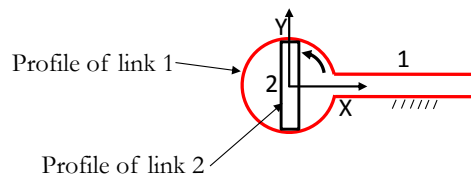


Figure 1.2: Example Rotational to Translational Variable Joint

properties these profiles need to have to enforce this type of motion.

1.4 Profile Synthesis of an Example Variable Joint

An example of the results from this research is shown in Fig. 1.3. The variable joint contains two links. Link 1 is assumed fixed, and link 2 moves relative to link 1. Link 2 starts in the initial configuration, as shown in Fig. 1.3(A), and rotates counterclockwise to the position, as shown in Fig. 1.3(B). Link 2 is then able to translate along the fixed slot as shown in Fig. 1.3(C). In determining the profiles for link 1 and link 2 of the variable joint, the design parameters are the

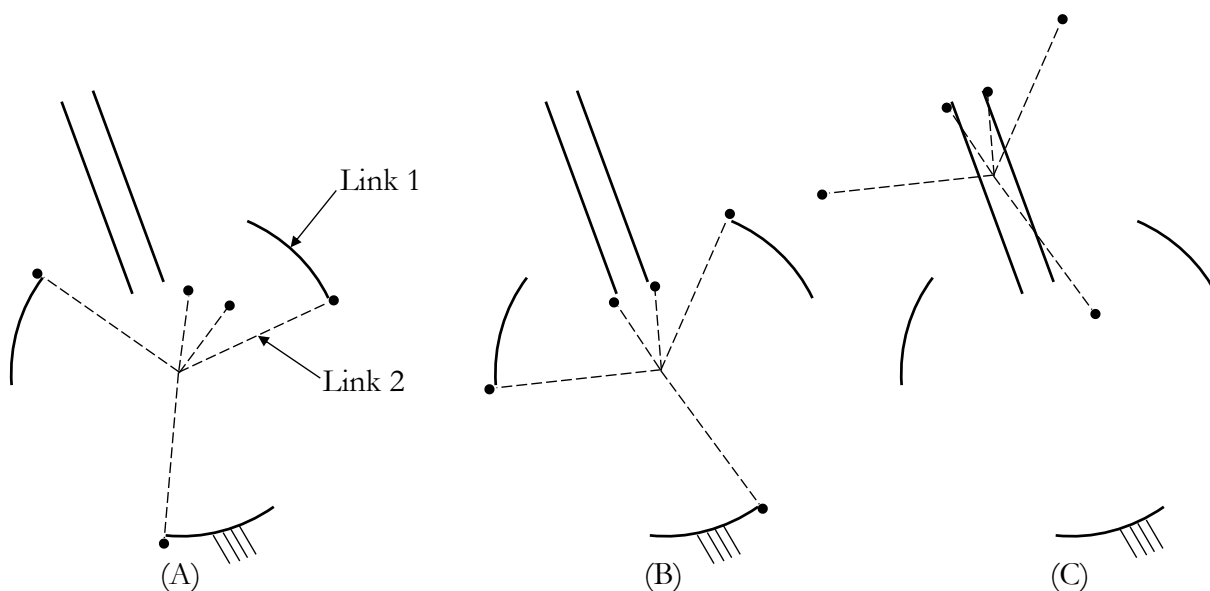


Figure 1.3: Rotational to Translational Variable Joint

amount of rotation, the direction of translation, and the distance link 2 translates. From specifying these design parameters, it is possible to automatically determine the profiles of two links that provide the desired planar motion.

In this dissertation, it is further shown how this type of variable joint can be used in a reconfigurable four-bar mechanism utilized in a manufacturing application. In addition, it is shown that using a variable joint that changes from a rotational motion to a translation motion can be used for singularity avoidance in a certain parallel manipulator (PM).

1.5 Organization of the Dissertation

This dissertation is organized as follows: Chapter 2 outlines the relevant literature and motivation for this work. Chapter 3 introduces planar, higher variable joints as essential components of Type II MVTs. Chapter 4 presents a procedure for the profile synthesis of R_uP_v variable joints. Chapter 5 shows an example of a reconfigurable four-bar mechanism that uses R_uP_v variable joints in a manufacturing application. Chapter 6 shows how an R_uP_v variable joint can be used to help avoid singularities in a 3-RPR² mechanism, and Chapter 7 provides a conclusion and remarks for future work.

²The underlined P in 3-RPR² denotes the actuated joints.

CHAPTER 2

Motivation and Literature Review

This work is motivated by the fact that variable joints are fundamental components of certain reconfigurable mechanisms¹. Reconfigurable mechanisms were introduced as recently as 1996 [4], and these will be discussed in greater detail in Section 2.3. However, in order to place this work in proper context, a brief history of kinematics will be presented.

2.1 A Brief History of Kinematics

Mechanisms analysis and synthesis was first formalized in the 1800s by Reuleaux [5], Kennedy [6], and Burmester [7]. Ingenious mechanisms were created prior to this time, but there were no standard analysis or synthesis techniques in use. In the early 1800's, many kinematicians were focused on synthesizing mechanisms that provide straight-line (or approximate straight line) motions. Examples include the Peaucellier-Lipkin linkage, the Sarrus linkage, Watt's linkage, Hoeken's linkage, and the Chebyshev linkage. In 1875 Reuleaux published his famous book, *Kinematics of Machinery*, in which he was the first to develop a notation to represent the topology of mechanisms. He also introduced the concept of kinematic pairs as well as kinematic inversions. In 1886, Alexander

¹The term reconfigurable mechanism should not be confused with self-reconfigurable robots which are not the focus of this work.

Kennedy translated *Kinematics of Machinery* into English, and Kennedy's Theorem [6] was a major contribution to the field. Around the same time frame, Burmester provided solutions for finite position synthesis for planar mechanisms. Over the next fifty years mechanisms were synthesized to trace a particular path.

In the 1950s, Denavit and Hartenberg introduced a standard matrix notation that is used as a convention for attaching reference frames to the links of a serial kinematic chain [8]. The advent of the digital computer in the allowed for the use of the vector loop equations [9, 10] to perform automated analysis and synthesis of linkages [11]. In 1985 Tsai and Morgan were able to solve the forward and inverse kinematics for general five and six DOF manipulators [12]. In 1992, Wampler and Morgan provided a complete solution of the nine-point path synthesis problem for four-bar linkages [13]. Following in 1996 Wohlhart introduced kinematotropic mechanisms [4]. In 1997, Ruth and McCarthy introduced computer aided synthesis for spherical linkages [14]. By 1999 Dai and Jones introduced metamorphic mechanisms [15]. The early 2000s led to the synthesis of compliant mechanisms [16]. In 2001 Yan et al. introduced mechanisms with variable topology (MVTs) [17], and in 2008 Murray and Schmiedeler did work with shape changing mechanisms [18].

This brief history of kinematics shows that since the 1950s many of the advances in the field have relied on advances in computer algebra and the solution of complex systems of equations. It is only recently that reconfigurable mechanisms (kinematotropic mechanisms, metamorphic mechanisms, MVTs) have been used to solve complex kinematics problems.

2.2 Reconfigurable Mechanisms

Recently, there has been an increasing demand to create reconfigurable mechanisms that can perform multiple tasks. As mentioned previously, reconfigurable mechanisms can be defined as mechanisms that change either their topology or DOF. These mechanisms are useful because they can provide quick changeover and reduced costs for low volume manufacturing applications. In addition, reconfigurable mechanisms can provide added flexibility in the context of a constrained environment. Specific areas of application include manufacturing, space exploration, medical devices, robotic end-effectors, and hand tools.

Much of the research on reconfigurable mechanisms focuses on reconfigurable mechanisms analysis. Dai [19], Kuo [20], Lan [21], and Slaboch [22] have proposed different ways to represent the topological characteristics of reconfigurable mechanisms using a matrix notation. In 2005 Dai and Jones [19] proposed an EU-elementary matrix operation to represent the state changes of metamorphic mechanisms. Dai and Jones realized that upon a change in the number of effective links, the dimension of an adjacency matrix changes as well as the order of the elements. The EU-elementary matrix operation is useful in capturing this change. This was followed in 2006 when Yan and Kuo [20] proposed directionality topology matrices. These matrices improved upon Dai's method by including information about the type of kinematic pair. In 2008 Lan and Du [21] proposed a -1 element to indicate a fixed kinematic pair. This ensured that the size of the adjacency matrix remained the same after a change in configuration

occurred. Finally, in 2011 Slaboch and Voglewede [22] introduced Mechanism State Matrices (M_{sm}) which combined the best qualities of the previous representations. (A more in depth review of reconfigurable mechanisms analysis and Mechanism State Matrices is presented in Appendix A.)

While reconfigurable mechanism analysis can be used as a common tool for discussing reconfigurable mechanisms, the more important type of research involves reconfigurable mechanisms synthesis. That is, determining what types of links and joints are required for a reconfigurable mechanisms to perform a certain task.

In 2001 Galletti [23] showed how to create single-loop kinematotropic mechanisms followed up in 2002 by Multiloop Kinematotropic Mechanisms [24]. In this work, different geometric conditions (i.e., parallel axes or coincident axes) were exploited to create mechanisms that would move through a singular configuration to change the DOF for a finite motion. Following in 2006, Yan and Kuo [20] showed how to use graph theory and generalized transition pairs to form a semi-automated procedure in synthesizing new mechanisms. This procedure involves determining different joint sequences based on design requirements. However, this procedure requires heavily on intuition. In 2006 Herve [25] showed how to create translational parallel manipulators using Lie-group algebra. In 2009 there was much work presented at the Reconfigurable Mechanisms and Robotics (ReMAR) conference in London. Ma et al. [26] showed how to use a characteristic matrix to produce new designs. Yang et al. [27] showed how to use a genetic algorithm approach to determine an optimal reconfigurable mechanism. Their algorithm uses different building blocks that are combined together using an

optimization. Kong and Huang [28] examined the type synthesis of single-DOF single loop mechanisms that have two operation modes, and Yan and Kang [29] showed how to perform configuration synthesis of mechanisms with variable topologies using graph theory.

Previous research on reconfigurable mechanism synthesis has relied exclusively on the classic lower and higher pairs. The synthesis work in this dissertation is different than prior research in that the focus is on the profile synthesis of the variable joints that change from rotational to translational motion. Once the profiles of the joints have been determined, the joints can be used to create new reconfigurable mechanisms. This type of synthesis work is novel, and the synthesized joint profiles are intended to help in the reconfigurable mechanism synthesis process.

This section has provided an overview of the analysis and synthesis of reconfigurable mechanisms. Section 2.3 will provide an overview of the three main types of reconfigurable mechanisms that are found in the literature. A subset of these mechanisms rely on variable joints (Type II MVTs), and so a fundamental understanding of the different types of reconfigurable mechanisms is necessary. This will help to show why the profile synthesis of variable joints that change from a rotational motion to a translational motion is an important problem.

2.3 Types of Reconfigurable Mechanisms

Different types of reconfigurable mechanisms were formally defined starting in the early 1990s, but they have been used informally prior to this time. For

example, in 1954 Wunderlich [30] introduced a 12-bar mechanism that changes from one DOF to two DOF. Even though reconfigurable mechanisms existed, they were not formally defined because most of the research was focused on what are today considered standard mechanisms analysis and synthesis procedures. In addition, each reconfigurable mechanism was considered an anomaly, and a broader classification system did not exist.

2.3.1 Kinematotropic Mechanisms

Reconfigurable mechanisms can be categorized as kinematotropic mechanisms, metamorphic mechanisms, or mechanisms with variable topology (MVTs)². Kinematotropic mechanisms were first proposed by Wohlhart in 1996 [4, 31]. In 2001, Galletti [23] showed how to create single-loop kinematotropic mechanisms, and in 2002 synthesized multiloop kinematotropic mechanisms [24]. Kinematotropic mechanisms are defined as follows:

Kinematotropic Mechanisms: “Mechanisms that, in passing a singularity position (in which a certain transitory infinitesimal mobility is attained) these mechanisms permanently change their global mobilities.” [4]

Figures 2.1 and 2.2 depict a typical kinematotropic mechanism in which the mechanism moves into a singularity which permanently changes the DOF of the linkage from one DOF to two DOF. A singularity occurs when ψ is equal to zero which causes the mechanism change its DOF. This example shows that kinematotropic mechanisms can change their global mobility by passing through a

²All reconfigurable mechanisms are MVTs. There are three different types of MVTs that are used to further classify the type of reconfigurable mechanism.

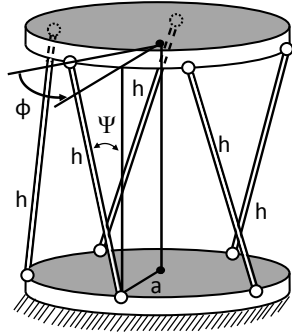


Figure 2.1: One DOF Wren Platform

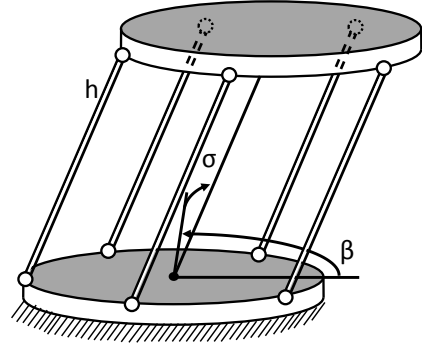


Figure 2.2: Two DOF Wren Platform

singular configuration.

2.3.2 Metamorphic Mechanisms

Following the work performed on kinematotropic mechanisms, Dai and Jones introduced metamorphic mechanisms [15]. A metamorphic mechanism is defined as follows:

Metamorphic Mechanism: “A mechanism whose number, the total of all effective links, changes as they move from one configuration to another or a singular condition makes it behave differently.” [15]

An example of this type of reconfigurable mechanism is shown in Fig. 2.3. This is a five-link metamorphic mechanism that oscillates between pins P_1 and P_2 . The spring embedded in link 2 pushes link 3 along the slot in link 2. In this case the state of the mechanism changes as it oscillates between pins P_1 and P_2 . The difference between this mechanism and a kinematotropic mechanisms is that there is a change in topology due to an external force as opposed to a singularity in the mechanism. This leads to the most common type of reconfigurable mechanisms, which are mechanisms with variable topology.

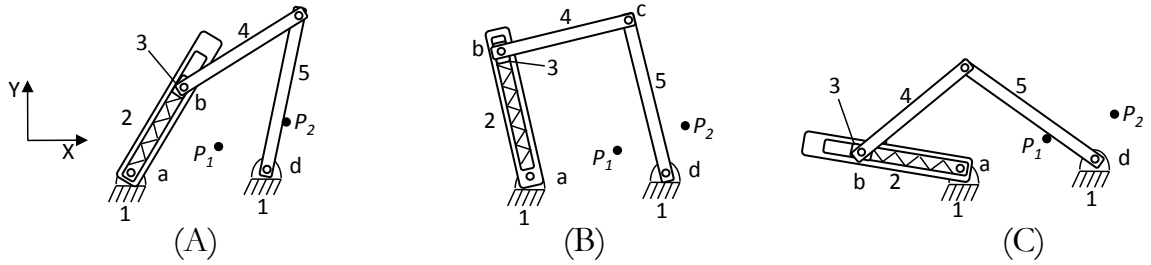


Figure 2.3: The Mechanisms Oscillate Between Pins P_1 and P_2 .

2.3.3 Mechanisms with Variable Topology

The topology of a mechanism refers to determining the types of joints in a mechanisms as well as the connectivity of those joints. A mechanism with variable topology is defined as follows:

Mechanism with Variable Topology (MVT): “A mechanisms with variable topology is a mechanism whose topology changes during operation.” [32]

MVTs can be further classified as one of the following three types [33]:

- I. MVTs that change topology due to an intrinsic constraint (kinematotropic or metamorphic mechanisms)
- II. MVTs that change topology due to a joint geometry change
- III. MVTs that change topology due to an external constraint (metamorphic mechanism)

Metamorphic mechanisms and kinematotropic mechanisms are simply subsets of Mechanisms with Variable Topology as shown in the diagram in Fig. 2.4. Both Type I MVTs and Type III MVTs have been studied more extensively than other types of reconfigurable mechanisms, and these types of mechanisms were discussed in Section 2.3.1 and Section 2.3.2. However, this research will be motivated by MVTs that change topology due to a joint geometry

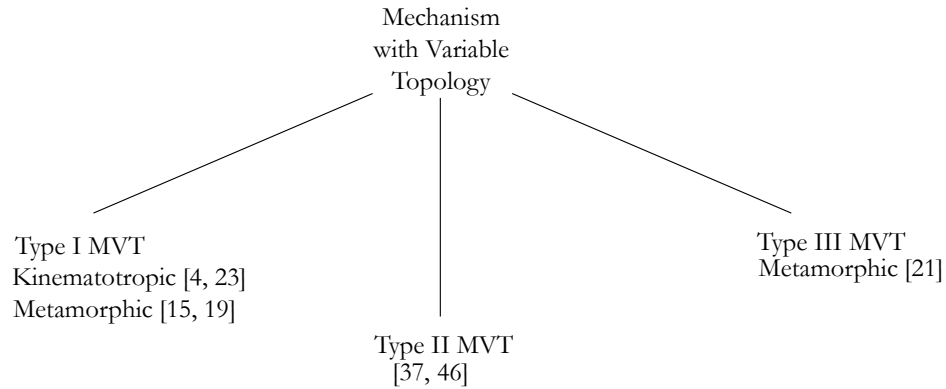


Figure 2.4: Classification of Mechanisms with Variable Topology

change (Type II), which are not as well understood. An example of an MVT that changes topology due to a joint geometry change is given in Figs. 2.5 and 2.6. This mechanism is able to change from performing skew-axial motion to performing straight line motion.

This mechanism is able to change its topology by using a variable joint that changes its orientation. In particular, the joint is able to change its axis of rotation. This type of joint is not a joint used in conventional mechanisms. In order to physically create this joint, the joint profiles had to be determined. It is assumed that the profiles of the variable joints in this mechanism were created using intuition. While this may work in some cases, it is the goal of this research to determine the theory behind the profile synthesis of variable joints. Specifically, the profiles of planar variable joints that change from a rotational to a translational motion will be determined.

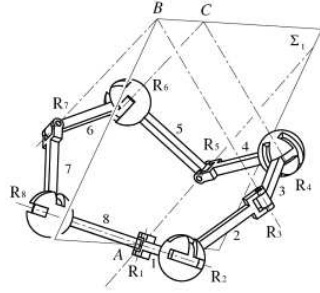


Figure 2.5: Mechanism Performing Straight Line Motion [34]

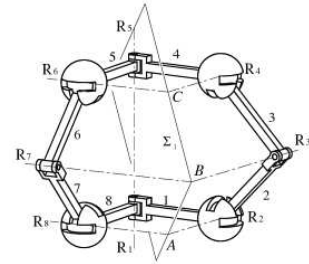


Figure 2.6: Mechanism Performing Straight Line Motion [34]

2.4 Summary of Reconfigurable Mechanisms

This section has shown that there are three types of reconfigurable mechanisms (kinematotropic, metamorphic, MVTs). Kinematotropic, metamorphic, and MVTs of Type I and Type III have been widely studied. Type II MVTs are reconfigurable mechanisms that change topology due to a joint geometry change. The joints that make up Type II MVTs will be the focus of this research. In order to fully comprehend what is meant by a “joint geometry change” it is important to first understand the definition of a joint.

2.5 Joints

Joints were first defined by Franz Reuleaux in 1876 [5], and their definition has not changed since that time. This section provides an overview of the different types of joints used for both conventional mechanisms and reconfigurable mechanisms. Joints are categorized as either lower pairs or higher pairs depending on the connection between two links (rigid bodies). Reuleaux was the first to formalize the idea that links in a mechanism are connected in pairs.

2.5.1 Lower Pairs

Reuleaux states that the closed pairs (lower pairs) must satisfy three criteria:

1. “Must have surface contact.
2. The two elements must be geometrically identical.
3. The elements prevent every motion except the one that is required.” [5]

Reuleaux determined that, by this definition, there are only six lower pairs (revolute, prismatic, cylindrical, helical, spherical, plane), and in 1972 Waldron [35] mathematically proved that Reuleaux was correct. Formal definitions of lower pairs taken from Tsai [36] are given in Appendix B.

2.5.2 Higher Pairs

Higher pairs can be distinguished from lower pairs in that the pair of elements do not enclose each other. From Reuleaux’s definition, higher pairs must satisfy the following criteria:

1. Require a point or line contact.
2. It must be shown that in all consecutive mutual positions relative sliding is impossible. [5]

An example of a higher pair is Reuleaux’s triangle, which is commonly used in rotary engines. In both lower and higher pairs it was assumed that the two bodies in contact were constrained solely by the geometric profiles of the two links. This important assumption, which is often overlooked in conventional kinematics texts, is an important concept as it relates to this research. In this research only higher pairs that are constrained solely by the geometric profiles of the two links

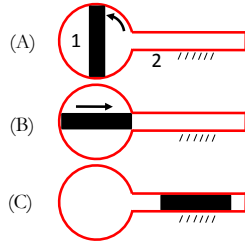


Figure 2.7: Change in Kinematic Pair

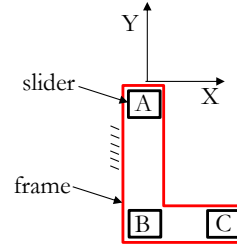


Figure 2.8: Change in Orientation

will be considered. Incomplete pairs [5] will not be considered. For example, a rack and pinion gear pair is not considered because it depends upon the application of a closing force.

2.5.3 Variable Joints

All MVTs that change topology due to a joint geometry change contain variable joints. Variable joints were first introduced by Yan and Kuo in 2006 [37], and are defined as joints that can change either their kinematic pair or representative orientation with respect to a local coordinate system.

An example of a variable joint that changes its kinematic pair is shown in Fig. 2.7. This variable joint changes its kinematic pair from a revolute pair to a prismatic pair. In configuration (A) link 1 rotates relative to the ground link. In configuration (B) link 1 is in a transition stage in which link 1 may instantaneously either rotate or translate relative to link 2. Finally, in configuration (C) link 1 may slide relative to the ground link.

Variable joints are also used to capture changes in the representative orientation of a joint. For instance, Fig. 2.8 shows a variable slider joint in which a sliding block moves relative to a fixed frame. The slider begins in configuration (A)

and translates along the $-Y$ axis to configuration (B). In configuration (B) the slider is in a transition stage in which it may either slide along the X or Y axes. The slider is then able to translate along the X axis as shown in configuration (C).

2.5.4 Practical Considerations for Variable Joints

In this dissertation, only the profile synthesis (i.e., the kinematics) of variable joints that change from a rotational motion to a translational motion is considered. However, there are many practical issues that would need to be considered in order to create these variable joints. This section will outline some of the practical issues that need to be considered. This is not meant to fully address every practical consideration, but rather, to show that understanding the kinematics is just the first part of the joint design process. While practical considerations are similar to those that are used for current design of standard lower and higher pairs, there are some design criteria that will be more challenging for variable joints than conventional lower and higher pairs.

After determining the required joint profiles, each of the joint profiles must be considered from a manufacturing point of view. An important first step in this process is to determine kinematic redundancies based on the nominal joint profile design. Kinematic redundancies can be used to add mechanical stops, reduce stress concentrations, and provide added stability to the design.

Appropriate bearings must be designed to accommodate the different joint profiles. Standard ball bearings are not designed for use with variable joints. Ball bearing designs for variable joints is an important area of future research.

However, one potential option could be to place steel balls around the joint profiles similar to what is done for current revolute joints.

Tolerances must be analyzed which can be completed using the work by Sacks et. al [38]. Tolerances are critical for R_uP_v variable joint due to the transition configuration from rotational to translational motion. In order to use R_uP_v variable joints in an automated process it must be shown that they are robust and do not jam during the transition from one motion to another.

When an R_uP_v variable joint is used within a mechanism the dynamics must be considered because different joint profiles may be better than others depending on the loading conditions of the joint. Care must be taken to ensure that the forces acting on the joint are within an appropriate range.

Other important factors include the stiffness of the joint as well as possible backlash. Many of the design considerations are identical to those for standard joints. Appropriate materials must be selected based on the specific application. While each of the design considerations are important, it is critical to first understand the joint profiles so that the required kinematic constraints are satisfied, and that will be the focus of this dissertation.

2.6 Summary

There is a need for reconfigurable mechanisms due to the fact that they can be used to provide quick changeover and reduced costs for low volume manufacturing applications. In addition, reconfigurable mechanisms can provide added flexibility in the context of a constrained environment. Reconfigurable

mechanisms can be categorized as kinematotropic, metamorphic, or mechanisms with variable topology. This research will focus on Type II MVTs because variable joints are fundamental components of Type II MVTs. Thus, in order to create Type II MVTs it is important to understand the profile synthesis variable joints.

In this research, the profile synthesis of planar, variable joints that change from a specific rotational motion to a specific translational motion will be investigated. Rotational and translation joints were chosen because these are the most common types of joints used in mechanisms.

CHAPTER 3

Higher Variable Joints

This chapter introduces planar, higher variable joints as essential components of Type II MVTs. It will be shown that profile synthesis of variable joints cannot be achieved using a conventional centroid approach. Finally, it will be proven that second order effects, or surface curvature, of higher variable joints is critical to achieve a particular joint motion. Higher variable joints will be used in Chapter 4 when performing profile synthesis of variable joints that change from a specific rotational motion to a specific translational motion.

3.1 Overview of Higher Variable Joints

In this section, planar revolute and prismatic *higher variable joints* are introduced. The term *higher variable joints* comes from the fact that each joint performs the *higher* characteristic of a lower pair motion, and this motion is intended to be used in a variable joint. Revolute higher variable joints are denoted as Type R_u , where $u = 1, 2, \text{ or } 3$. Prismatic higher variable joints are denoted as Type P_v , where $v = 1 \text{ or } 2$. Figure 3.1 shows that each of the higher variable joints is the discrete form of lower pair motion.

For example, the first row of Fig. 3.1 shows a Type R_1 higher variable joint. The body defined by points (1,2,3) rotates by an angle θ to points (1', 2', 3') as

shown in Fig. 3.1. Note that the angles between the contact normals (α, β, γ) must be less than 180° . The advantage of higher variable joints is that they are able to provide geometrically different forms of identical rotational or translational motion. In Section 3.2 and Section 3.3 it will be proven that there are three types of R_u higher variable joints, and there are two types of P_v type higher variable joints. Prior to this, it will be shown why standard kinematic theory cannot be used to determine the profiles of joints that change from a specific rotational motion to a specific translational motion.

3.1.1 Motivation for Higher Variable Joints

Profile synthesis has been studied since the time of Reuleaux [5]. Reuleaux proposed various methods to determine the profiles of higher pair joints, based on

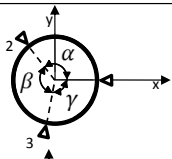
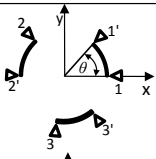
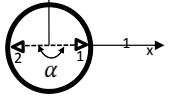
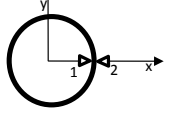
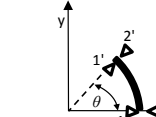
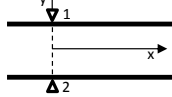
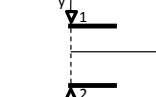
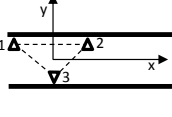
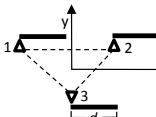
Lower Pair Motion	Higher Variable Joint	Type	Constraints
		R_1	$\alpha < 180^\circ$ $\beta < 180^\circ$ $\gamma < 180^\circ$
		R_2	$\alpha = 180^\circ$
		R_3	Contact normals aligned
		P_1	Contact normals aligned
		P_2	Contact normal for point 3 between contact normal for points 1 and 2

Figure 3.1: Higher Variable Joints

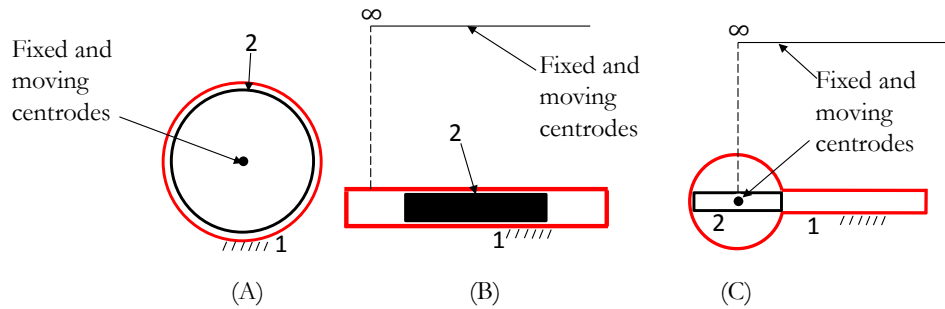


Figure 3.2: Fixed and Moving Centroides of a Variable Joint

a centrode approach. Centroides can be used to represent the planar motion of one body relative to another. Thus, any body moving relative to another can be represented by a fixed and moving centrode where the moving centrode rolls upon the fixed centrode and remains continually in contact.

The two most widely used planar lower pairs, the revolute and prismatic pair, are unique in that their respective fixed and moving centroides are identical. For a revolute pair the fixed and moving centroides are both a point as shown in Fig. 3.2(A) because the instantaneous center of rotation does not change. For a prismatic pair, the fixed and moving centroides are considered to be a line at infinity as shown in Fig. 3.2(B). When combined into a variable joint as shown in Fig. 3.2, the fixed and moving centroides are still identical, but there is a discontinuity in which the centroides move from a point to a line at infinity as the variable joint changes from a revolute pair to a prismatic pair. Thus, there is not a moving centrode rolling on a fixed centrode. Due to this fact, a standard joint profile synthesis technique using a centroid approach is not applicable to variable joints.

In order to determine the profile synthesis of a variable joint that changes

from a rotational motion to a translational motion, it is important to know the minimum number of frictionless point contacts necessary to constrain a body (either circular or rectangular) to either rotational or translational motion. By determining the minimum number of contact points necessary, it allows one to develop a nominal design which can be used to design these types of variable joints. In order to determine the minimum number of contact points necessary, a theory developed by Rimon and Burdick [39] was used, and the fundamentals of this theory are provided in Section 3.1.2.

3.1.2 Mobility of Bodies in Contact

In 1995 Rimon and Burdick [39,40] showed how configuration space may be used to determine the mobility of an object, B , that is in contact with constraint bodies ¹ A_1, \dots, A_n . Figures 3.3 and 3.4 show two bodies, each constrained by frictionless point contacts. First order theories, such as screw theory or Reuleaux's instant center approach, would correctly indicate that both bodies may instantaneously rotate about the z -axis. However, body B in Fig. 3.3 is able to rotate freely about the z -axis, while body B in Fig. 3.4 is immobile. Rimon and Burdick showed that second order effects (i.e., curvature effects) are needed to determine the mobility of bodies in contact because the relative motion between the two bodies is a finite, rather than an infinitesimal motion. The results from this prior work have been used in grasp planning and fixturing as well as other application areas in which the goal is to determine the minimal number of

¹Constraint bodies may be thought of as frictionless point contacts. The constraint bodies do not need to be circular, but must only make contact with body B at one point.

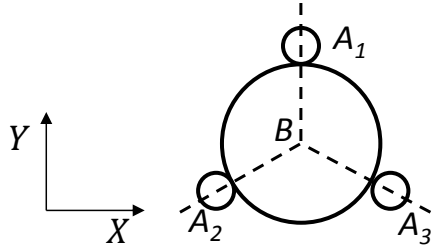


Figure 3.3: Rotation About the Z-axis is Possible

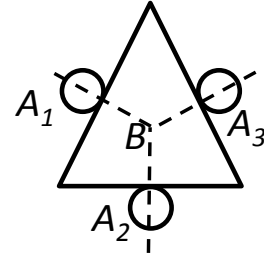


Figure 3.4: Immobile Object due to Frictionless Contacts

constraint bodies necessary to completely immobilize a body, B .

This chapter uses the approach proposed by Rimon and Burdick to determine the minimum number of constraint bodies necessary to constrain a body, B , to either rotational motion or translational motion depending on whether a Type R_u or Type P_v higher variable joint is required. Section 3.1.3 will review the configuration space (c-space) terminology associated with this theory.

3.1.3 Configuration Space Terminology

A rigid object, B , is in contact with rigid, stationary, constraint bodies A_1, \dots, A_n . It is assumed that the boundaries of all bodies are smooth (i.e., frictionless) and that the surface normals are well defined. This analysis will focus on the configuration space of B rather than the combined configuration space of the constraint bodies.

A planar configuration space representation requires three configuration variables. The configuration variables (x_B, y_B, θ_B) can be thought of as describing the motion of the center of body B relative to a fixed body A . Both x_B and y_B have units of length, and $-180 < \theta_B < 180^\circ$. Points are denoted by $q = (d, \theta)$, where $d = (x_B, y_B)$.

C-space obstacles will be denoted by CA_i , which is the set of all configurations, q , in which $B(q)$ intersects the i^{th} constraint body, A_i . The boundaries of CA_i are denoted as S_i , and consist of the configurations in which the surfaces $B(q)$ and A_i touch each other, while their interiors are not touching. The freespace, F_i , is the complement to the c-obstacles' interior. Therefore, curves in F correspond to the free motions of B . If a body, B , is in contact with n frictionless point contacts then the freespace may be expressed as $F = \bigcap_{i=1}^n F_i$.

3.2 Type R_u Variable Kinematic Joints

In order to determine the types of R_u higher variable joints, it is important to review the fundamentals of lower pair revolute joints. Lower pairs consist of touching surfaces, one solid and the other hollow which can move relative to each other while maintaining contact. For example, in the plane, revolute joints can be represented by a solid circle of radius R rotating relative to a hollow outer circle as shown in Fig. 3.5(A). Reuleaux [5], and subsequently Waldron [35], proved that these are the only profiles in the plane that can be used to produce revolute motion. Therefore, to produce a joint that has a variable amount of rotation, one of the joint profiles must be a circular arc.

Suppose now that the solid inner circle of the revolute joint is removed and only the hollow outer circle remains. In creating a higher variable revolute joint, the goal is to determine the *minimum number of constraint bodies* necessary to ensure that the circle of radius R remains constrained to rotational motion. There are three possible cases as shown in Fig. 3.5:

Case 1: Frictionless point contacts are placed on the outside of the circle (Fig. 3.5(B)).

Case 2: Frictionless point contacts are placed on the inside of the circle (Fig. 3.5(C)).

Case 3: Frictionless point contacts are placed on both the inside and the outside of the circle (Fig. 3.5(D)).

3.2.1 Case 1: Type R_1 Higher Variable Joints

For Type R_1 higher variable joints three constraint bodies are necessary to completely constrain a circular body, B , to rotational motion. In addition, the angles between the contact normals of the three constraint bodies (α, β, γ) must be less than 180° . In order to prove that three constraint bodies is the *minimum* number of bodies necessary to constrain body B to rotational motion, it must be shown that motions other than rotational motion are possible with one or two constraint bodies. Three sub-cases will be examined corresponding to the number of constraint bodies that are used to attempt to constrain body B to rotational motion. All of the sub-cases will be shown for R_1 higher variable joint, but for the other higher variable joints only the final result will be presented.

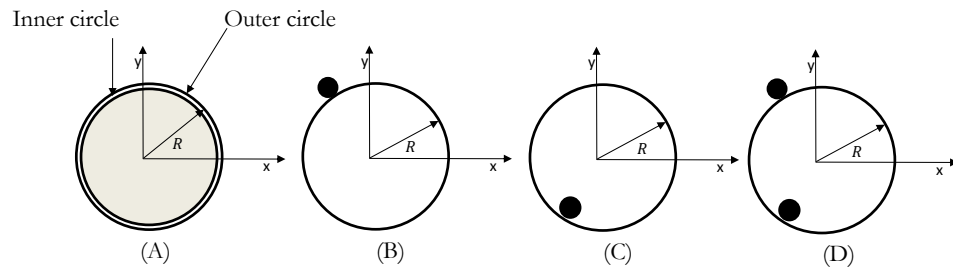


Figure 3.5: Different Cases for Revolute Higher Variable Joints

One Constraint Body

In this sub-case, it will be shown that one constraint body located on the outside of circle B is not sufficient to completely constrain the body to rotational motion. Figure 3.6(A) consists of a circle of radius R (body B) that is in contact with a constraint body (body A) with radius r . A fixed $XY\theta$ coordinate system is located at the center of body B . A local $X_B Y_B \theta_B$ coordinate system is attached to body B , and it is initially aligned with $XY\theta$ in configuration q_1 . Figure 3.6(B) shows body B in two different contact configurations, q_1 and q_2 . Note that in configuration 2, body B is rotated relative to the fixed coordinate system. The c-space obstacle, represented by CA , is shown in Fig. 3.6(C). The boundary of the c-obstacle is given by S . The free space, F , is the complement of the c-obstacles interior.

A tangent plane can be drawn at configuration q_1 that provides a separation between the penetration Halfspace and the free Halfspace. First order theories show that body B can break away from constraint body A along a path within the free Halfspace as shown in Fig. 3.6(C). However, due to the curvature of body B , there are paths in the penetration Halfspace in which body B may escape from body A as curves within F correspond to free motions of B . For instance, body B may break away from body A by moving along the curve $\alpha_1(t)$ or $\alpha_2(t)$. Due to the existence of an infinite number of free paths within F , one constraint body is not sufficient to constrain body B to pure rotation.

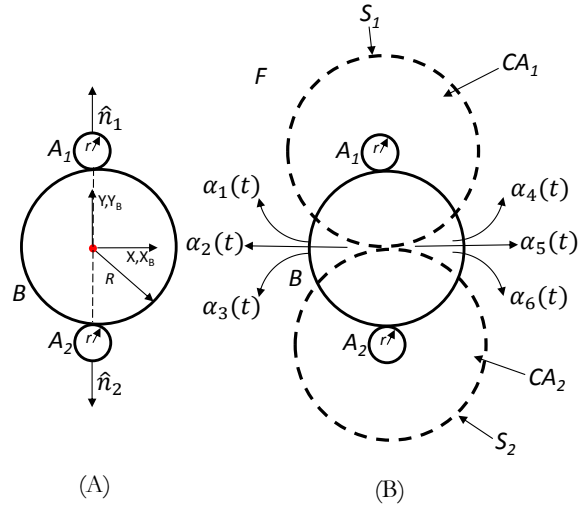


Figure 3.7: Two Constraint Bodies, A_1 and A_2 are Placed on the Outside of Body B .

Three Constraint Bodies

In this sub-case it will be shown that three constraint bodies located on the outside of circle B are sufficient to completely constrain the body to rotational motion. Figure 3.8(A) shows that in the plane, the c-obstacles form three circles that intersect about the center point of body B . This means that only pure rotation is possible. Figure 3.8(B) shows that the possible configurations is a vertical line in the configuration space corresponding to a pure rotation. Any path taken other than along the vertical line would cause body B to collide with a c-obstacle. It is important to note that the angles between the contact normal of the bodies (α, β, γ) must be greater than 180° . If the contact normals are less than 180° then the c-obstacles do not intersect at a point (in the XY -plane) and motion other than rotational motion is possible.

3.2.2 Case 2: Type R_2 Higher Variable Joints

For Type R_2 higher variable joints two constraint bodies are necessary to completely constrain a circular body, B , to rotational motion. This corresponds to the case in Fig. 3.5(C), in which the contact bodies make contact on the inside of body B . For this case, it can be proven that only two contact bodies are necessary to completely restrain body B to rotational motion. The normals of the two contact bodies must be aligned for this to be possible, and the contact normals must also be in opposite directions. Figure 3.9 shows body B , in contact with two constraint bodies, A_1 and A_2 . The contact normals, \hat{n}_1 and \hat{n}_2 , of A_1 and A_2 are aligned. In the XY -plane, the c-obstacles form two circles that meet at the origin. This is similar to the two constraint body case for R_1 higher variable joint. The difference is that the freespace, F , is now the c-obstacles *interior*, as opposed to the complement of the c-obstacles interior. The reason for this is the body B is

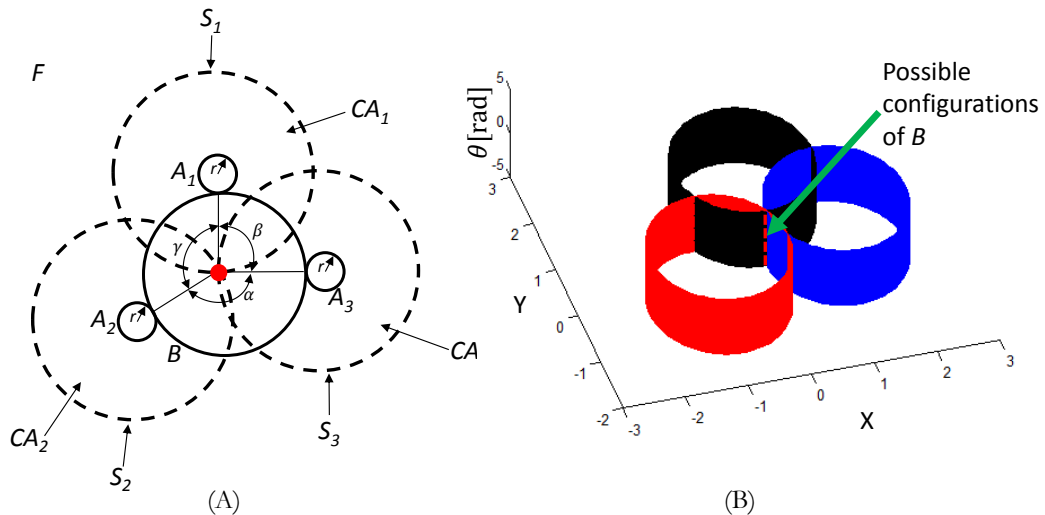


Figure 3.8: (A) The C-obstacles Intersect at the Origin. (B) Only Pure Rotation is Possible Along the θ Axis.

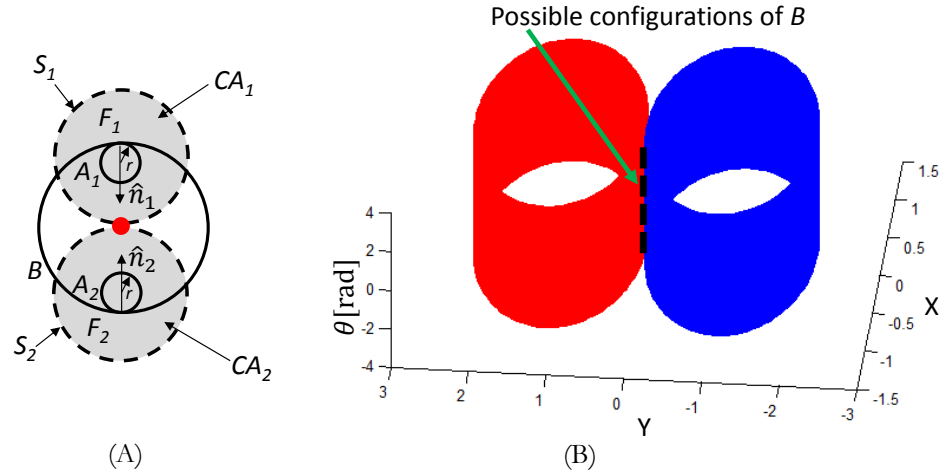


Figure 3.9: (A) The Only Free Motion is Rotation About the Center of Body B . (B) Only Pure Rotation is Possible Along the θ axis.

now imposing a boundary around the constraint bodies which forces them to remain within that boundary. Recall that only paths within the freespace are possible. Therefore, the only free path occurs at the intersection of the c-obstacles. This corresponds to a vertical line as shown in Fig. 3.9(B). Similar to R_1 higher variable joints, only rotational motion is possible.

3.2.3 Case 3: Type R_3 Higher Variable Joints

For Type R_3 higher variable joints two constraint bodies are necessary to completely constrain a circular body, B , to rotational motion. Type R_3 higher variable joints correspond to the case in Fig. 3.5(D) in which there are contacts on both the inside and the outside of body B . For this case, two constraint bodies, A_1 and A_2 , are needed to constrain body B to rotational motion as shown in Fig. 3.10(A). The contact normals must be aligned, and the contact normals must be in opposite directions. In this case, F_1 is on the interior of CA_1 , and F_2 is the

complement to the CA_2 . Therefore, the intersection of the freespace in the XY -plane is again a point at the origin. Figure 3.10(B) shows that the possible configurations of body B correspond to pure rotation about the center of body B .

3.2.4 Review of Type R_u Higher Variable Joints

In this section three types of R_u higher variable joints were presented. In each case, a different number of contact point were necessary to constrain body B to purely rotational motion, depending on the location of the contact points. The three types of R_u higher variable joints are all kinematically equivalent to a lower pair revolute joint, but each higher variable joint has a different physical implementation.

3.3 Type P_v Higher Variable Joints

This section presents Type P_v higher variable joints as shown in Fig. 3.12. These will be derived in a similar manner as for Type R_u higher variable joints. In

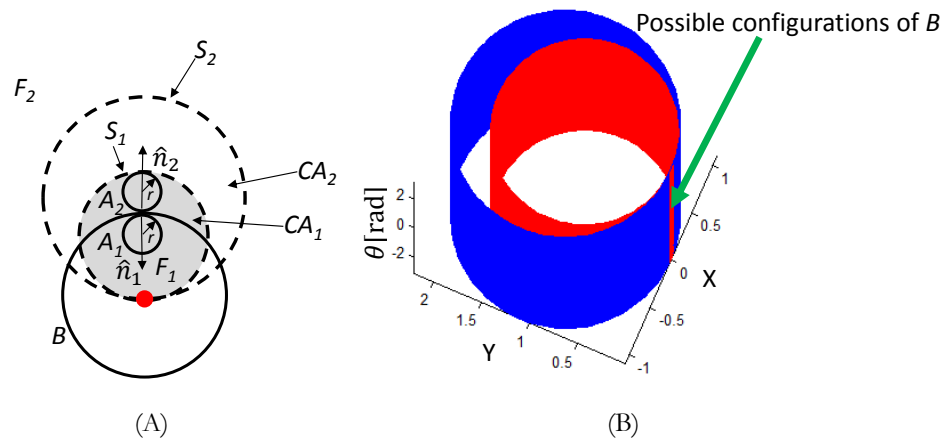


Figure 3.10: (A) The only free motion is rotation about the center of body B . (B) Only pure rotation is possible along the θ axis.

the plane, a prismatic joint may be thought of as two rectangles, one solid and the other hollow, that move relative to each other. Similarly to revolute joints, Waldron [35] proved that these are the only profiles in the plane that can be used for translational motion. Thus, any joint containing a variable amount of translational motion must contain two parallel lines as part of the constraint profiles. In creating a higher variable prismatic joint, the goal is to determine the *minimum number of constraint bodies* necessary to ensure that the outer rectangle remains constrained to translational motion. There are three possible cases as shown in Fig. 3.11:

Case 1: Frictionless point contacts are placed on the outside of the rectangle (Fig. 3.11(B)).

Case 2: Frictionless point contacts are placed on the inside of the rectangle (Fig. 3.11(C)).

Case 3: Frictionless point contacts are placed on both the inside and the outside of the rectangle (Fig. 3.11(D)).

For a prismatic joint, case 1 and case 3 are equivalent if it is assumed the lines forming the outer rectangle have some finite thickness.

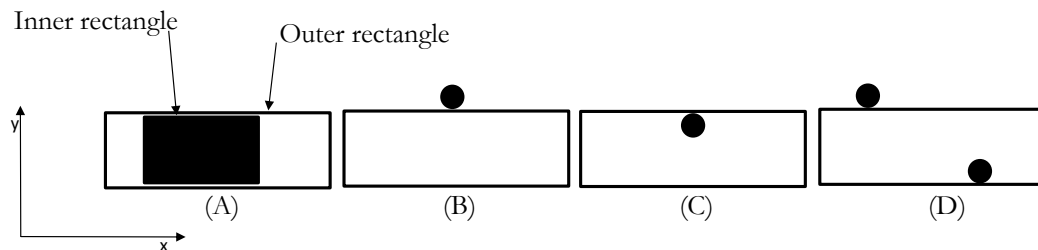


Figure 3.11: Different Cases for Prismatic Higher Variable Joints

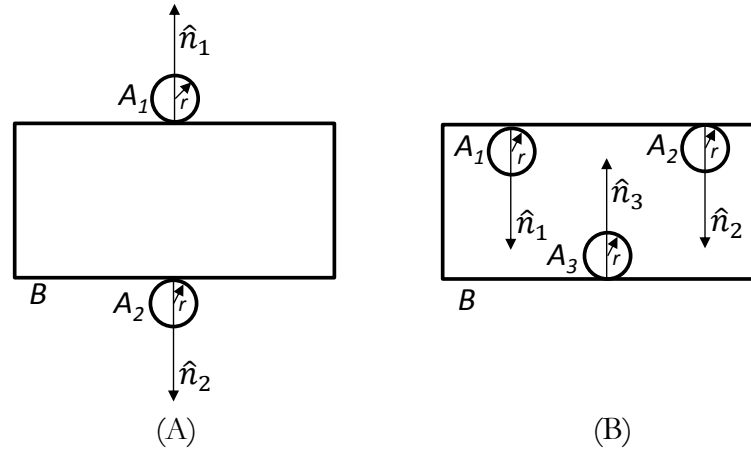


Figure 3.12: (A) Two Point Contacts are Needed for Translational Motion. (B) Three Point Contacts are Needed for Translational Motion.

3.3.1 Case 1: Type P_1 Higher Variable Joints

For Type P_1 higher variable joints, two constraint bodies are necessary to completely constrain a rectangular body, B , to translational motion. The contact normals of both constraint bodies must be aligned, and they must be in opposite directions. Type P_1 higher variable joints are shown in Fig. 3.11(A). The two constraint bodies, A_1 and A_2 make contact with body B . Figure 3.13 shows the three dimensional c-obstacles, CA_1 and CA_2 . The only available motion is translational motion along the X -axis.

Figure 3.14 shows a cross section of Fig. 3.13 at different values of θ .

Figures 3.13 (A) and (C) show that when $\theta = -10^\circ$ or $\theta = 10^\circ$ any possible motion from the origin causes body B to collide with either body A_1 or A_2 . This is due to the fact that the c-obstacles overlap, and there is no free path. However, Fig. 3.13(B) shows that when $\theta = 0^\circ$ the only possible motion is translational motion. The free space is a line along the X -axis. Figure 3.15 show a case in

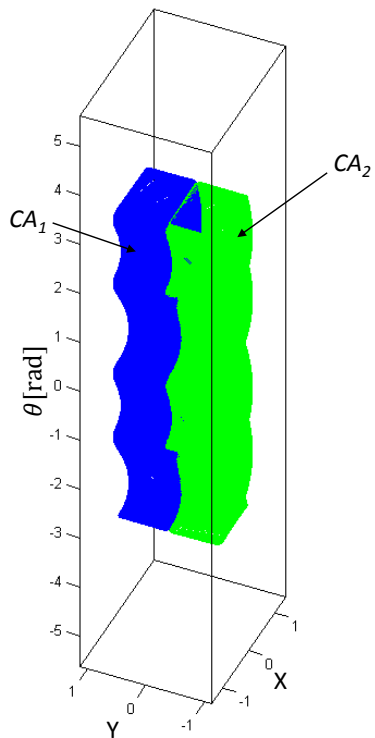


Figure 3.13: Only Translational Motion is Possible due to the C-obstacles

which the contact normals of the constraint bodies, A_1 and A_2 , are not aligned. In this situation, intuition reveals that body B should be able to rotate clockwise,

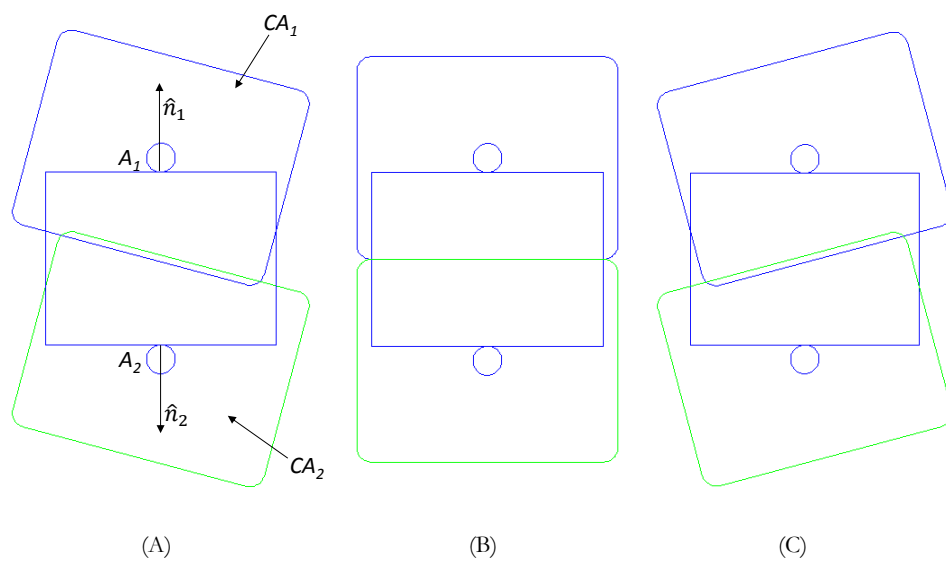


Figure 3.14: Cross Sections for: (A) $\theta = -10^\circ$. (B) $\theta = 0^\circ$ (C) $\theta = 10^\circ$

but counterclockwise rotation should be prevented. The cross section at $\theta = -10^\circ$ (Fig. 3.15) shows that because the c-obstacles do not overlap there is an available free path. However, Fig. 3.15(C) with $\theta = 10^\circ$ shows that if positive rotation is attempted the c-obstacles overlap and there is no available free path.

3.3.2 Case 2: Type P_2 Higher Variable Joints

For Type P_2 higher variable joints three constraint bodies are necessary to completely constrain a rectangular body, B , to translational motion. Type P_2 higher variable joints are shown in Fig. 3.11(B). The three constraint bodies, A_1 , A_2 , and A_3 make contact with body B . The contact normal for body A_3 must be between the contact normal for bodies A_1 and A_2 . Figure 3.16 shows the three dimensional configuration space for a Type P_2 higher variable joint. To analyze this plot it is best to examine different cross sections. Figure 3.17 shows the cross section of Fig. 3.16 when $\theta = -10^\circ$, $\theta = 0^\circ$, or $\theta = 10^\circ$. As shown in Figs. 3.17(A) and (C) there is no overlap in the possible free space (the

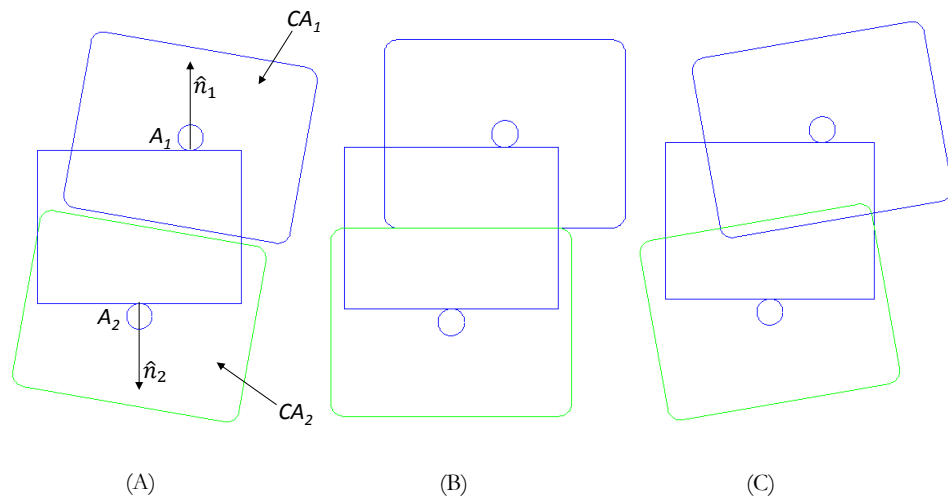


Figure 3.15: Cross Sections for: (A) $\theta = -10^\circ$. (B) $\theta = 0^\circ$ (C) $\theta = 10^\circ$

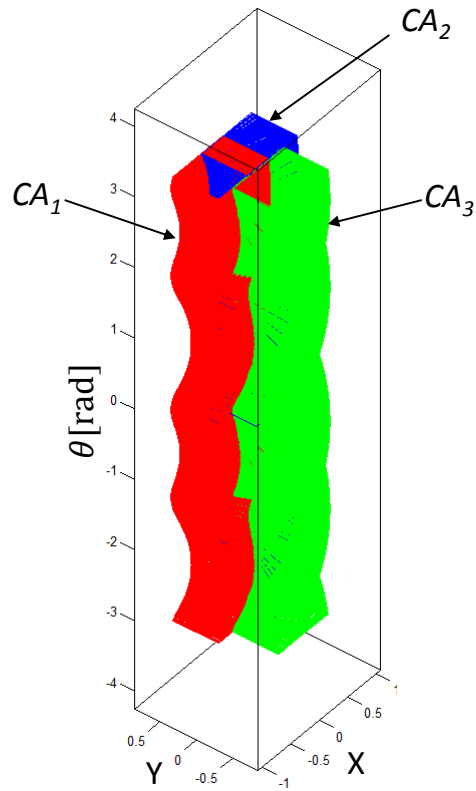


Figure 3.16: Only translational motion is possible due to the c-obstacles

c-obstacle's interior). The only possible free motion is a translational motion along the X -axis. Consider another situation in which the contact normals from constraint bodies A_2 and A_3 are aligned as shown in Fig. 3.18(A). In this situation

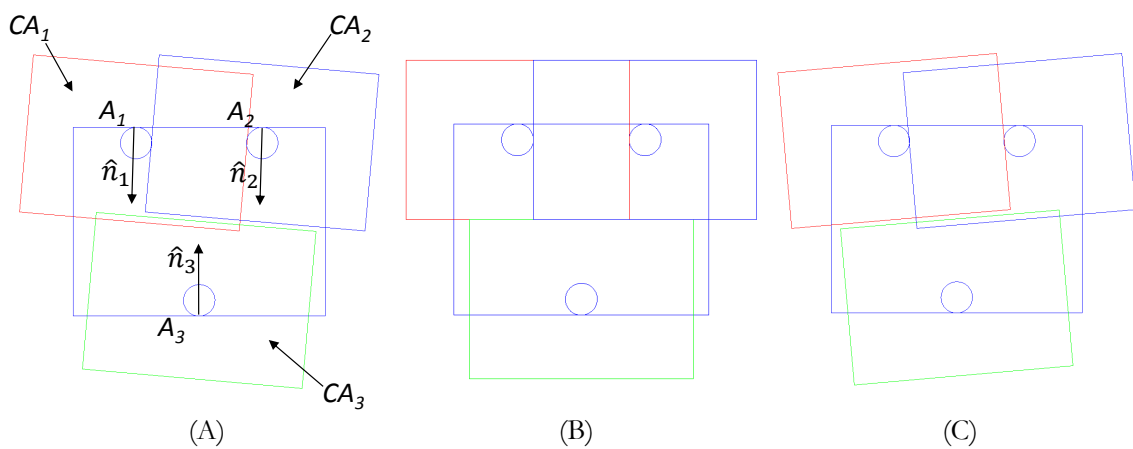


Figure 3.17: Cross Sections for: (A) $\theta = -10^\circ$. (B) $\theta = 0^\circ$ (C) $\theta = 10^\circ$

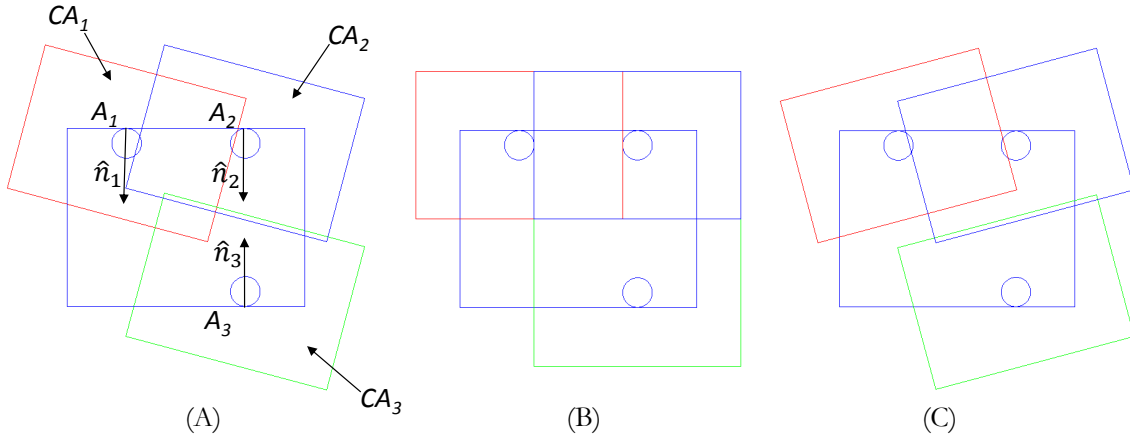


Figure 3.18: Cross Sections for: (A) $\theta = -15^\circ$. (B) $\theta = 0^\circ$ (C) $\theta = 15^\circ$

intuition dictates that body B can rotate clockwise, but counterclockwise rotation should be prevented. The results from this configurations space analysis agree with intuition. Figure 3.17(A) shows that at $\theta = -15^\circ$ there is an area of overlap of the c-obstacles interior which shows that there are available free motions. However, when body B is rotated counterclockwise (Fig. 3.18(C) there is no overlap in the c-obstacles, and therefore there are no available free motions.

3.3.3 Review of Type P_v Higher Variable Joints

In this section two types of P_v higher variable joints were presented. In each case, a different number of contact points were necessary to constrain body B to purely translational motion, depending on the location of the contact points. The two types of P_v higher variable joints are all kinematically equivalent to a lower pair prismatic joint, but each higher variable joint has a different physical implementation.

3.4 Summary

In this chapter it was shown that surface curvature of higher variable joints is important to achieve a particular joint motion. Higher variable joints will be used in Chapter 4 when performing the profile synthesis of variable joints that change from a specific rotational motion to a specific translational motion. These variable joints can then be used in reconfigurable mechanisms.

CHAPTER 4

Profile Synthesis of R_uP_v Variable Joints

This chapter presents a method that can be used for profile synthesis of planar, variable joints that change from a revolute pair to a prismatic pair. The method utilizes the minimum number of points necessary for the profiles of the two links. The method provides a nominal design for R_uP_v variable joints that can be modified based on the required application.

4.1 Profile Synthesis of an Example R_1P_1 Variable Joint

The goal of this section is to provide an example of the profile synthesis for a specific variable joint that changes from a rotational motion to a translational motion. Figure 4.1 shows an example R_1P_1 variable joint that was synthesized using the method from this chapter. The notation R_1P_1 means that a R_1 higher variable joint is combined with a P_1 higher variable joint to create a R_1P_1 variable joint.

The R_1P_1 variable joint is comprised of two links. Link 1 is assumed to be attached to ground, and link 2 is assumed to move relative to link 1. Link 1 is denoted by the solid lines, and link 2 is denoted by the dashed lines connected to five point contacts. Note that all of the dashed lines are rigidly attached. In Fig. 4.1 (A)-(C) link 2 rotates CCW relative to link 1. The three outer point

contacts make this a Type R_1 higher variable joint motion. In Fig. 4.1 (D) and (E) link 2 translates relative to link 1. The two outer point contacts required for translation make this a Type P_1 higher variable joint motion.

The resulting profiles of two links provide the desired rotational to translational motion. The profiles shown utilize the minimum number of point contacts necessary to generate the required rotational to translational motion for a R_1P_1 variable joint. After creating a R_uP_v variable joint it can be used in a reconfigurable mechanism for applications in which adaptability is required. Examples of this will be presented in Chapters 5 and 6.

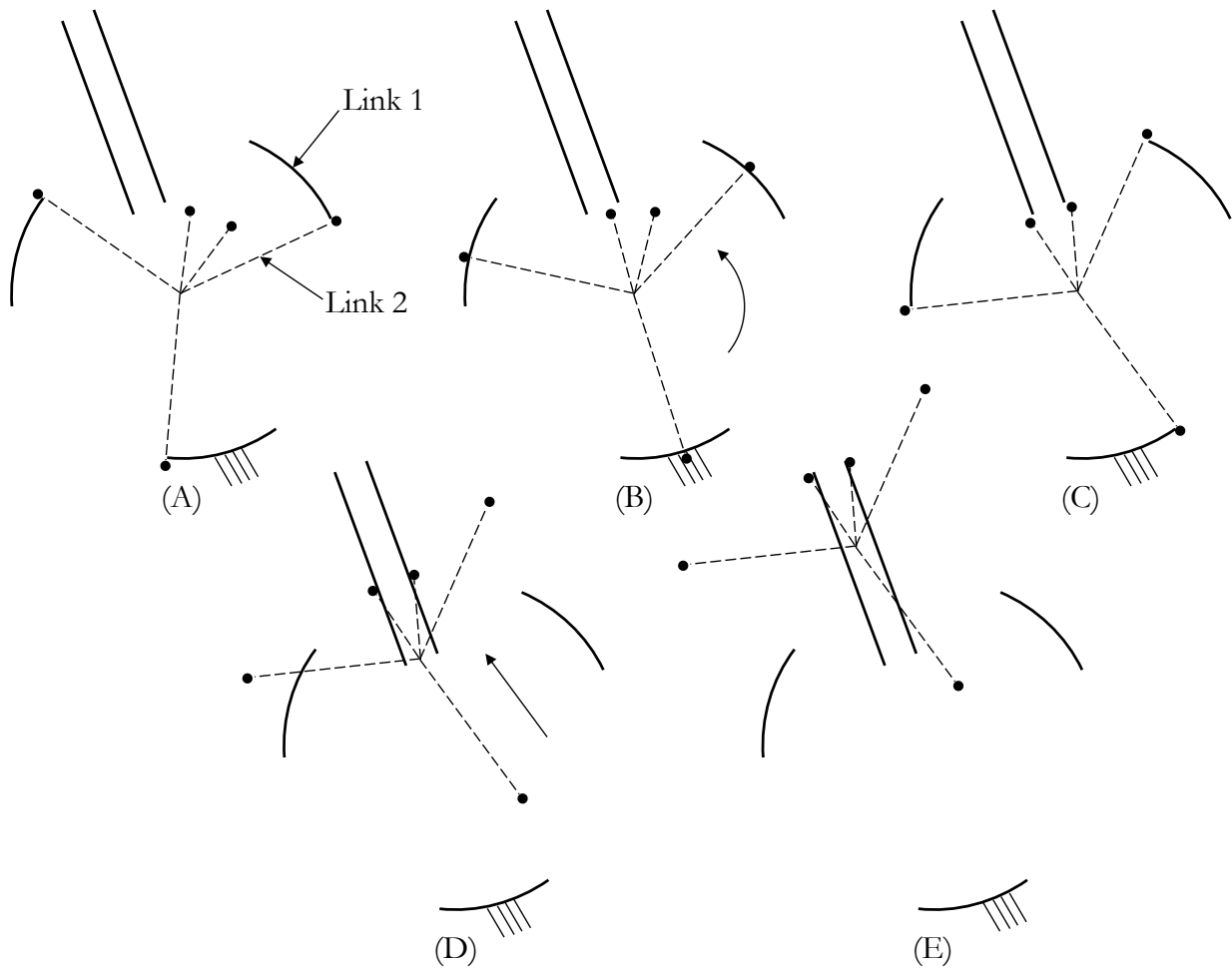
4.2 Enumeration of Rotational to Translational Variable Joints

Before presenting the equations for the specific profiles, it is important to enumerate all possible permutations of planar, higher variable joints that change from a rotational motion to a translational motion. These joints will be represented by generalized variable joints which are created by combining the different types of higher variable joints from Chapter 3. For instance, in creating a generalized R_uP_v variable joint there are three Type R_u higher variable joints and two Type P_v higher variable joints. This leads to six different R_uP_v variable joints as shown in Eq. 4.1:

$$R_1P_1 \quad R_1P_2 \tag{4.1}$$

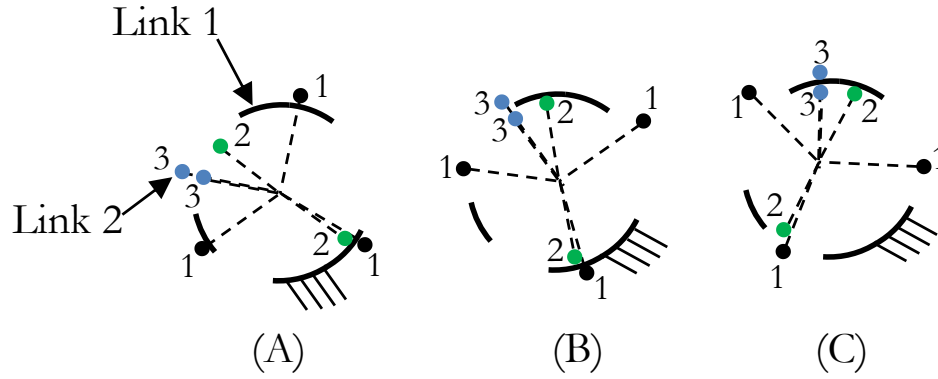
$$R_2P_1 \quad R_2P_2$$

$$R_3P_1 \quad R_3P_2$$

Figure 4.1: R_1P_1 Variable Joint

$R_uP_v^1$ variable joints are not the only generalized variable joints that provide rotational to translational motion. Table 4.1 shows that there are 60 permutations of generalized variable joints that allow for a change from a rotational motion to a translational motion. The six variable joints presented in Eq. 4.1 correspond to the first row of Tab. 4.1. Each of these geometric representations corresponds to identical joint motions; however, the profiles of each of the joints are distinctly different.

¹Note that R_uP_v variable joints are kinematically equivalent to P_vR_u variable joints.

Figure 4.2: $R_1R_2R_3$ Variable Joint

Even though there are 60 possible permutations available, many of them are not useful for practical applications. For instance, there are 24 generalized variable joints in Tab. 4.1 that contain an $R_uR_uR_u$ combination. An example of an $R_1R_2R_3$ variable joint is provided in Fig. 4.2. In Fig. 4.2(A) three contact points are used to constrain link 2 to rotational motion (Type R_1 higher variable joint). In Fig. 4.2(B) the contact points change, and two contact points are needed to constrain link 2 to rotational motion (Type R_2 higher variable joint). Finally, in Fig. 4.2(C) two contact points are used to constrain the system to rotational motion (Type R_3 higher variable joint). While the $R_1R_2R_3$ variable joint is a theoretically possible solution as shown, it would not be used in any practical design. The manufacturing of this type of joint would be difficult, and the joint

Table 4.1: General Variable Joint Permutations

Generalized Variable Joint	Number of Permutations
R_uP_v	6
$R_uP_vP_v$	6
$R_uR_uP_v$	12
$R_uR_uP_vP_v$	12
$R_uR_uR_uP_v$	12
$R_uR_uR_uP_vP_v$	12

would be overly complicated for its intended purpose. The other generalized variable joints also have similar practical issues, and therefore R_uP_v generalized variable joints will be the focus of this work.

4.3 Design Configuration Space of Variable Joints

Each of the profiles of the six R_uP_v variable joints must be created by specifying the desired joint motion in some manner. Typically, the joint design requirements will start in written form, but it is helpful to have a more formal mathematical formulation. In this dissertation, configuration space will be used to specify the design parameters. The “design configuration space” is a way to generalize the joint motion, and it represents the movement of link 2 relative to link 1. The joint design requirements could be specified in a tabular or some other form, but configuration space ensures joint motions are not missed, and the design configuration space representation can be expanded to spatial joints as well.

Configuration space has been widely studied in terms of robot motion planning [41], and it can be thought of as the space of possible poses that a physical system may attain. A planar configuration space representation requires three configuration variables $(x, y, \theta)^\top$. Both x and y have units of length, and $-180^\circ < \theta < 180^\circ$. By its definition, this is the same configuration space as was used in Chapter 3. However, the design configuration space in this chapter is used for a different purpose than the configuration space from Chapter 3.

The configuration space for an example R_uP_v joint is shown in Fig. 4.3. This can be manifested physically in the R_1P_1 variable joint in Fig. 4.1, but there

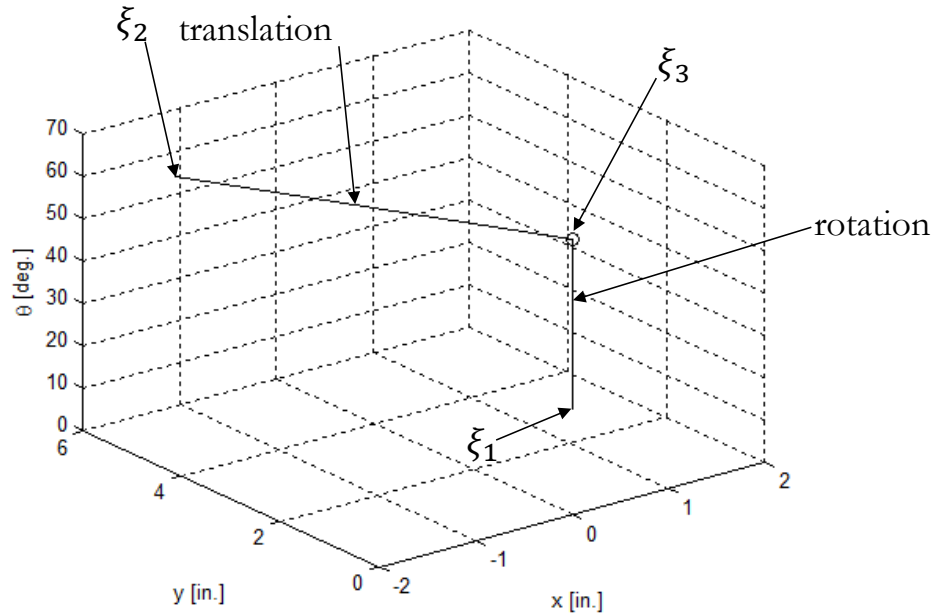


Figure 4.3: Configuration Space for a $R_u P_v$ Variable Joint

are five other $R_u P_v$ designs that would provide the same kinematic motion. The vertical line represents the rotational motion of the moving link relative to the fixed link, and the line in a plane parallel to the XY -plane represents translational motion. The circle in Fig. 4.3 represents the transition between rotational motion and translational motion. For a $R_u P_v$ variable joint, there are specific constraints on the configuration space as shown:

1. There must be exactly one vertical line and exactly one horizontal line.
2. The vertical line and the horizontal line must meet at a point.
3. The point of intersection between the two lines must be at either end of the vertical line.

Each of the points in the configuration space corresponds to a different configuration of a joint. For example, point ξ_1 in Fig. 4.3 corresponds to the initial configuration for the $R_1 P_1$ variable joint in Fig. 4.1(A). Similarly, ξ_3 and ξ_2

correspond to Fig. 4.1(C) and Fig. 4.1(E), respectively. Properly specifying the joint motion is an important part of determining the joint profiles.

4.4 Profile Synthesis Equations for R_uP_v Variable Joints

Once the design requirements have been expressed in the design configuration space, it is possible to automatically determine the profiles for the R_uP_v variable joints. The profile for link 1 can be generated by determining equations for the constraint arcs required for rotational motion as well as the lines required for translational motion. The profile for link 2 is specified by the minimum number of points that need to be rigidly attached to generate the required rotational or translational motion. The profiles for all six R_uP_v variable joints can be represented by general equations, and each of the R_uP_v variable joint profiles can be synthesized by changing parameters in the general equations.

4.4.1 Assumptions

In determining the general profiles for both link 1 and link 2 the following assumptions are made:

1. The constraint points for both the rotational and translational motion are in the same plane.
2. All bodies are rigid.
3. The system dynamics are ignored.
4. Tolerances and machining errors are ignored².
5. The design configuration space is known based on the design requirements.

²Tolerances are ignored because there has been much work done by Sacks et al. [38] on the tolerance analysis of higher pairs. The focus of this work is purely on the kinematic analysis.

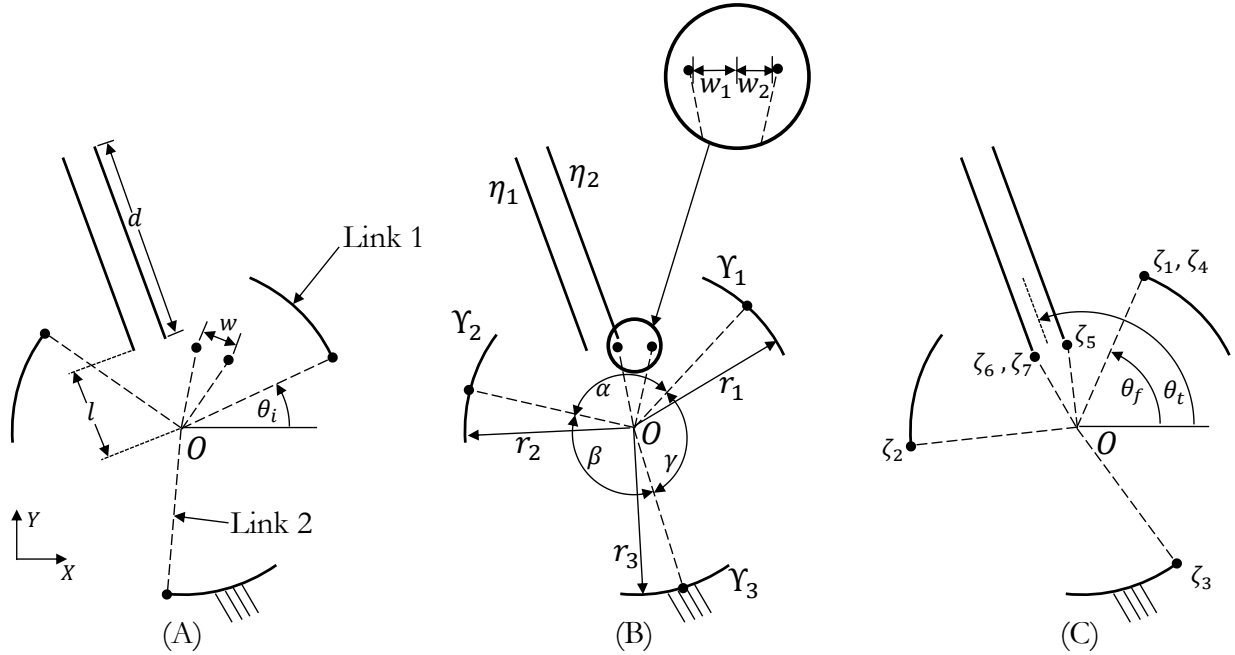


Figure 4.4: General Joint Profile

The assumptions were chosen so that the majority of this work will focus on the kinematics of the joints. The kinematics are fundamental to understanding issues associated with dynamics and tolerances. This is not within the scope of this work.

4.4.2 Profile of Link 1

From the design configuration space, it is possible to extract all the information necessary to perform the profile synthesis of R_uP_v variable joints. The variables in the equations are separated into the design configuration space inputs, joint design parameters, and the outputs as shown below:

design configuration space inputs: ξ_1, ξ_2, ξ_3

joint design parameters: $l, w_j, r_n, \alpha, \beta, \gamma, \delta_k, \delta_{po}, \theta_R$

outputs: $\Upsilon_n, \eta_j, \zeta_k$

The design configuration space inputs have already been defined in Section 4.3.

The joint design parameters and the outputs will be defined throughout the derivation.

Link 1 is assumed fixed to ground, and it is defined by the three constraint arcs required for rotational motion, and the two line segments required for translational motion. The arcs required for rotational motion are given by Υ_n , and the lines required for translational motion are given by η_j , where $n = 1, 2, 3$ and $j = 1, 2$ as shown in Fig. 4.4(B). In order to determine Υ_n and η_j it is helpful to determine θ_i , θ_f , θ_t , and d , where θ_i is the initial angle of rotation of link 2, θ_f is the final angle of rotation of link 2, θ_t is the angle of translation of link 2, and d is the distance of translation. The design configuration space inputs are used to determine θ_i , θ_f , θ_t , and d in Eq. 4.2

$$\theta_i = \xi_{1z} \quad (4.2)$$

$$\theta_f = \xi_{3z}$$

$$\theta_t = \text{atan2}(\xi_{2y}, \xi_{2x})$$

$$d = \sqrt{(\xi_{2x} - \xi_{1x})^2 + (\xi_{2y} - \xi_{1y})^2}.$$

The three arcs in a general R_uP_v variable joint are separated by the angles α , β , and γ . These angles change based on the potential joint design, and they will be referred to as the separation angles. The general R_uP_v variable joint must include all three arcs because a R_1 higher variable joint requires all three. The outer boundaries, Υ_n , are then given as

$$\Upsilon_n = (r_n \cos \theta_n, r_n \sin \theta_n) \mid \phi_{ni} \leq \theta_n \leq \phi_{nf} \quad (\theta_i > \theta_f) \quad (4.3)$$

$$\phi_{ni} \geq \theta_n \geq \phi_{nf} \quad (\theta_i < \theta_f)$$

where

$$\phi_{ni} = \phi_n + \theta_i \quad (4.4)$$

$$\phi_{nf} = \phi_n + \theta_f$$

and

$$\phi_1 = \theta_R \quad (4.5)$$

$$\phi_2 = \phi_1 + \alpha$$

$$\phi_3 = \phi_2 + \beta,$$

r_n is the radius of each of the arcs, and i and f correspond to the initial and final states. θ_R provides an added amount of rotation to Υ_n .

The lines required for translational motion, η_j , are given in Eq. 4.6 as

$$\eta_1 = (-w_1 \sin \theta_t + (l + d_1) \cos \theta_t, w_1 \cos \theta_t + (l + d_1) \sin \theta_t) \mid 0 \leq d_1 \leq d \quad (4.6)$$

$$\eta_2 = (w_2 \sin \theta_t + (l + d_2) \cos \theta_t, -w_2 \cos \theta_t + (l + d_2) \sin \theta_t) \mid 0 \leq d_2 \leq d,$$

where w_j is the width of the sliding track and l is the distance the track is offset from the origin in the radial direction. The profile for link 1 has now been fully defined by Υ_n and η_j .

4.4.3 Profile of Link 2

The general profile of link 1 consists of the three arcs for the rotational constraint and the two lines for translational constraint. The general profile of

link 2 consists of a set of contact points that are rigidly connected.³ These points constrain the motion of link 2 to be either rotational motion or translational motion relative to link 1. The profile of link 2 is defined by the points ζ_k , where $k = 1$ to 7 as shown in Fig. 4.4 (C). Even though there are seven ζ_k points in the general joint profile, only some of these points will be used at a time. The number of points that are used depends on which type of R_uP_v variable joint is being synthesized. All values of ζ_k will be defined based on the transition configuration between rotational and translational motion. The values of ζ_k are expressed in Eq. 4.7 as

$$\zeta_n = ((r_n + \delta_n) \cos \phi_{nf}, (r_n + \delta_n) \sin \phi_{nf}) \quad (n = 1 \text{ to } 3) \quad (4.7)$$

$$\zeta_4 = ((r_n + \delta_4) \cos \phi_{1f}, (r_n + \delta_4) \sin \phi_{1f})$$

$$\zeta_5 = ((w_2 + \delta_5) \sin \theta_t + (l + \delta_{5o}) \cos \theta_t, -(w_2 + \delta_5) \cos \theta_t + (l + \delta_{5o}) \sin \theta_t)$$

$$\zeta_6 = (-(w_1 + \delta_6) \sin \theta_t + l \cos \theta_t, (w_1 + \delta_6) \cos \theta_t + l \sin \theta_t)$$

$$\zeta_7 = (-(w_1 + \delta_7) \sin \theta_t + (l + \delta_{7o}) \cos \theta_t, (w_2 + \delta_7) \cos \theta_t + (l + \delta_{7o}) \sin \theta_t)$$

The δ_k and δ_{po} ($p = 5$ or 7) values can be considered a small distance. For example, Fig. 4.5 shows a change of δ_1 in the radial direction for a R_1 higher variable joint. Changing the values of δ_k and δ_{po} allow for a change between the different types of R_uP_v variable joints. For example, moving δ_1 in the positive radial direction allows for a R_1 higher variable joint, but moving δ_1 in the negative radial direction allows for a R_2 variable joint.

³The profile of link 2 is considered to be a set of points as opposed to the lines and arcs that define link 1. It should also be noted that the points are rigidly connected to form the joint profile.

4.4.4 Constraints for R_uP_v Variable Joints

The two joint profiles for a general R_uP_v variable joint are fully specified using Eqs. 4.3, 4.6, and 4.7 which correspond to Υ_n , η_j , and ζ_k . The six different R_uP_v variable joints can be created by placing constraints on different values in the equations. Table 4.2 shows how different parameters change based on the desired R_uP_v variable joint. Example R_uP_v variable joints are shown for a specific design in Fig. 4.6.

Consider the R_1P_1 variable joint in Fig. 4.6 which corresponds to the first row in Tab. 4.2. For this variable joint α , β , and γ must all be less than 180° due to the R_1 constraint as was derived in Chapter 3. All three outer boundaries are used, and therefore Υ_2^4 and Υ_3 have a “1” to indicate that those arcs are needed for the rotational constraint. The values of δ_1 , δ_2 , and δ_3 all have a small positive distance, and are denoted with a “+” in Tab. 4.2. This ensures that ζ_1 , ζ_2 , and ζ_3 are all moved outwardly in the radial direction. δ_4 is not needed for a R_1 higher

⁴ Υ_1 is not placed in the table because it is used for every joint

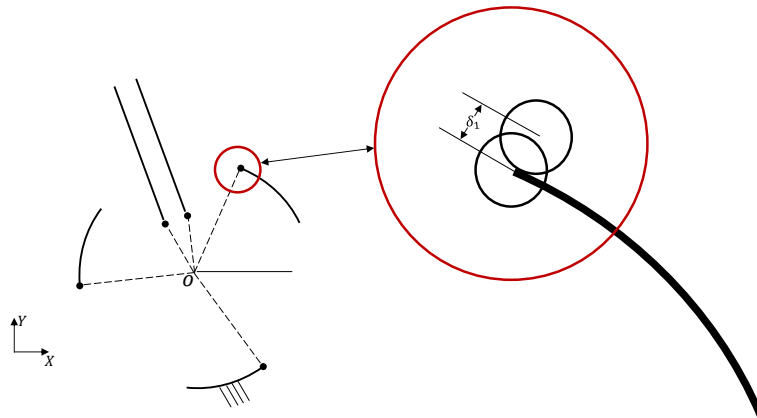


Figure 4.5: A Change of δ_1 in the Radial Direction

Table 4.2: Constraints for R_uP_v Variable Joints

Variable Joint	α	β	γ	Υ_2	Υ_3	δ_1	δ_2	δ_3	δ_4	δ_5	δ_{5o}	δ_6	δ_7	δ_{7o}
R_1P_1	$< 180^\circ$	$< 180^\circ$	$< 180^\circ$	1	1	+	+	+	\emptyset	+	0	+	\emptyset	\emptyset
R_2P_1	180°	180°	\emptyset	1	\emptyset	-	-	\emptyset	\emptyset	+	0	+	\emptyset	\emptyset
R_3P_1	\emptyset	\emptyset	\emptyset	\emptyset	\emptyset	+	\emptyset	\emptyset	-	+	0	+	\emptyset	\emptyset
R_1P_2	$< 180^\circ$	$< 180^\circ$	$< 180^\circ$	1	1	+	+	+	\emptyset	-	-	-	-	-
R_2P_2	180°	180°	\emptyset	1	\emptyset	-	-	\emptyset	\emptyset	-	-	-	-	-
R_3P_2	\emptyset	\emptyset	\emptyset	\emptyset	\emptyset	+	\emptyset	\emptyset	-	-	-	-	-	-

variable joint, and therefore it is denoted by \emptyset . Both δ_5 and δ_6 are given a positive value in order to apply the appropriate translational constraint for a P_1 higher variable joint. This will ensure that ζ_5 and ζ_6 are moved outward for a P_1 higher variable joint. δ_{5o} is 0 because ζ_5 and ζ_6 must be aligned. δ_7 and δ_{7o} are only used for P_2 higher variable (as shown in Fig. 4.6) joints and so both of these have a value of \emptyset .

Table 4.2 provides the constraints for all six R_uP_v variable joints.

Substituting these values into Eqs. 4.3, 4.6, and 4.7 yields the profiles of R_uP_v variable joints as shown in Fig. 4.6. The equations presented provide the minimum number of points necessary to create the two link profiles. A designer can then use these points as a nominal design for a joint that changes from a rotational motion to a translational motion.

4.5 Adjustable Plier Designs Based on R_uP_v Variable Joints

As an example of the theory presented in Section 4.4, consider the design of adjustable pliers that are commonly used to grip irregularly shaped objects. The adjustable pliers will be made of two links, one moving relative to another. This tool can be thought of as a variable joint because the motion of one link relative to

another requires both translational motion and rotational motion. It will be shown in this section how these designs can be generated in a systematic manner by using the method developed in Section 4.4.

The design requirements must first be determined. Figure 4.7 provides the design configuration space for standard adjustable pliers. Adjustable pliers must be able to rotate between 0° and 90° to provide different clamping configurations. Additionally, the pliers must be able to slide to accommodate different sized objects. The proposed design configuration space is shown in Fig. 4.7. The vertical lines in the design configuration space correspond to the rotation of one link

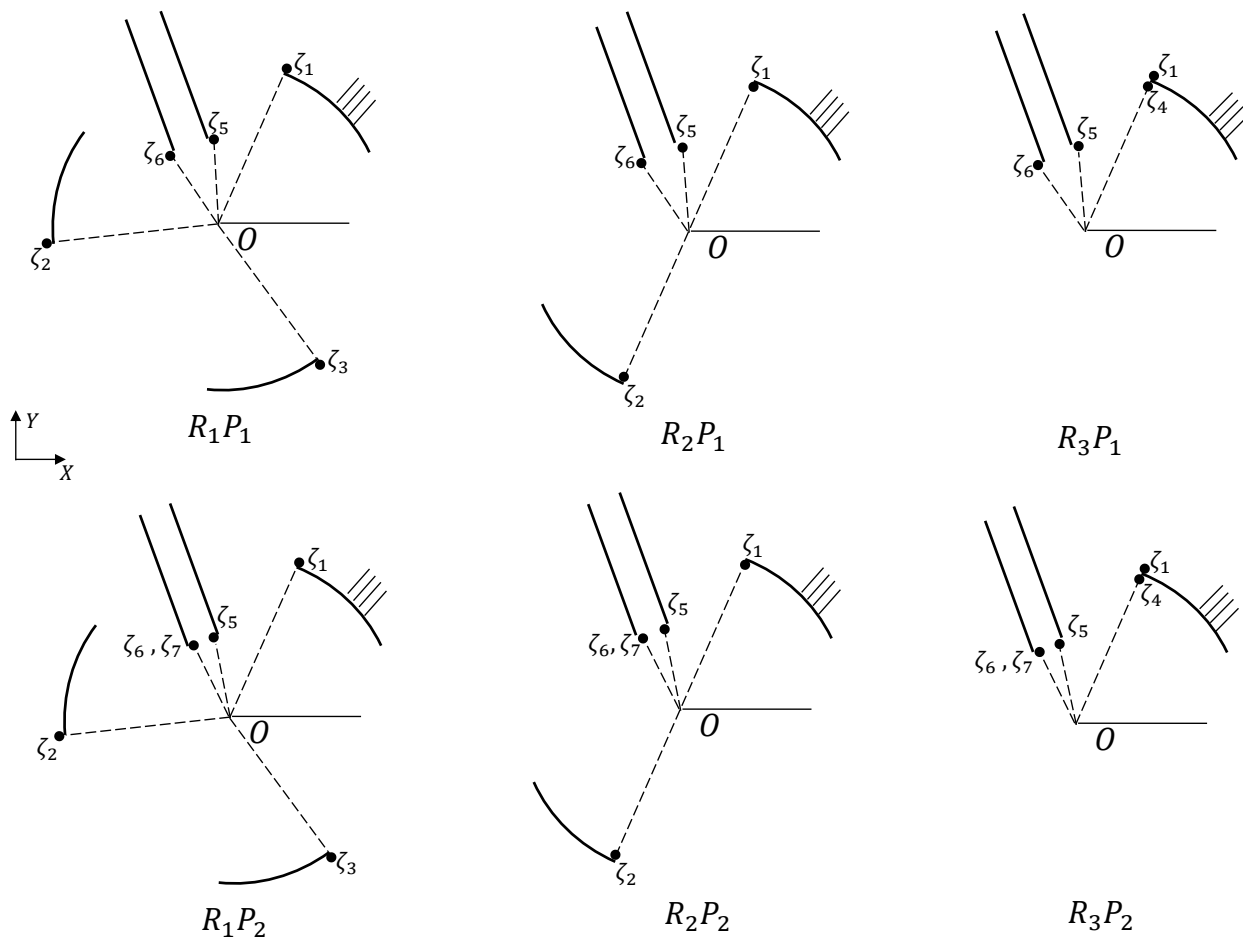


Figure 4.6: The R_uP_v Variable Joints

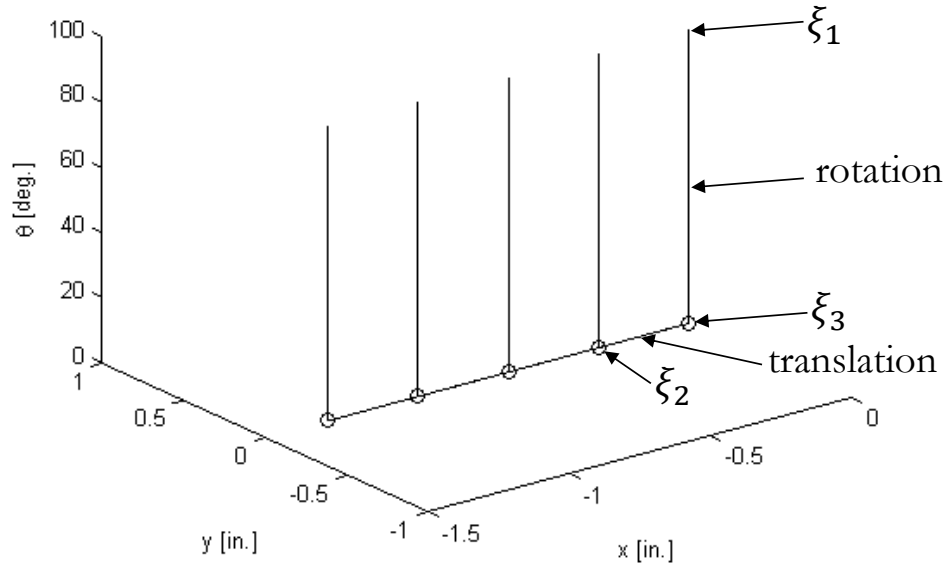


Figure 4.7: Design Configuration Space Representation of Adjustable Pliers.

relative to another, and the horizontal lines correspond to translation of one link relative to another.

Link 1 of the pliers begins at a position of $\xi_1 = (0, 0, 90)^\top$ relative to Link 2. This link then rotates from 90° to 0° to position ξ_3 . Finally, link 1 translates relative to link 2 to position ξ_2 . This process is repeated four more times to create different clamping configurations. Thus, the configuration space representation for the adjustable pliers can be thought of as multiple $R_u P_v$ variable joints connected in series.

4.5.1 Example $R_1 P_2$ Variable Joint for Adjustable Pliers

A $R_1 P_2$ variable joint is perhaps the most complicated type of $R_u P_v$ variable joint because three constraint arcs ($\Upsilon_1, \Upsilon_2, \Upsilon_3$) are needed to perform the rotational motion. It is this complicated design that will be explained with the theory. In designing a $R_1 P_2$ variable joint (or any $R_u P_v$ variable joint) ξ_1, ξ_2 , and

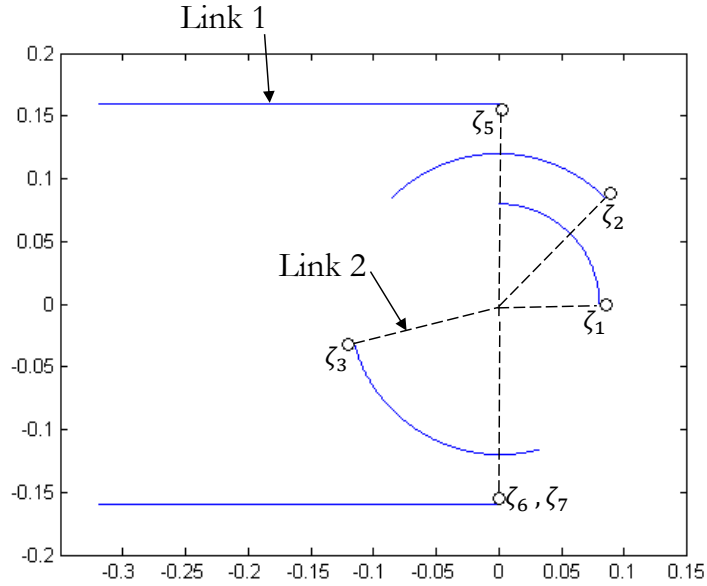


Figure 4.8: The R_1P_2 Variable Joint for Adjustable Pliers

ξ_3 must first be determined from the design configuration space. From Fig. 4.7, ξ_1 , ξ_2 , and ξ_3 are given in Eq. 4.8 as

$$\xi_1 = (0, 0, 90^\circ)^\top \quad (4.8)$$

$$\xi_2 = (-.32 \text{ in.}, 0, 0)^\top$$

$$\xi_3 = (0, 0, 0)^\top.$$

The resulting R_1P_2 variable joint is shown in Fig. 4.8. This joint was created by using Equations 4.3 through 4.7 presented in Section 4.4. To better visualize how link 2 moves relative to link 1, Fig. 4.9 shows link 2 in five different configurations. Link 2 starts at its initial configuration as shown in Fig. 4.9(A) and rotates 90° counterclockwise to configuration (C). Link 2 then translates from configuration (C) to configuration (E). Notice that each of these configurations corresponds to a point in the configuration space as shown in Fig. 4.10.

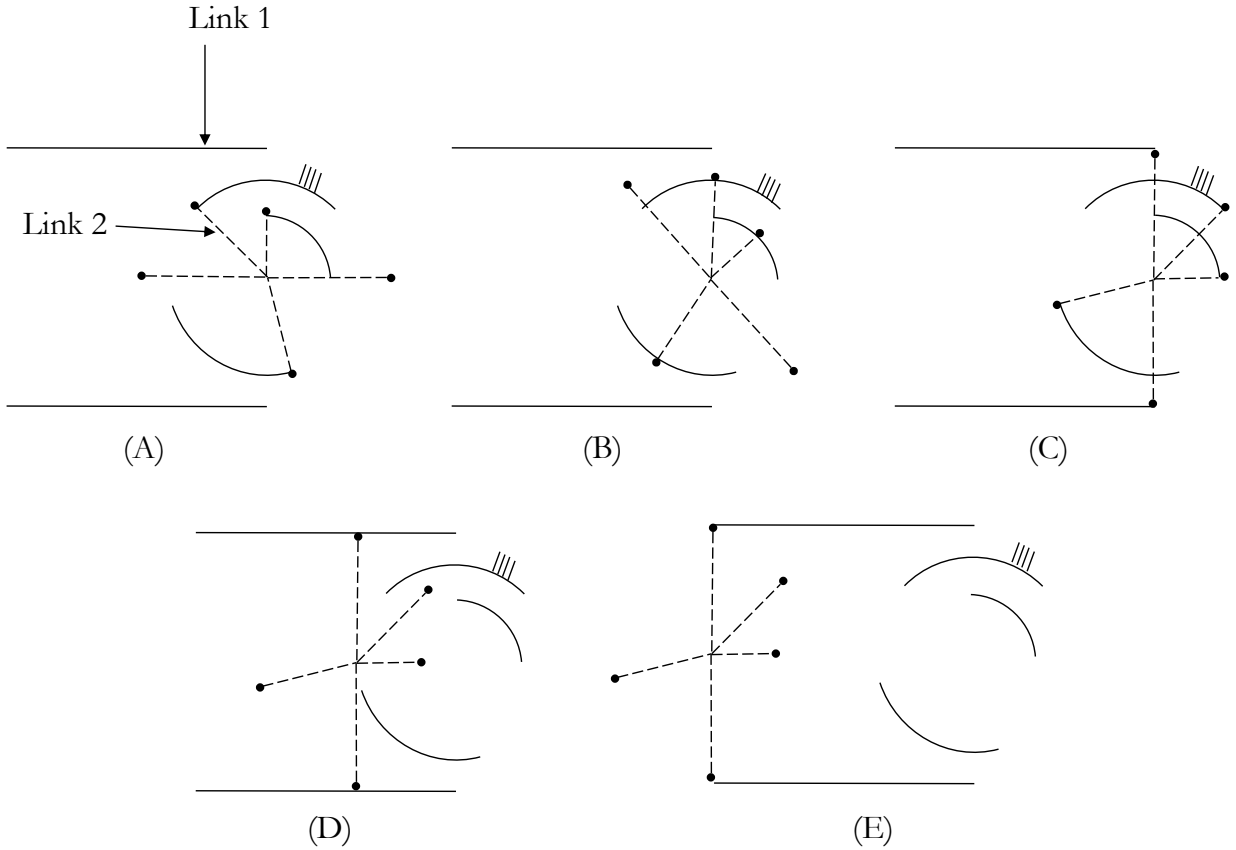


Figure 4.9: Different configurations of the R_1P_2 variable joint

The joint design parameters were chosen carefully to ensure that the joint performs the required kinematic function. The values for this joint design parameters are given in Tab. 4.3. All values have units of inches unless otherwise indicated. The value of l was chosen to be 0 in. so that the center of link 2 remains in the same xy position throughout the 90° rotation. The w_j values were chosen to be identical to ensure symmetry about the x -axis for the translational constraint. Additionally, these values were chosen to be greater than the r_n values; doing so

Table 4.3: Joint Design Parameters for a R_1P_2 Variable Joint

Joint Design Parameter	l	w_1	w_2	r_1	r_2	r_3	α	β	γ	δ_k	δ_{po}	θ_R
Value	0	0.16	0.16	0.08	0.12	0.12	45°	150°	165°	δ	δ	0

allows the rotational constraint points to be contained within the translational constraint points. This will be important when connecting this joint in series.

Both the values of r_2 and r_3 are identical, but r_1 was chosen to be smaller than r_2 and r_3 to ensure that during the translational motion ζ_2 does not make contact with Υ_1 . The separation angles, α , β , and γ were carefully chosen to ensure that when link 2 begins to slide there is no interference between the ζ_k rotational constraint points and the Υ_n boundaries. For instance, by choosing $\alpha = 45^\circ$ point ζ_2 is able to translate without interfering with Υ_2 . Finally, all of the δ_k and δ_{po} values were chosen to be a small finite distance denoted by δ .

After completing the R_1P_2 variable joint design, this variable joint can be connected in series to create the joint profile for the adjustable pliers. The final design is shown in Fig. 4.11(A) and Fig. 4.11(B). Figure 4.11(A) shows link 2 in its design position. The R_1P_2 joint is repeated four times which corresponds to the

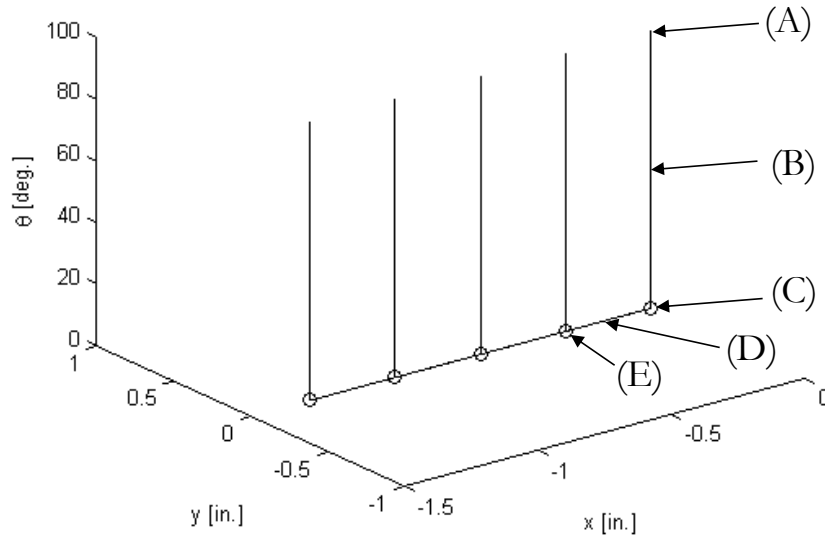


Figure 4.10: Design Configuration Space Representation of Adjustable Pliers.

configuration space shown in Fig. 4.10. Figure 4.11(B) shows link 2 as it moves through configurations C_1 through C_6 . This allows the pliers to move through different clamping configurations.

The next step in the R_uP_v variable joint design process is to add kinematic redundancies for a more practical solution. This step will not be completed for this example because the joint design has many drawbacks such as the complicated profile of link 1 as well as different r_n values. An example of adding kinematic redundancies to an R_uP_v variable joint will be shown in Section 4.5.3.

4.5.2 Alternative Solution

The design from Section 4.5.1 is one of an infinite number of design possibilities that can be generated using the method presented in Section 4.4. Consider an alternative solution for a R_3P_2 variable joint. The joint design parameters are shown in Tab. 4.4, and the resulting joint profile is given in

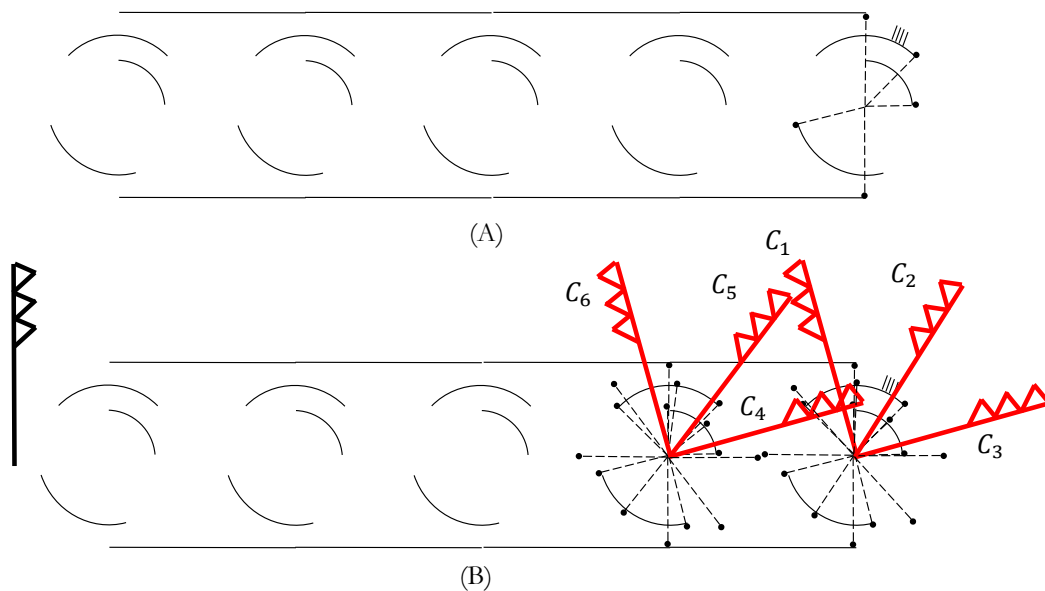


Figure 4.11: R_1P_2 Adjustable Plier Design

Table 4.4: Joint Design Parameters for a R_1P_2 Variable Joint

Joint Design Parameter	l	w_1	w_2	r_1	δ_k	δ_{po}	θ_R
Value	-0.32	0.005	0.005	0.32	δ	δ	0

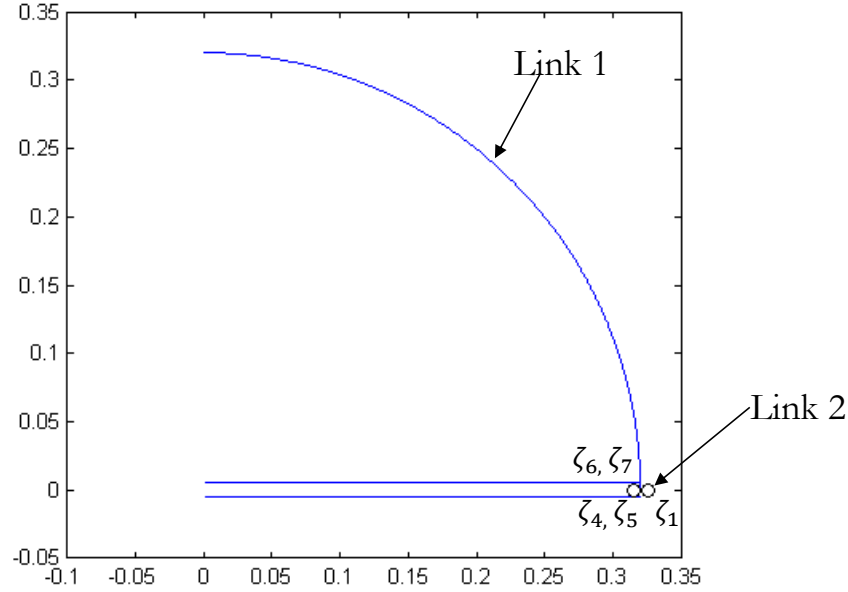
Figure 4.12: R_3P_2 Variable Joint

Fig. 4.12. The value of r_1 was chosen such that the radius equals the sliding distance, d . The value of l was chosen as -0.32 in. so that the translational constraint points are essentially coincident with the rotational constraint point, ζ_4 . The variable joint shown in Fig. 4.12 can then be attached together in series to produce the final design of the adjustable pliers as shown in Fig. 4.13

4.5.3 Kinematic Redundancies

The profile for the adjustable pliers in Fig. 4.13(A) provides the minimal number of point contacts necessary for the required joint motion. This is meant to be a nominal design that is used as the base for a more practical solution.

However, as part of the method presented in this chapter, kinematic redundancies

can be added for a more practical solution.

Figure 4.13(B) provides a R_3P_2 adjustable plier design based off of the joint design parameters from Tab. 4.4. The design shows the two links of the pliers as link 2 moves from configuration C_1 to configuration C_6 . Kinematic redundancies have been added to improve functionality of the joint. For instance, mechanical stops have been added to the design to prevent unwanted translational or rotational motion. As an example, in configuration C_3 a mechanical stop has been put in place to prevent unwanted translation in the x -direction.

Another kinematic redundancy is that the point contacts of ζ_1 and ζ_4 have been changed to surface contacts. The surface contacts occur during both the rotational motion and the translational motion. The surface contacts allow for a more stable design, and the device is able to handle larger loads.

Care must be taken when changing any point contacts to surface contacts. In this example, when ζ_1 and ζ_4 were changed to surface contacts, part of the profile of link 1 had to be removed to account for the expansion of ζ_1 and ζ_4 from a point contact to a surface contact. For instance, in configuration C_3 link 2 must be able to translate. Therefore, a section of link 1 was removed. The section that is removed was critical for the joint design shown in Fig. 4.13(A). However, due to the change from point contacts to surface contacts, the joint is able to maintain the rotational constraint at the desired configuration. A similar approach was taken for the translational part of the motion.

Other kinematic redundancies can be added to ensure that the links do not move relative to one another along the z -axis. The kinematic redundancies are just

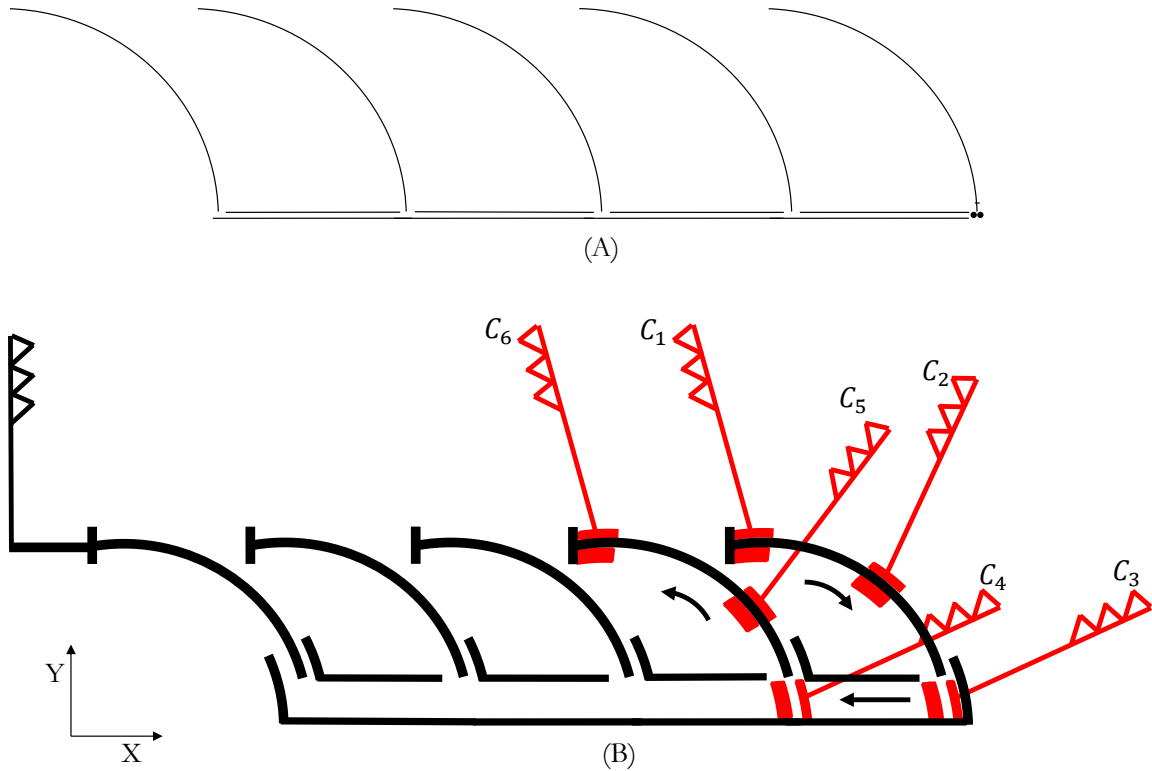


Figure 4.13: R_3P_2 Adjustable Plier Design

some of the redundancies that would need to be added to create a practical design. However, it is shown in this section how understanding the joint profiles allows one to choose kinematic redundancies appropriately.

4.5.4 Summary of Adjustable Plier Designs

In this section it was shown how different adjustable plier designs can be created based off of the required design configuration space. Both a R_3P_2 and a R_1P_2 variable joint were created using the method from Section 4.4. Any other R_uP_v joint could be synthesized. The synthesized profiles are used as a nominal joint design that can be modified for practical purposes. Each of R_uP_v variable joints has the same kinematic motion but different joint profiles. The R_uP_v

variable joint can be connected in series to form a new design for adjustable pliers. Figure 4.14 provides a comparison between the two adjustable plier designs presented in this chapter (Fig. 4.14(A) and Fig. 4.14(B)) as well as an adjustable plier design based on a R_2P_2 variable joint (Fig. 4.14(C)). Notice that all three of the adjustable plier profiles are distinctly different, but they all provide the required kinematic motion. For instance, a comparison of the translational distance, d , shows that the translational distance is equal for all three joint designs. It is interesting to note that adjustable plier designs are commercially available that are based on both an R_2 higher variable joint and an R_1 higher variable joint as shown in Figs. 4.15 and 4.16. These adjustable pliers do not impose translational constraints, and therefore a P_v variable joint is not utilized for these designs.

4.6 Constraints on the Direction of Translation

During the design of the adjustable pliers, there were certain directions of translation that were not possible. Depending on the joint design parameters, not all directions of translation are possible for all R_uP_v variable joints. Constraints exist on the direction of translation due to the Υ_n constraint arcs. The two types of constraints are denoted as external arc interference and internal arc interference.

4.6.1 External Arc Interference

External arc interference occurs when ζ_k ($k = 1$ to 4) interferes with either of the two arcs it does not make contact with during the initial rotation. For instance, during external arc interference, ζ_1 could potentially make contact with

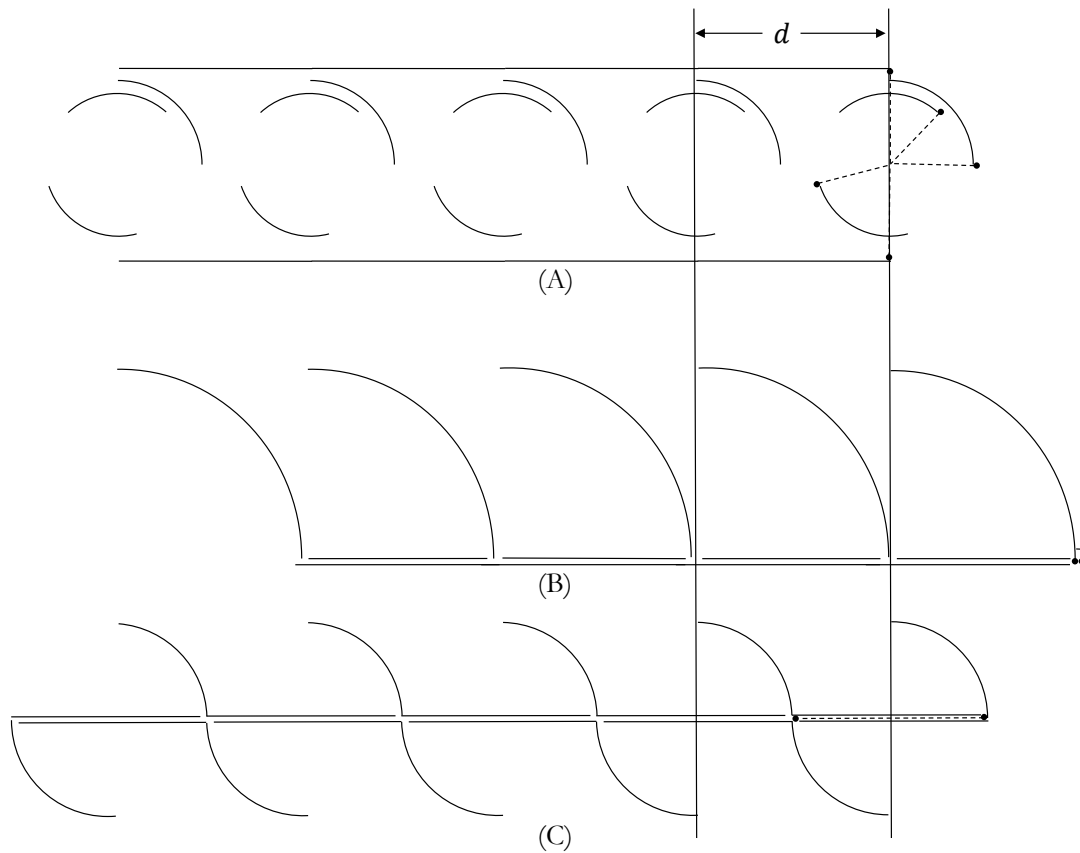


Figure 4.14: Adjustable Plier Designs

either Υ_2 or Υ_3 as shown in Fig. 4.17. Link 2 begins at the position shown in Fig. 4.17(A) and slides through to the position shown in Fig. 4.17(C). In



Figure 4.15: Knipex R_2 adjustable plier design

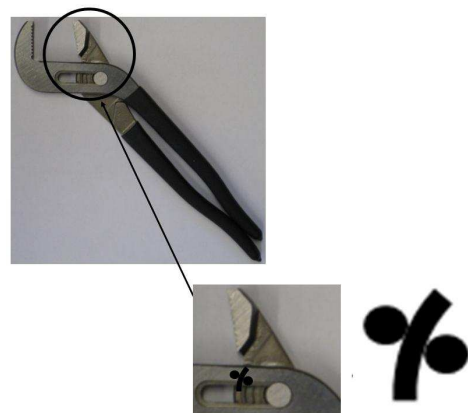


Figure 4.16: Craftsman R_1 adjustable plier design

Fig. 4.17(C) ζ_1 makes unwanted contact with Υ_2 . External arc interference must be determined during the joint design process to avoid this unwanted contact.

Figure 4.18 shows a graphical representation of how the external arc interference regions can be calculated. A unit vector can be formed between point λ_1 and λ_2 and points λ_1 and λ_3 . The direction of translation, θ_t , must lie outside the region formed by the unit vectors $\vec{U}_{\lambda_1\lambda_2}$ and $\vec{U}_{\lambda_1\lambda_3}$. This region is indicated by the red arc in Fig. 4.18. Repeating this process for ζ_1 , ζ_2 , and ζ_3 results in six different regions in which external arc interference occurs. This is shown in Fig. 4.19. Care must be taken to ensure that external arc interference does not occur during the joint design process. These constraints can easily be added to the requirements of Section 4.4.

4.6.2 Internal Arc Interference

Internal arc interference occurs when ζ_k interferes with Υ_n . For example, ζ_1 may interfere with Υ_1 as shown in Fig. 4.20. It is assumed that link 2 can move in the tangent direction of Υ_n or in the direction of the unit vector that connects the initial angle of rotation to the final angle of rotation. Figure 4.21 shows all of the

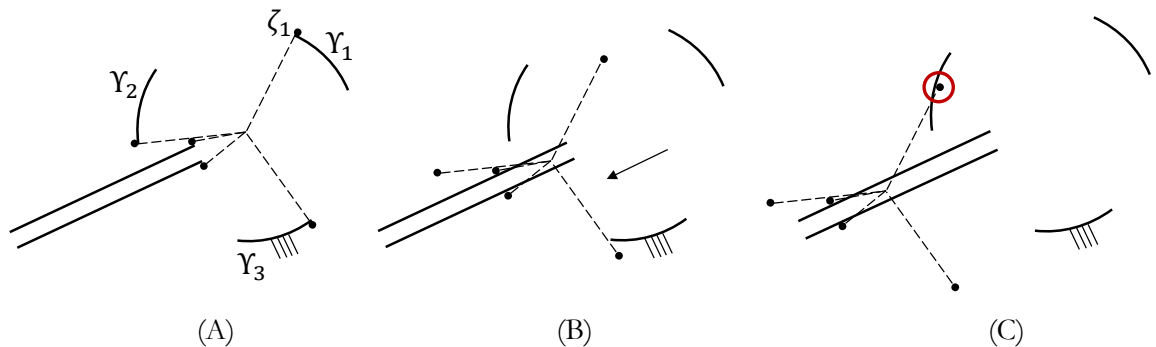


Figure 4.17: External Arc Interference Example.

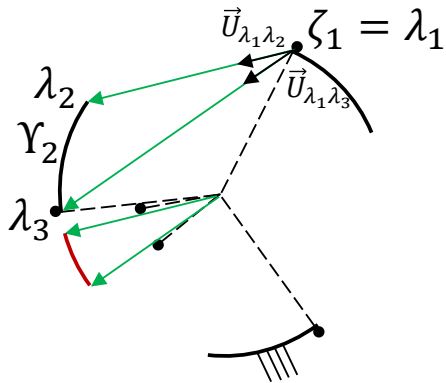


Figure 4.18: External Arc Interference

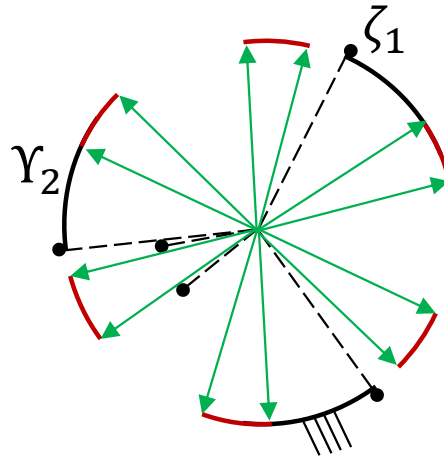


Figure 4.19: All External Arc Interference Regions

internal arc interference regions for the joint in Fig.4.20. It is important that these regions for translation are avoided.

4.6.3 Determining the Separation Angles for an R_1P_v Joint

The R_1P_v variable joint is unique in that there is variability in the location of two of the three arcs that form the outer boundary. For most R_1P_v joint designs there are multiple combinations of separation angles that may be used to generate

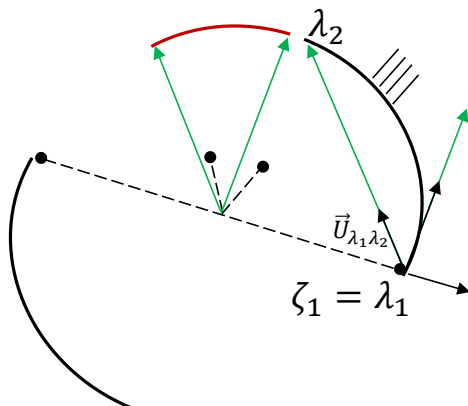


Figure 4.20: Internal Arc Interference

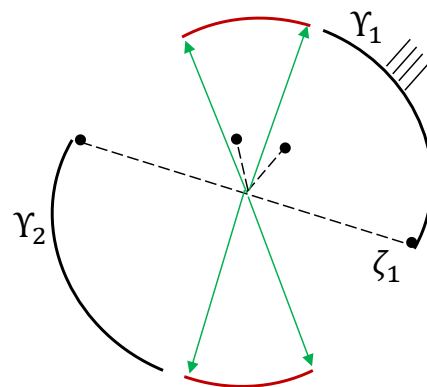


Figure 4.21: All Internal Arc Interference Regions

the desired motion. This section will look at different ways to determine appropriate separation angles. Figure 4.22 shows a plot of all theoretically possible α , β , and γ combinations for the example R_uP_v variable joint presented in Section 4.3. This plot was generated based on the internal and external arc interference equations presented in Section 4.6 with the following range of α , β , and γ values:

$$0^\circ \leq \alpha, \beta, \gamma \leq 180^\circ \quad (4.9)$$

Notice that Fig. 4.22 is a plane due to the constraint that $\alpha + \beta + \gamma = 360^\circ$. While Fig. 4.22 shows the theoretically possible values of the separation angles, many of the separation angle combinations are not practical. Further constraints can be placed on the separation angles to ensure the solutions are practical. Eq. 4.10

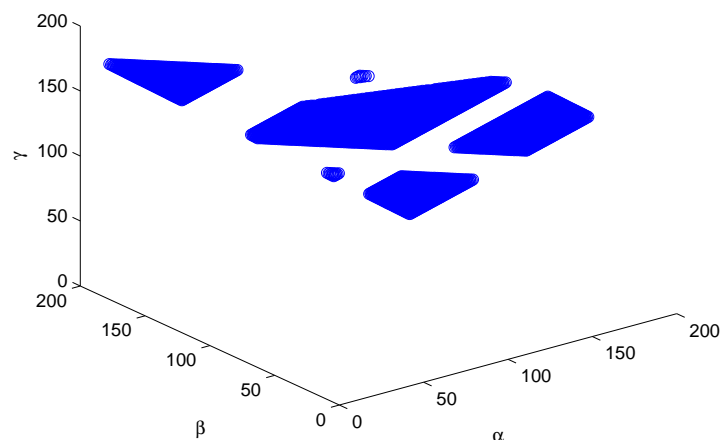


Figure 4.22: Possible α , β , γ Combinations with $\theta_i = 25^\circ$, $\theta_f = 65^\circ$, $\theta_t = 110^\circ$, $\theta_R = 0^\circ$, and $d = 5$ in.

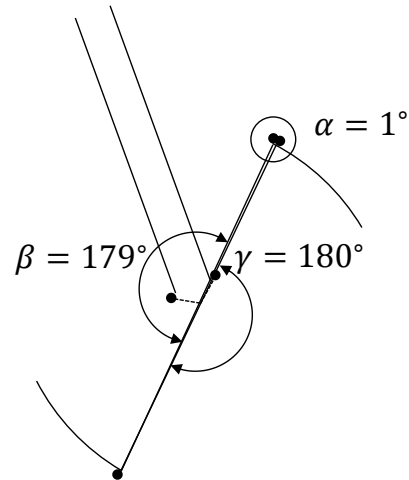


Figure 4.23: Unrealistic Joint Design

shows an additional constraint that

$$\alpha \geq \theta_f - \theta_i + \Delta\theta \quad (4.10)$$

$$\beta \geq \theta_f - \theta_i + \Delta\theta$$

$$\gamma \geq \theta_f - \theta_i + \Delta\theta,$$

which ensures that the arcs will not overlap, and there will be a separation of $\Delta\theta$ degrees between each arc. Figure. 4.24 shows updated separation angles after imposing the constraints in Eq. 4.10. After imposing the constraints in Eq. 4.10 it is up to the designer to choose appropriate values for the separation angles.

4.7 Summary

This chapter presented a method that can be for the profile synthesis of R_uP_v variable joints. General equations were developed based on a general joint profile that includes all R_uP_v variable joints. By changing parameters in the

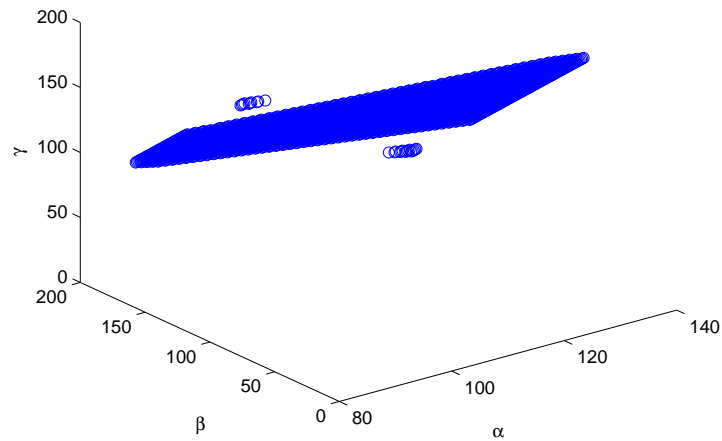


Figure 4.24: Separation Angles after Imposing the Constraints from Eq. 4.10

equations, the profiles of the six different R_uP_v variable joints were determined. It was further shown how the profiles of R_uP_v variable joints can be created based on a design configuration space. An example was provided in which different adjustable pliers were created by placing multiple R_uP_v variable joints in series. In addition, it was shown that there are constraints on the direction of translation of R_uP_v variable joints due to the arcs used for rotational constraint. Finally, different combinations of separation angles were considered for R_1P_v variable joints.

CHAPTER 5

Four-Bar Mechanism with Variable Topology

This chapter presents a four-bar Type II MVT that may be used in an industrial manufacturing application. The four-bar Type II MVT uses a R_uP_v variable joint to perform a manufacturing task. Using a R_uP_v variable joint allows for fewer actuators to be used in the mechanism. It is further shown how to determine an appropriate transmission ratio to reduce the forces seen by the variable joint.

5.1 Problem Setup

Figure 5.1 shows the setup for this manufacturing application. The application requires the assembly of part A to part B. An even layer of adhesive must be applied to part A by a dispenser that is at a height, h , above ground level. Dispensing the adhesive in the vertical direction allows for a uniform application. Part A must be moved from configuration I to configuration II where it must be able to slide a distance, l , to make an even surface contact with part B as shown in configuration III. This process must be automated to ensure both the speed and the accuracy of the manufacturing operation.

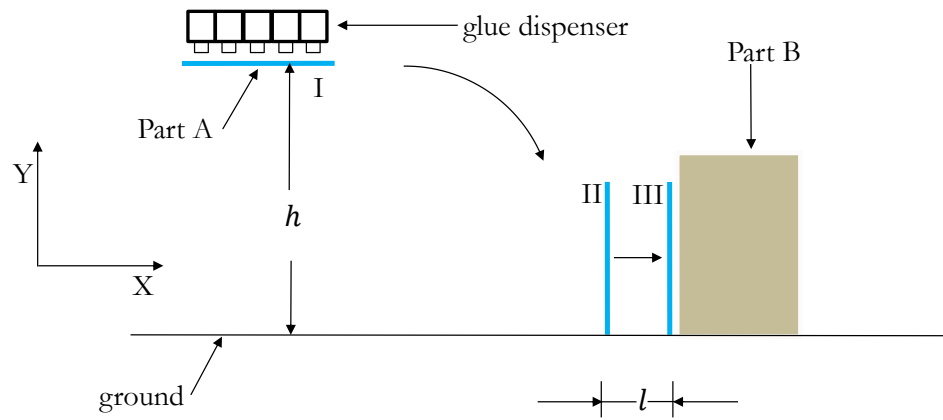


Figure 5.1: Problem Setup for Manufacturing Application

5.2 Solution Method using R_uP_v Variable Joints

This rigid body guidance problem can be completed using a four-bar mechanism that uses a R_uP_v variable joint for one of the base pivots. Doing so allows the four-bar linkage to change its topology from an $RRRR$ mechanism shown in Fig. 5.2 to a $RRRP$ mechanism¹ shown in Fig. 5.3. Figure 5.4 shows how an R_uP_v variable joint can be incorporated into the base pivot of the ground link

¹Note that an inline $RRRP$ mechanism is not necessary for this application, but an inline $RRRP$ mechanism is used as a simplifying assumption.

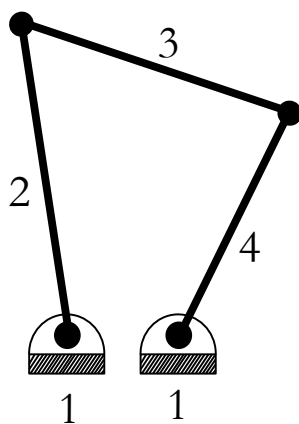


Figure 5.2: RRRR Four-Bar Mechanism

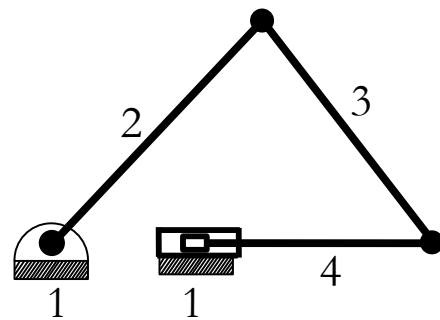


Figure 5.3: RRRP Four-Bar Mechanism

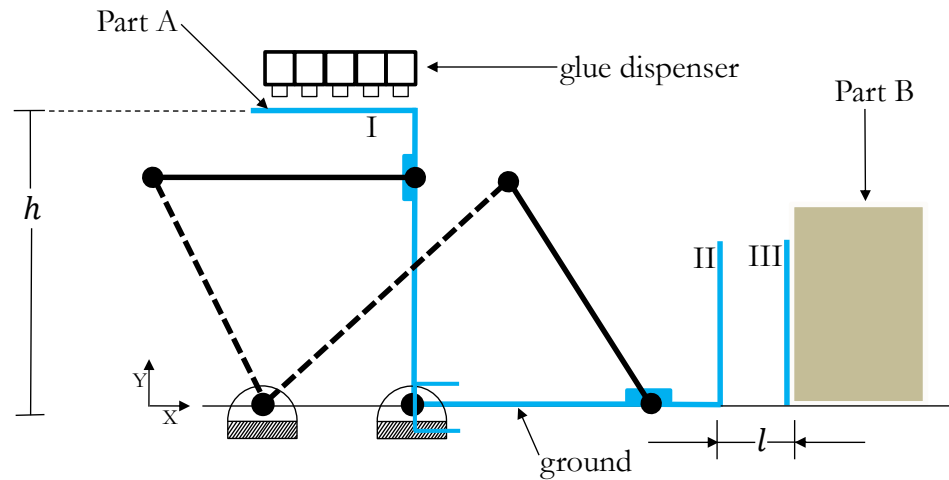


Figure 5.4: Solution Using a R_uP_v Variable Joint

to produce a four-bar mechanism capable of completing the required rigid body guidance. Notice the graphical symbol from Fig. 5.5 is used to denote the variable joint. This is a new symbol introduced in this dissertation. As shown in Fig. 5.4, a $RRRR$ four-bar mechanism is used to move part A from configuration I to configuration II. At this instant, due to the variable joint, a $RRRP$ mechanism is used to translate from configuration II to configuration III. Changing to a $RRRP$ mechanism allows the adhesive to be applied evenly to part B. Fig. 5.6 shows how the mechanism moves from the initial configuration to the final configuration. Six different configurations are shown. After the input link rotates clockwise through the six configurations, the input link rotates counterclockwise back to configuration I, and the cycle is repeated. The joint used in Fig. 5.6 is for demonstration only. Section 5.7 will explore the particular joint design in greater detail. However, prior to this, the mechanism will be analyzed to understand the topology and DOF.

5.3 Four-Bar Mechanism Analysis

It is important to understand the topology and DOF of the mechanism prior to performing the mechanism synthesis. Often, the analysis techniques can then be used to help with the mechanism synthesis. The mechanisms in Figs. 5.2 and 5.3 can be conveniently represented with one schematic representation as shown in Fig. 5.7. It can further be shown that the topology for this mechanisms can be represented by the augmented mechanism state matrix in Eq. 5.1.

$$M_{ASM} = \left[\begin{array}{ccc|c} \alpha 2_Z^R, 4_Z^R & \beta 3_Z^R & \beta 4_Z^R & \beta \\ \alpha 2_Z^R, 4_X^P & \beta 3_Z^R & \beta 4_Z^R & \beta \end{array} \right] \begin{array}{c} 1 \\ 1 \end{array} \quad (5.1)$$

This provides a convenient way to communicate the topology and degrees of freedom of this mechanism in a mathematical form. Appendix A contains more information on mechanism state matrices. There are many other forms of graphical analysis such as conventional adjacency matrices [36], EU-matrix transformations [15, 19], improved adjacency matrices [21], and directionality topology matrices [37]. However, all of these contain a subset of the information found in mechanism state matrices, and that is why mechanism state matrices are used in this section.

The analysis techniques have a limit to their usefulness in mechanism



Figure 5.5: Graphical Symbol for an $R_u P_v$ Variable Joint

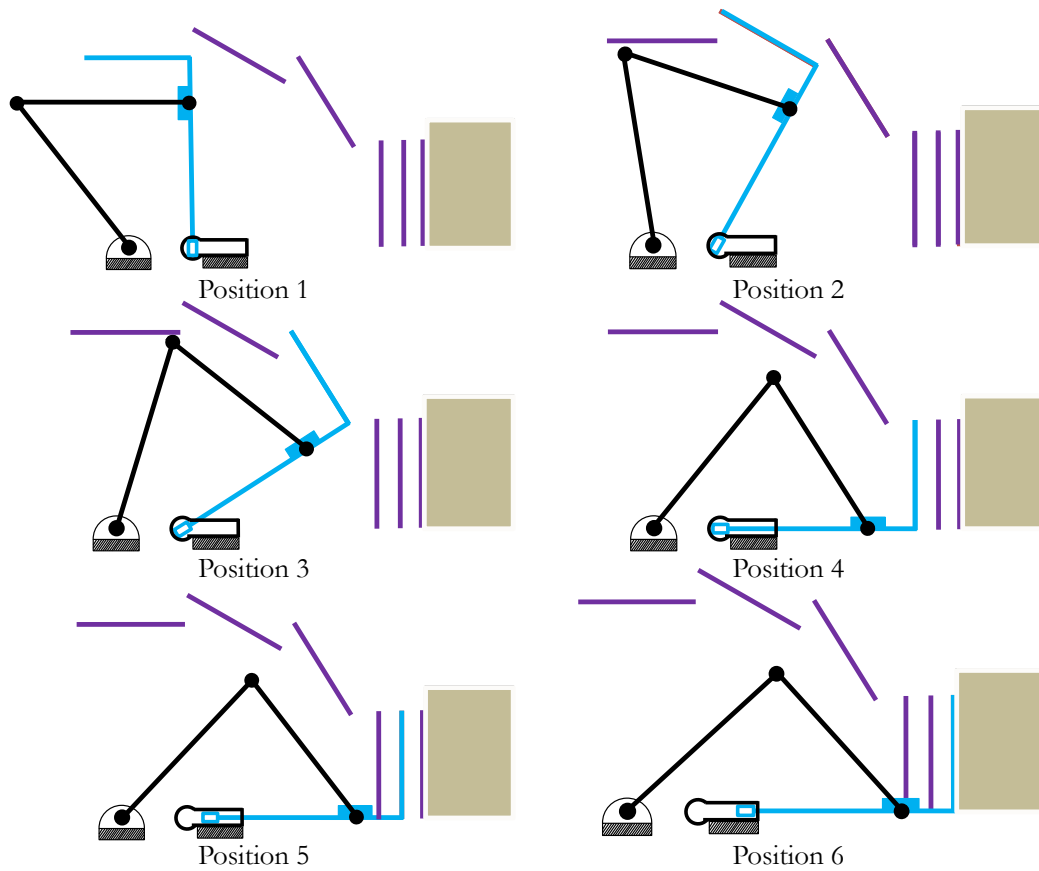
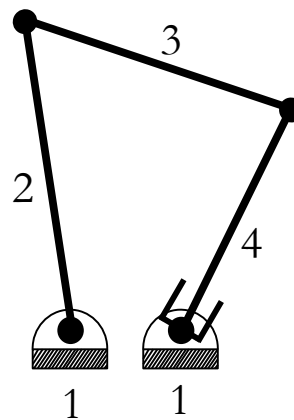


Figure 5.6: Final Result

design of reconfigurable mechanisms. Simply expressing the topology and degrees of freedom of the mechanism is not enough to synthesize a mechanism for a

Figure 5.7: Combined *RRRR* and *RRRP* Four-Bar Mechanism

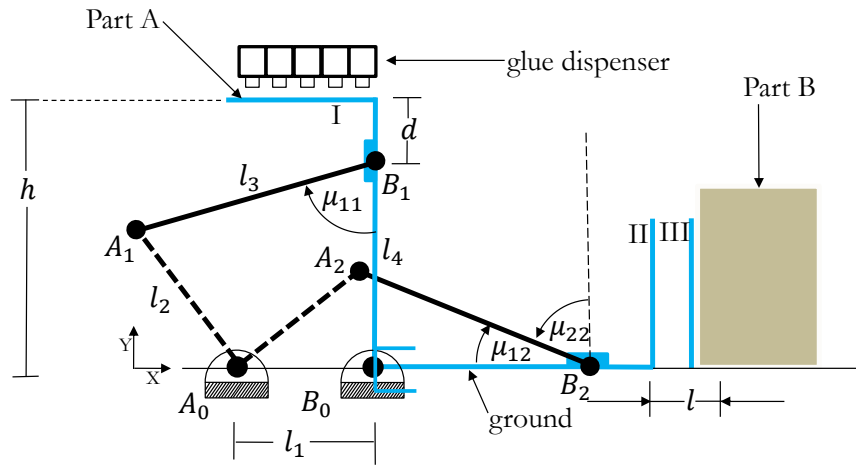


Figure 5.8: Solution Using a R_uP_v Variable Joint

particular task. The remainder of this chapter will be used to show how the theory developed in Chapter 4 can be used to design the joint required for this mechanism. In addition, classic four-bar mechanism theory can be applied in a new way because a variable joint is used in the design. Using a variable joint allows for a four-bar mechanism to perform a rigid body guidance task that is not possible using a conventional four-bar mechanism.

5.3.1 Overview of Solution Methodology

Figure 5.8 shows the schematic that is used to determine the solution to this problem. The links of the mechanism are numbered one through four, and their lengths are given by l_1 , l_2 , l_3 , and l_4 . Part A is at a distance, h , from the ground. There is an offset of a distance, d , which is trivial. The mechanism moves a distance l when moving from configuration II to configuration III.

The solution to this problem is separated into four different tasks. The first task is to determine the constraint equations necessary to move the four-bar linkage from configuration I to configuration II. The second task is to determine

the constraint equations to move the four-bar mechanism from configuration II to configuration III. Once all of the constraint equations are determined, the next task is to determine optimal transmission angles, μ_{11} and μ_{22} where the transmission angles in different configurations are denoted by μ_{ij} where $i = 1$ corresponds to the $RRRR$ mechanism, $i = 2$ corresponds to the $RRRP$ mechanism, and j corresponds to the configuration of the mechanism. Finally, an appropriate R_uP_v variable joint will be determined using the theory from Chapter 4.

5.3.2 Two Position Rigid Body Guidance for an $RRRR$

The first task is to determine the constraint equations necessary to move from configuration I to configuration II. To move from configuration I to configuration II, the coupler of the four-bar mechanism moves from position A_1B_1 to position A_2B_2 . Determining a four-bar mechanism in which the coupler moves between two known configurations is known in the literature as two position rigid body guidance [42]. This can be formally defined as follows:

- Two Position Rigid Body Guidance: Given two positions and orientations of a coupler link, synthesize a planar $RRRR$ four-bar mechanism such that its coupler assumes these two positions and orientations during the course of the the motion of the mechanism.

For this manufacturing application, the equations used for two position rigid body guidance, along with constraint equations, can be used to determine a mechanism to perform the required task.

Figure 5.9 provides the schematic for the solution to the two position rigid body guidance of a planar $RRRR$ four-bar mechanism. The coupler moves from position A_1B_1 to position A_2B_2 . The fixed pivots are located at points A_0 and B_0 .

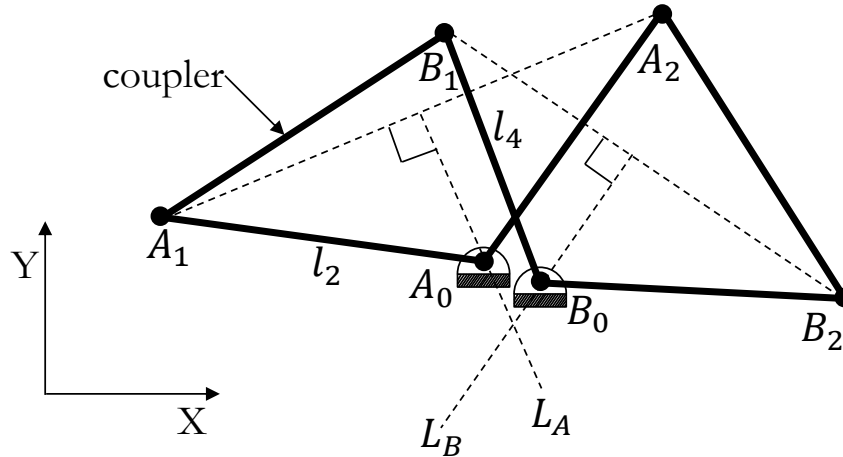


Figure 5.9: Two Position Rigid Body Guidance: RRRR

The pivots may be located anywhere along the perpendicular bisector of A_1A_2 and B_1B_2 . These lines will be denoted as L_A and L_B . This graphical solution can be written in algebraic form in Eq. 5.2:

$$(A_{1x} - A_{0x})^2 + (A_{1y} - A_{0y})^2 = l_2^2 \quad (5.2)$$

$$(A_{2x} - A_{0x})^2 + (A_{2y} - A_{0y})^2 = l_2^2$$

$$(B_{1x} - B_{0x})^2 + (B_{1y} - B_{0y})^2 = l_4^2$$

$$(B_{2x} - B_{0x})^2 + (B_{2y} - B_{0y})^2 = l_4^2$$

Equation 5.2 provides the general constraint equations for the two position rigid body guidance problem of an $RRRR$, but in this manufacturing application, there are further constraints that must be used in conjunction with Eq. 5.2.

Link four must be constrained so that it is able to slide relative the ground once the coupler reaches position A_2B_2 . Therefore, link 4 must rotate 90°

clockwise from the vertical position to the horizontal position as shown in Fig. 5.8. Further, the ground pivots, A_0 and B_0 , are assumed to be along the x -axis which will allow for an inline $RRRP$ mechanism. The constraint equations are given in Eq. 5.3. Note that y -axis of the coordinate system is aligned with point A_1 .

$$\begin{aligned}
 A_{0y} = B_{0y} = A_{1x} = B_{2y} &= 0 & (5.3) \\
 B_{0x} &= B_{1x} = l_3 \sin \mu_{11} \\
 B_{1y} &= h - d \\
 B_{2x} &= B_{1x} + B_{1y} \\
 A_{1y} &= B_{1y} - l_3 \cos \mu_{11} \\
 A_{2x} &= B_{2x} - l_3 \sin \mu_{22} \\
 A_{2y} &= l_3 \cos \mu_{22} \\
 l_4 &= B_{1y},
 \end{aligned}$$

Substituting the constraint equations from Eq. 5.3 into Eq. 5.2 and solving for the unknowns A_{0x} and l_2 gives

$$\begin{aligned}
 A_{0x} &= \frac{A_{2x}^2 + A_{2y}^2 - A_{1y}^2}{2A_{2x}} & (5.4) \\
 l_2 &= \sqrt{(A_{1x} - A_{0x})^2 + (A_{1y} - A_{0y})^2}.
 \end{aligned}$$

The $RRRR$ four-bar mechanism has now been fully defined based on the constraints.

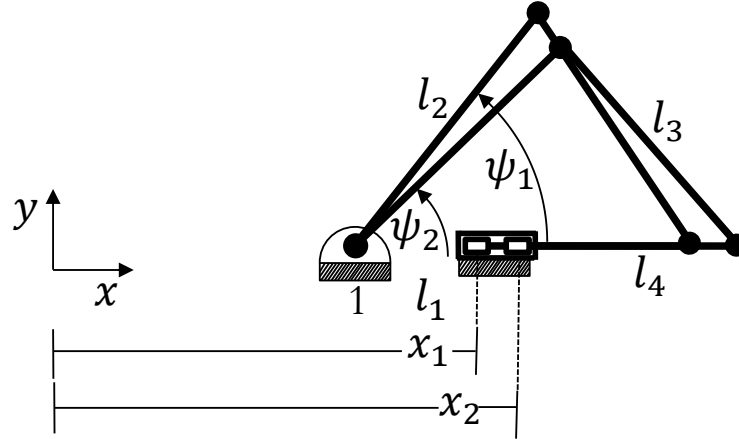


Figure 5.10: Two Position Rigid Body Guidance: RRRP

5.4 Two Position Rigid Body Guidance for an *RRRP*

After completing the two position synthesis of an *RRRR* to move from configuration I to configuration II, two position rigid body guidance must be completed for an *RRRP* in order to move part A from configuration II to configuration III. For an *RRRP* mechanism, the two position rigid body guidance problem can be formally defined as follows (see Fig. 5.10):

- Two Position Rigid Body Guidance: Given two positions of the slider, x_1 and x_2 , synthesize a planar *RRRP* four-bar mechanism such that its input link changes its angle from ψ_1 to ψ_2 .

$$\psi_1 = \arcsin\left(\frac{l_3 \cos \mu_{22}}{l_2}\right) \quad (5.5)$$

$$x_1 = B_{0x}.$$

Thus, it is possible to solve for ψ_2 using the law of cosines. The result is given in Eq. 5.6 as

$$\psi_2 = \arccos \frac{l_2^2 + (B_{2x} + l - A_{0x})^2 - l_3^2}{2l_2(B_{2x} + l - A_{0x})}. \quad (5.6)$$

Different choices of l_3 , μ_{11} , and μ_{22} will lead to different values of both ψ_1 and ψ_2 . Therefore, a designer has a choice of different four-bar mechanisms that can perform the desired task. The next section will provide insight on how to determine appropriate transmission angles for the design.

5.5 Determining Transmission Angles for a Reconfigurable Four-Bar

Transmission angles used in four-bar mechanism design to estimate the dynamic forces of the mechanism during the kinematic design process. The transmission angles for both an *RRRR* four-bar mechanism and a *RRRP* mechanism are shown in Figs. 5.11 and 5.12, and the general transmission angles are denoted by μ_R and μ_P , respectively. However, the transmission angles change as the mechanisms moves from one configuration to another. The transmission angles in different configurations are given by μ_{ij} . Furthermore, the transmission angles are kinematic parameters, and do not rely on the system dynamics.

For both mechanisms, it is best to keep the transmission angles as close to 90° as possible because this is the optimal value for force transmission. This helps to ensure that most of the torque from the input link is transferred to the output link. It also reduces the forces felt by the joint of the output link. A rule of thumb used in four-bar mechanism design is to keep the transmission angle between 45°

and 90° . Therefore, the maximum and minimum transmission angles must be determined during the design process to ensure that the transmission angles fall within the required range.

To determine the maximum and minimum transmission angles, equations can be derived for the transmission angle of both mechanisms. For the *RRRR* four-bar mechanism the transmission angle can be determined by writing the law of cosines for both triangles $A_0A_1B_0$ and $B_0A_1B_1$ and equating the distance A_1B_0 as shown in Fig. 5.11 which leads to Eq. 5.7

$$\cos \mu_R = \frac{l_4^2 + l_3^2 - l_1^2 - l_2^2}{2l_3l_4} + \frac{l_1l_2}{l_3l_4} \cos \theta_2. \quad (5.7)$$

Similarly, the expression for the transmission angle for the *RRRP* four-bar mechanism in configuration II is given in Eq. 5.8 as

$$\cos \mu_P = \frac{l_2}{l_3} \sin \theta_2. \quad (5.8)$$

The expressions for the transmission angles are both continuous and differentiable,

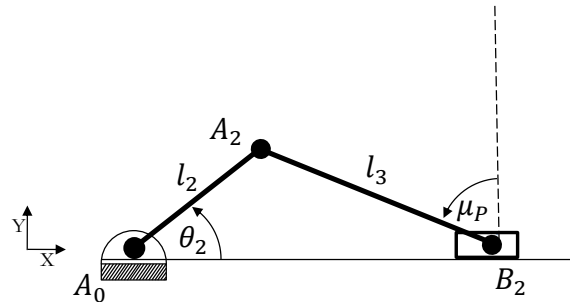
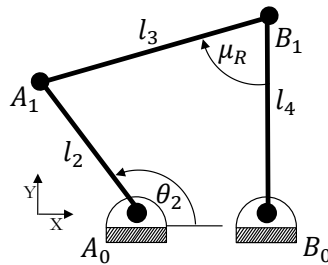


Figure 5.11: *RRRR* Transmission Angle

Figure 5.12: *RRRP* Transmission Angle

and therefore to find maximum and minimum transmission angles the equations for the transmission angles must be evaluated at all critical points as well as the boundaries.

The global maximum and minimum transmission angles are the critical points and can be found by differentiating Eqs. 5.7 and 5.8 with respect to θ_2 and setting equal to zero as shown in Eqs. 5.9 and 5.10, respectively.

$$\frac{d\mu_R}{d\theta_2} = \frac{l_1 l_2 \sin \theta_2}{l_3 l_4 \sin \mu_R} = 0 \quad (5.9)$$

$$\frac{d\mu_P}{d\theta_2} = -\frac{\cos \theta_2 l_2}{\sin \mu_P l_3} = 0 \quad (5.10)$$

Solving Eq. 5.9 for θ_2 shows that the global maximum and minimum transmission angles for a *RRRR* four-bar mechanism occur at $\theta_2 = 0^\circ$ or $\theta_2 = 180^\circ$. Similarly, solving Eq. 5.10 for θ_2 shows that the maximum and minimum transmission angles occur at $\theta_2 = 90^\circ$ or $\theta_2 = 270^\circ$.

If the mechanism does not pass through the the θ_2 values corresponding to the maximum and minimum transmission angles, then the maximum and minimum transmission angles must occur at the values of θ_2 corresponding to either the starting configuration or ending configuration (i.e. the boundary conditions). An example will be provided in Section 5.6.

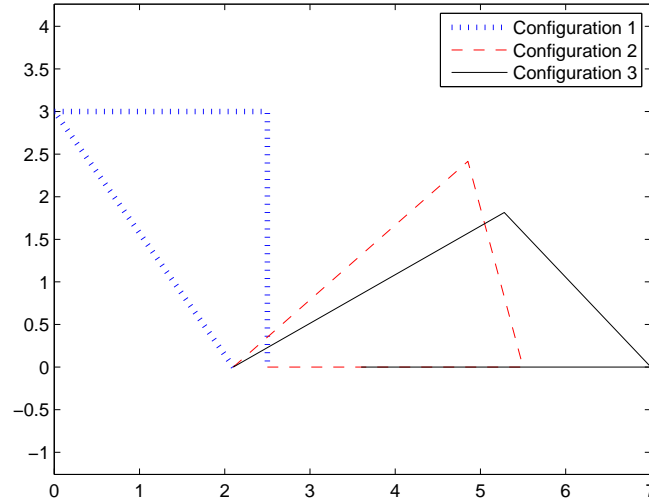


Figure 5.13: Resulting Four-Bar Mechanism

5.6 Numerical Example

A numerical example is presented in this section to verify the results of the derived equations, and to show how appropriate transmission angles can be determined for a reconfigurable four-bar mechanism. Part A begins at a height of $h = 3$ ft. above ground level. Bar A_1B_1 is offset in the vertical direction $d = 0.5$ ft. The required sliding distance is $l = 1.6$ ft. The final inputs were determined to be $l_3 = 3$ ft., $\mu_{11} = 90^\circ$, and $\mu_{22} = 45^\circ$. Substituting the known values into Eqs. 5.4, 5.5, and 5.6 gives

$$A_{0x} = 1.4304 \quad (5.11)$$

$$l_2 = 2.8803 \text{ ft.}$$

$$\psi_1 = 47.4342^\circ$$

$$\psi_2 = 15.706^\circ.$$

Figure 5.13 shows the four-bar mechanism as it moves from configuration I to configuration II to configuration III.

The transmission angles, μ_{11} and μ_{22} , were chosen to reduce the reaction forces seen by the joints of the output link. A unique problem for choosing transmission angles for this reconfigurable mechanism is that in configuration II there is a constraint on the transmission angle for the *RRRR* four-bar (μ_{12}) and the transmission angle for the *RRRP* four-bar (μ_{22}) given by:

$$\mu_{12} + \mu_{22} = 90^\circ \quad (5.12)$$

In this design both μ_{12} and μ_{22} were chosen to be 45° in order to satisfy the constraint that the transmission angles do not deviate more than 45° from the optimal value of 90° . The transmission angle for the *RRRR* four-bar (μ_{11}) was chosen to be 90° , as this is the optimal value. The calculated boundary conditions of

$$\theta_{2i} = 119.7765^\circ \quad (5.13)$$

$$\theta_{2f} = \psi_1 = 47.4342^\circ.$$

show that the mechanism does not pass through $\theta_2 = 0^\circ$ or $\theta_2 = 180^\circ$ (the critical points), and therefore the the maximum and minimum values of the transmission angles for the *RRRR* four-bar are 90° and 45° , respectively. Similarly, for the *RRRP* mechanism the mechanism does not pass through $\theta_2 = 180^\circ$ or $\theta_2 = 270^\circ$

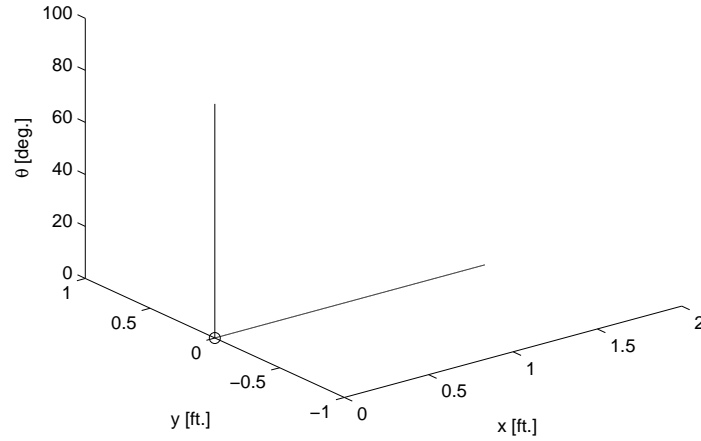


Figure 5.14: Design Configuration Space

(the critical points), and therefore the minimum and maximum transmission angles for the RRRP four-bar are 45° and 67.556° , respectively.

5.7 Joint Design for the Four-Bar Mechanism

The R_2P_2 variable joint designed in this section is for the example in Section 5.6. The joint is required to rotate from 90° to 0° and then translate a distance, l , of 1.6 ft . This can be seen in the design configuration space shown in Fig. 5.14 where the values of ξ_1 , ξ_2 , and ξ_3 can be given in Eq. 5.14

$$\xi_1 = (0, 0, 90^\circ)^\top \quad (5.14)$$

$$\xi_2 = (1.6, 0, 0)^\top$$

$$\xi_3 = (0, 0, 0)^\top.$$

The units are in ft unless otherwise indicated. Notice that the transition point

between rotational and translational motion occurs at the origin.

The resulting joint is shown in Fig. 5.15, and the corresponding parameters table is given in Tab 5.1. For this design, the values of the joint design parameters were chosen so that ζ_1 coincides with the translational constraint point. The calculated R_2P_2 variable joint is shown in the final mechanism in Fig. 5.16. A version of this design that includes redundant contact points is given in Fig. 5.17. In this modified design, the rotational constraint points are expanded to be surfaces to allow for a smoother rotation. In addition, the translational constraint points are extended to be lines in order to have a more stable design. Mechanical stops are also placed at both the end of the rotational motion and the end of the translational motion. Note that the mechanical stop at the end of the translation is used for a dual purpose. It is meant to stop the rotation of link 2, but it will also force link 2 to transition from a rotational motion to a translational motion.

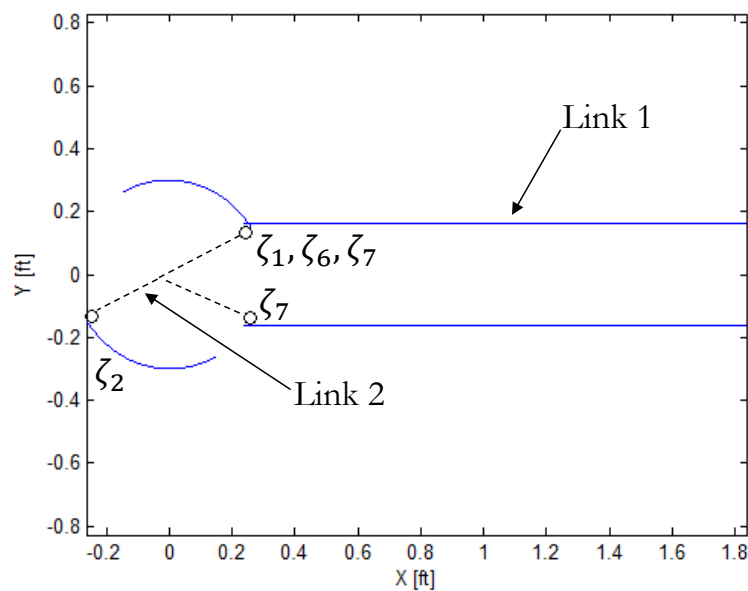


Figure 5.15: Calculated R_2P_2 Joint

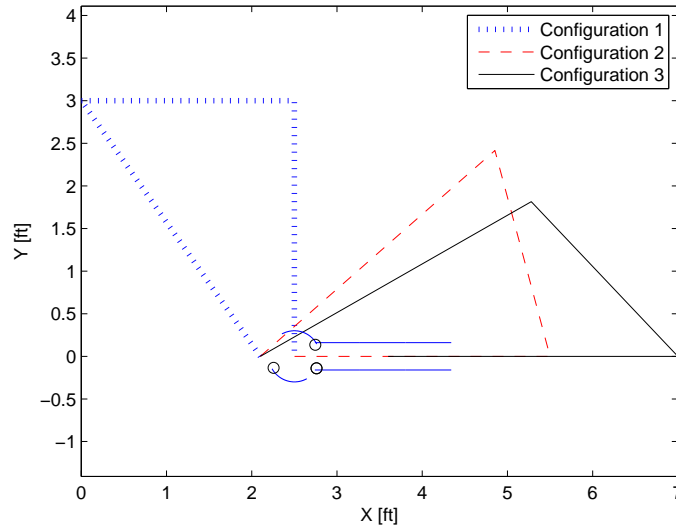


Figure 5.16: Mechanism Design with an R_2P_2 Variable Joint

The mechanical stop could be made longer if the width of link 2 were reduced.

However, this would reduce the surface contact during rotation. This is an important tradeoff that must be considered.

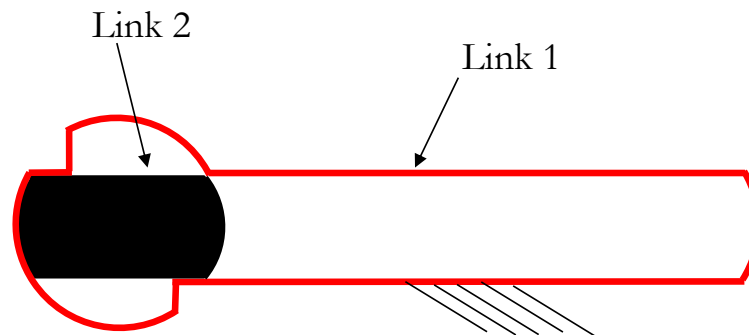


Figure 5.17: Final Joint Design for the R_2P_2 Variable Joint

Table 5.1: Joint Design Parameters for a R_2P_2 Variable Joint

Joint Design Parameter	l	w_1	w_2	r_1	r_2	r_3	α	β	δ_k	δ_{po}	θ_R
Value	0.24	0.16	0.16	0.3	0.3	0.3	180°	180°	δ	δ	29°

5.8 Discussion of Alternative Solutions

In any rigid body guidance task (or other motion specification) there are typically multiple different mechanisms that can provide the same kinematic motion. For example, there are multiple mechanisms that can be used to perform straight line motion (Peaucellier linkage, Sarrus linkage, etc.). Determining which mechanism to use for a particular application is typically referred to as type synthesis. This provides the basic topology of the mechanism. After type synthesis occurs, dimensional synthesis is completed to determine specific link lengths that will provide the desired kinematic motion.

There are multiple mechanisms that can be used to complete the rigid body guidance problem for this particular assembly application. For instance, a planar RP serial mechanism can be used to perform the required task. Additionally, an additional linear actuator can be used in combination with a $RRRR$ four-bar mechanism to produce the same result. However, both of these solutions require more than one actuator.

The advantage of using an R_uP_v variable joint is that it is possible to produce the required motion with a one DOF four-bar mechanism. This is not possible with a four-bar mechanism unless a variable joint is used. The four-bar mechanism is one of the most widely used mechanisms. The most common type of four-bar mechanism is an $RRRR$ chain, but other options include an $RRRP$, $RRPP$, or an $RPRP$. By assigning various links of each of these as a fixed link there are seven basic one DOF four-bar mechanisms that result [36]. These

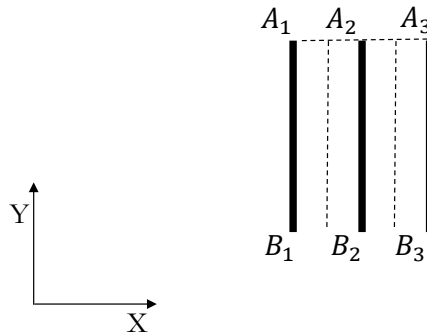


Figure 5.18: Three Position Rigid Body Guidance: RRRR

mechanisms have common names such as the turning-block linkage, swinging-block-linkage, scotch yoke mechanism, etc., and are used extensively in industry. Each of these mechanisms have their own specific use, but none of these four-bar mechanisms can be used to solve the rigid body guidance problem posed in this chapter.

For example, it can quickly be shown that it is not possible to move a rigid body in pure translation using an *RRRR* linkage. Consider the three position rigid body guidance problem shown in Fig. 5.18. The coupler link of a four-bar mechanism must be moved from position A_1B_1 to position A_2B_2 to position A_3B_3 . The graphical solution procedure for the three position problem follows the same method as that for the two position problem. Figure 5.18 shows that the perpendicular bisector of A_1A_2 and the perpendicular bisector of A_2A_3 do not cross, and therefore there is no solution. A similar example can be used to show that the other types of four-bar mechanisms cannot be used for this manufacturing application.

5.9 Summary

In this chapter it was shown that a four-bar mechanism with a variable joint (a Type II MVT) can be used in a practical manufacturing application. The mechanism uses an R_2P_2 variable joint as one of the fixed pivots. This allows for a combined $RRRR$ and an $RRRP$ four-bar mechanism that can be used to perform a rigid body guidance task that changes from a rotational motion to a translational motion. It was also shown that this type of problem could not be solved using a conventional four-bar mechanisms without adding an additional actuator.

CHAPTER 6

Singularity Avoidance in a 3-RPR Parallel Manipulator

This chapter shows how an R_uP_v variable joint can be used for singularity avoidance when a 3-RPR parallel manipulator (PM)¹ is moved in the vertical direction. The advantage of this approach is that the end-effector of the 3-RPR mechanism can pass through a singular configuration without redundant actuation. This is accomplished by replacing one of the passive revolute joints on the end-effector with an R_uP_v variable joint that changes one of the legs of the mechanism to an RPP kinematic chain.

6.1 Introduction

In general, PMs have lower inertia and higher end-effector speeds than serial end-effectors. In addition, PMs often have higher stiffness and are more accurate than serial manipulators. The tradeoff is that PMs have a reduced workspace and an increased number of singularities [43]. Singularities that are unique to parallel manipulators are called platform singularities [44]. When platform singularities occur, a parallel mechanism can instantaneously gain a degree of freedom. That is, the end-effector can move instantaneously even if all of the actuators are locked.

Platform singularities can lead to large internal forces, reduced accuracy,

¹The prismatic joint in 3-RPR is underlined to indicate that this is the actuated joint

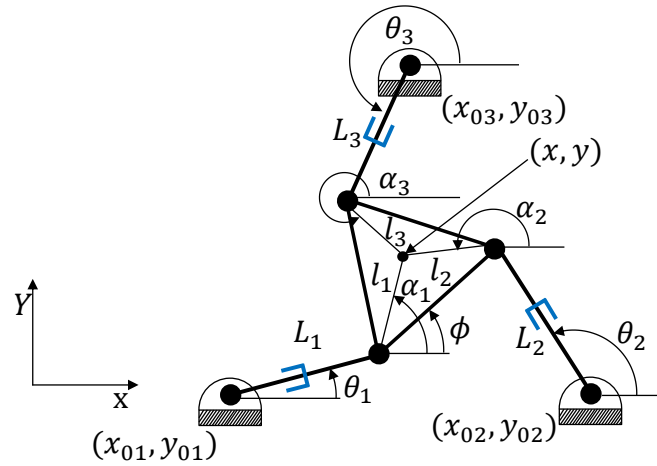


Figure 6.1: 3-RPR Parallel Mechanism

and an uncontrollable degree of freedom. Two options are often used to overcome platform singularities: avoiding the singularities or redundant actuation. Avoiding singularities in the workspace may not be feasible due to the required path of the end-effector. Redundant actuation can be used for singularity avoidance, but this adds unwanted inertia [43]. In this chapter, it is shown how an R_uP_v variable joint provides a passive solution to singularity avoidance for a 3-RPR moving in the vertical direction.

6.2 3RPR Singularities

In this section the singularities of a 3-RPR are found by way of the standard Jacobian method. This method is used in order to easily determine the singularity curve of the mechanism. Another method using Kennedy's Theorem will be presented later in this chapter as a more graphical approach to the problem. Either approach is valid, but both an analytical as well as graphical solution provide insight into the problem at hand.

Figure 6.1 shows a typical 3-RPR mechanism. There are three passive revolute joints located at a grounded pivot (x_{0i}, y_{0i}) , where $i = 1, 2, 3$. The prismatic joints are active and have a variable length, L_i . The end-effector (represented by a triangular piece) is connected to the prismatic joints by three passive revolute joints. The lengths l_i are at an angle of α_i , and are the distance from the distal passive revolute joint (i.e., on the end-effector) to the centroid of the end-effector. The end-effector configuration is given by $(x, y, \phi)^\top$, where ϕ is the angle of the end-effector relative to the horizontal. The values of α_i are related to ϕ as shown in Eq. 6.1.

$$\begin{aligned}\alpha_1 &= \phi + \frac{\pi}{6} \\ \alpha_2 &= \phi + \frac{5\pi}{6} \\ \alpha_3 &= \phi - \frac{\pi}{2}\end{aligned}\tag{6.1}$$

In order to determine the singularities of the 3-RPR the determinant of the Jacobian must be determined. The Jacobian relationship for this manipulator can be given in Eq. 6.2 as:

$$\begin{bmatrix} 1 & 0 & 0 \\ 0 & 1 & 0 \\ 0 & 0 & 1 \end{bmatrix} \begin{bmatrix} \dot{L}_1 \\ \dot{L}_2 \\ \dot{L}_3 \end{bmatrix} = \begin{bmatrix} \cos \theta_1 & \sin \theta_1 & l_1 \sin(\alpha_1 - \theta_1) \\ \cos \theta_2 & \sin \theta_2 & l_2 \sin(\alpha_2 - \theta_2) \\ \cos \theta_3 & \sin \theta_3 & l_3 \sin(\alpha_3 - \theta_3) \end{bmatrix} \begin{bmatrix} \dot{x} \\ \dot{y} \\ \dot{\phi} \end{bmatrix}\tag{6.2}$$

The Jacobian relationship is in the form of

$$\mathbf{A}\dot{L} = \mathbf{B}\dot{X},\tag{6.3}$$

and singular configurations occur when either matrix \mathbf{A} or \mathbf{B} is singular [44].

When \mathbf{A} is singular the manipulator has inverse kinematic singularities. For the 3-RPR there are no inverse kinematic singularities. When \mathbf{B} is singular the manipulator undergoes a platform singularity. Platform singularities are found by setting the determinant of \mathbf{B} equal to 0. This leads to the expression in Eq. 6.4:

$$\begin{aligned} l_1 \sin(\alpha_1 - \theta_1) \sin(\theta_3 - \theta_2) + l_2 \sin(\alpha_2 - \theta_2) \sin(\theta_1 - \theta_3) \\ + l_3 \sin(\alpha_3 - \theta_3) \sin(\theta_2 - \theta_1) = 0. \end{aligned} \quad (6.4)$$

Substituting in the values of α_i gives

$$\begin{aligned} l_1 \sin\left(\phi + \frac{\pi}{6} - \theta_1\right) \sin(\theta_3 - \theta_2) + l_2 \sin\left(\phi + \frac{5\pi}{6} - \theta_2\right) \sin(\theta_1 - \theta_3) \\ + l_3 \sin\left(\phi - \frac{\pi}{2} - \theta_3\right) \sin(\theta_2 - \theta_1) = 0. \end{aligned} \quad (6.5)$$

While the singular configurations can be determined by solving Eq. 6.5, the

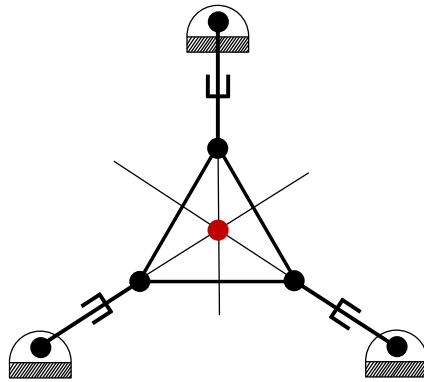


Figure 6.2: 3-RPR Singular Configuration

equation can be interpreted geometrically by looking at the Jacobian relationship of matrix \mathbf{B} . The first two columns for each row are the unit vectors of the L_i links. The third column can be thought of as the “moment” of that unit vector about the center point of the end-effector. Thus, the geometric interpretation of Eq. 6.5 is that singularities occur when the values of θ_i are such that axes of all three prismatic actuators meet at a point (including infinity) as shown in Fig. 6.2 [45]. At this instant in time the end-effector can instantaneously rotate about the point of intersection even if all three prismatic actuators are locked.

Another approach to determining singularities is to use Kennedy’s theorem. Kennedy’s theorem is stated as follows:

- Kennedy’s Theorem: The three instant centers shared by three rigid bodies in relative planar motion all lie on the same straight line [6].

The results from Kennedy’s theorem are the same as the results from analyzing the determinant of the Jacobian in Eq. 6.5. However, Kennedy’s theorem provides a more intuitive and graphical result, and can be easily applied to a mechanism at a particular instant. Kennedy’s theorem will also be used to analyze the mechanism when one of the legs changes from an RPR to a RPP.

There are currently two common ways to overcome a platform singularity. One method involves avoiding the singular configuration altogether. However, avoiding singular configurations reduces the effective workspace of the PM, and avoiding the singular configuration may not be an option due to the required trajectory of the end-effector.

An alternative solution is to add redundant actuation. For example, an extra actuator may be placed on one of the passive revolute joints. Adding this additional actuator ensures that when the end-effector reaches a platform singularity the actuator can be locked to prevent unwanted rotation. The drawback from adding a redundant actuator is that the actuator adds unwanted inertia to the system. One of the main advantages of a PM is its increased speed in comparison to a serial mechanism, but adding additional inertia reduces the effectiveness of this advantage.

Another solution to solving the problem of platform singularities is to add a redundant leg to the mechanism, a similar solution as adding a redundant actuator to one of the passive revolute joints. However, it also has similar drawbacks due to the unwanted inertia and an added actuator that must be controlled.

Each of the current popular solutions to solving the problem of platform singularities has different drawbacks such as an effectively reduced workspace or increased inertia in the system. In the following sections it will be shown how, for certain cases, platform singularities can be avoided using an R_uP_v variable joint. Eliminating the platform singularity allows one to maintain control of the end-effector and avoid any large internal forces that could have occurred at the singular configuration.

The advantage of the proposed approach is that no redundant actuators are necessary, and the singular configuration does not need to be avoided. By using an R_uP_v variable joint, it is possible to take advantage of the existing actuators used in the mechanism to overcome the platform singularity. In the next section, a

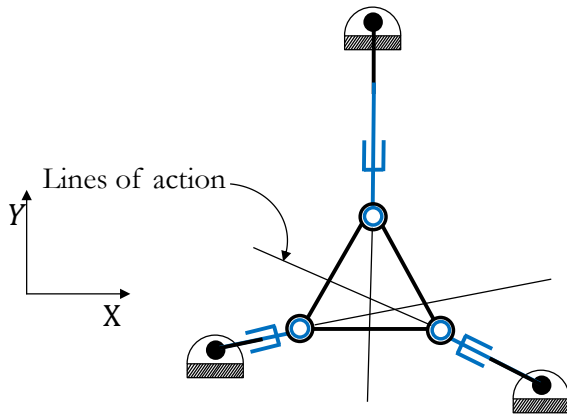


Figure 6.3: Non-Singular Configuration

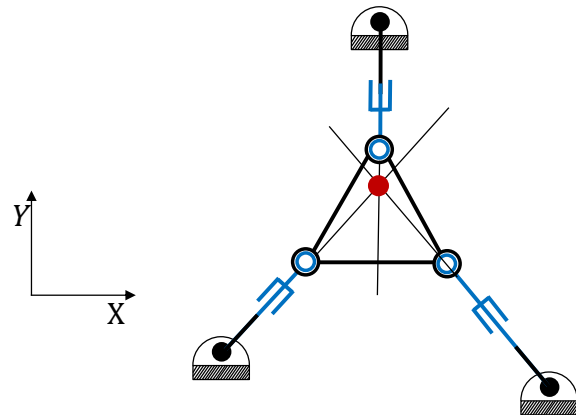


Figure 6.4: Singular Configuration

problem will be described in which a platform singularity will be avoided.

6.3 Problem Setup

The problem that will be considered will be for a potential manufacturing application. Consider the 3-RPR in Figs. 6.3 and 6.4. For a specific manufacturing application, it is necessary to move the end-effector in the Y -direction. The starting configuration (Fig. 6.3) is non-singular because the axes of the prismatic joints do not intersect at a point. As the end-effector moves in the Y -direction it eventually reaches a singular configuration where the axes of the prismatic joints intersect. Figure 6.5 shows how this problem could be solved using redundant actuation. An additional actuator could be used in place of one of the passive joints. By locking the actuator it can prevent the end-effector from gaining an extra DOF. However, adding this redundant actuator adds a significant amount of unwanted inertia to the system.

In the next section, it will be shown how this problem can be solved by adding an $R_u P_v$ variable joint in place of one of the passive revolute joints. Using

an R_uP_v variable joint in this way allows one to effectively lock the passive revolute joint. This is similar to how a redundant actuator can be used to lock the passive revolute joint. The difference between the two solution methodologies is that using a variable joint is a completely passive solution that does not require the added redundant actuator.

6.4 Solution Method using R_uP_v Variable Joints

Passing through this singularity can be accomplished using an R_uP_v variable joint in place of one of the passive revolute joints on the end-effector as shown in Fig. 6.6. This mechanism operates in two different states. When the R_uP_v variable joint is a revolute joint the mechanism will function exactly as a conventional 3-RPR mechanism would. However, when the R_uP_v variable joint becomes a prismatic joint, one of the legs in the mechanism becomes an RPP chain. In certain situations, changing the leg in the mechanism from a RPR to an RPP chain removes the platform singularity. Before explaining why this joint change removes the platform singularity, a conventional 3-RPR singularity will be

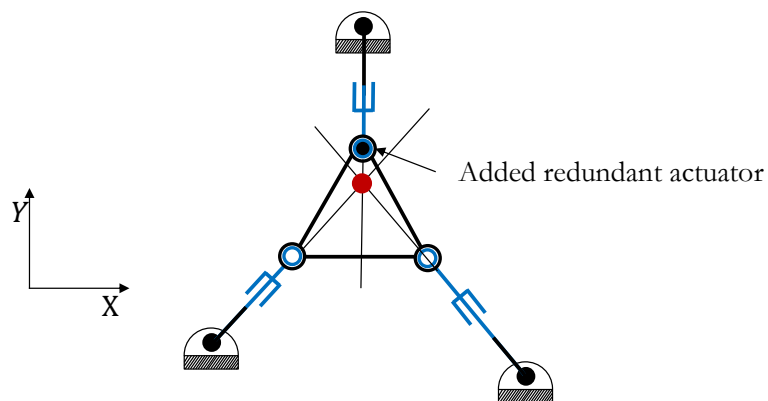


Figure 6.5: 3-RPR with Variable Topology

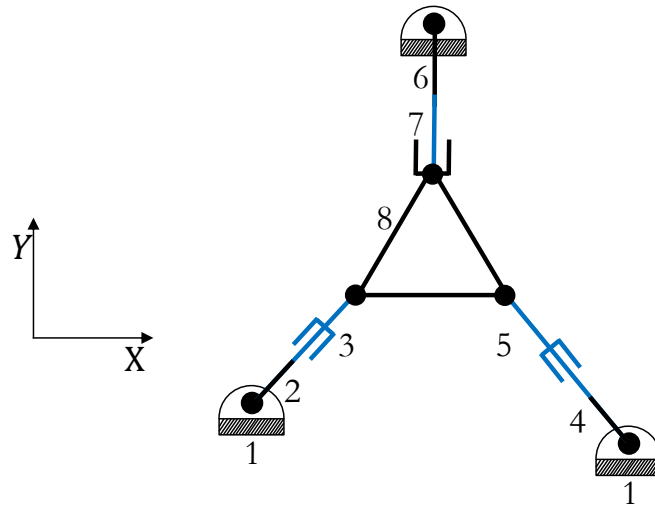


Figure 6.6: 3-RPR with Variable Topology

examined in more detail.

Platform singularities allow for instantaneous rotation of the end-effector even if all the actuators are locked. When all of the actuators are locked a standard 3-RPR can be thought of as a 3-RR mechanism as shown in Fig. 6.7. Even though it seems like the 3-RR mechanism should be a structure, the end-effector can still instantaneously rotate due to the platform singularity. The platform singularity can be shown by using Kennedy's theorem.

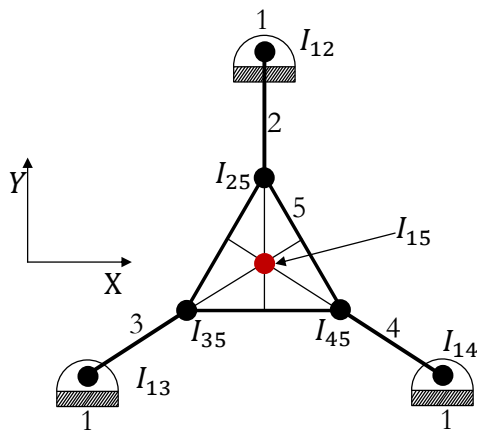


Figure 6.7: Singular Configuration

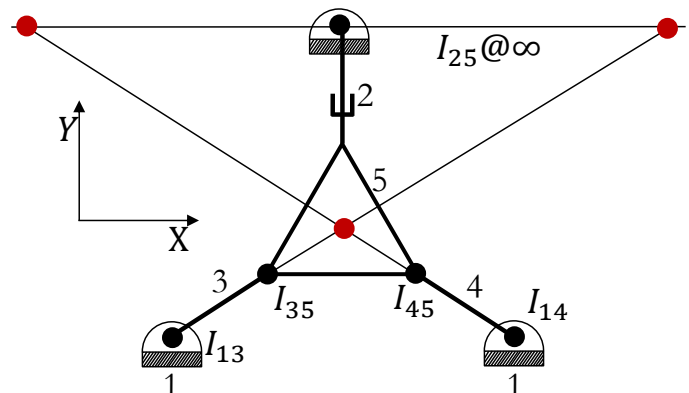


Figure 6.8: Structure

In Fig. 6.7 the instant center of link one and three is denoted by I_{13} , and the instant center between links three and five is denoted by I_{35} . Therefore, the instant center between link five and one must be on the line connecting I_{13} and I_{35} . For link five to move relative to link one, I_{15} must be a unique point. Because I_{15} in Fig. 6.7 is a unique point, the end-effector can instantaneously rotate around that point.

A similar analysis can be completed if one of the legs changes from \underline{RPR} to \underline{RPP} as shown in Fig. 6.8. The joint change can be completed using an R_uP_v variable joint. The joint change that occurs changes the position of the instant centers in the mechanism. When the joint between links two and five is changed from a revolute joint to a prismatic joint as shown in Fig. 6.8, the end-effector (link five) is instantaneously trying to rotate about three different points. Therefore, the mechanism is a structure. The instant center, I_{15} , that occurred in the mechanism in Fig. 6.7 no longer exists because the end-effector is instantaneously trying to rotate around three different points.

An animation showing the result using an example R_1P_2 variable joint is shown in Fig. 6.9. In position one the mechanism is not in a singular configuration because the axes of the prismatic joints do not intersect. In positions two and three, actuator one is moved along the Y -axis to change the joint from a rotational joint to a prismatic joint while the end-effector remains stationary. In positions four and five actuators two and three are actuated in order to move the end-effector along the Y -axis. During the movement along the Y -axis the end-effector passes through the singular position that would occur if the passive prismatic joint were a

revolute joint. Position six shows the end-effector rotating after passing through the singularity. The advantage of this approach is that no redundant actuators are required in order to pass through the singular configuration. Section 6.5 will present a numerical example to provide added clarity.

6.5 Numerical Example

The numerical example presented here relates back to the manufacturing application discussed in Section 6.3. The 3-RPR mechanism is shown in Fig. 6.10.

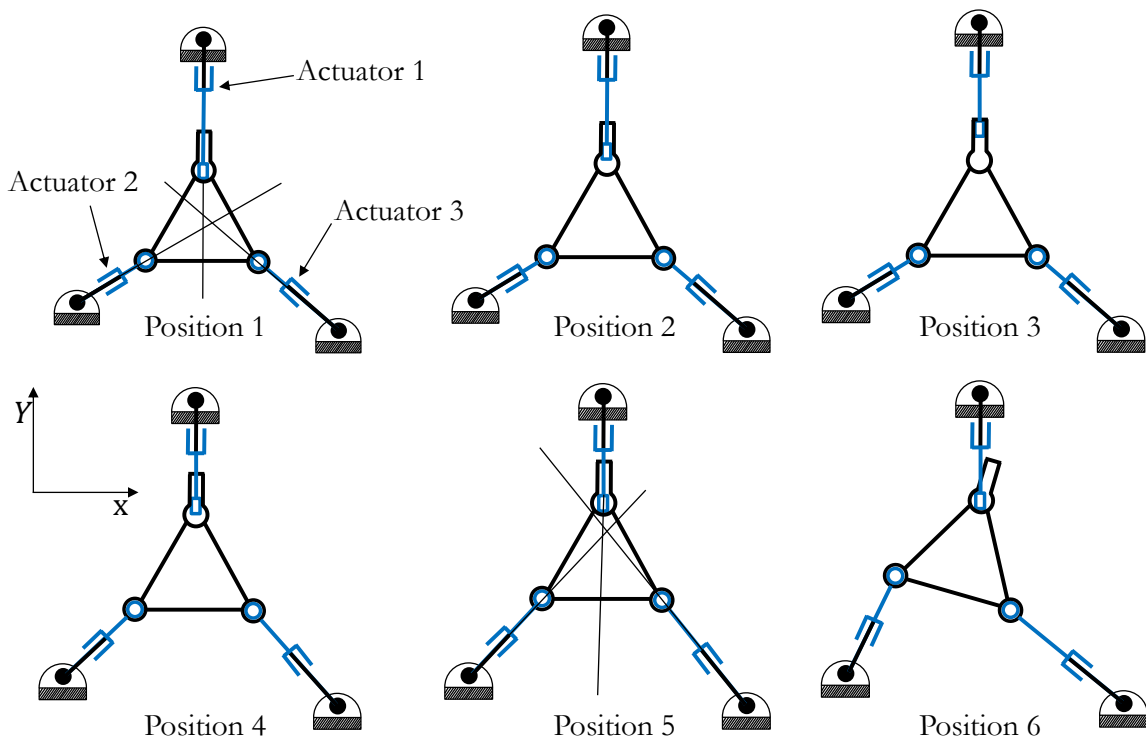


Figure 6.9: Animation Showing the Final Result

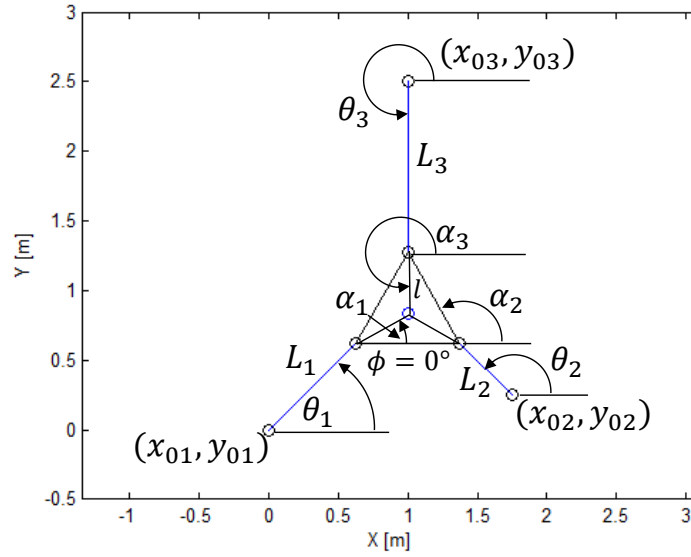


Figure 6.10: 3-RPR Mechanism Singular Configuration

The fixed pivots are located at the following location:

$$\begin{aligned} (x_{01}, y_{01})^T &= (0, 0)^T \\ (x_{02}, y_{02})^T &= (1.75, 2.5)^T \\ (x_{03}, y_{03})^T &= (1, 2.5)^T. \end{aligned} \quad (6.6)$$

The end-effector is an equilateral triangle with a side length of 0.75 m. Therefore, the lengths of each of the sides of the end-effector are $l_1 = l_2 = l_3 = \frac{0.75}{\sqrt{3}}$ m. The actuator lengths, L_i , are limited to a 1.5 m stroke length. Therefore, the reachable workspace for this mechanism is shown in Fig. 6.11. For the manufacturing application, the end-effector must move from the initial position to the final

position as shown in Eq. 6.7, which corresponds to Figs. 6.12 and 6.13, respectively.

$$(x, y, \phi)_{initial}^T = (1, 0.75, 0)^T \quad (6.7)$$

$$(x, y, \phi)_{final}^T = (1, 0.93, 0)^T$$

Due to the required end-effector path, the end-effector must pass through the singular position given by:

$$(x, y, \phi)_{singular}^T = (1, 0.84, 0)^T.$$

Figure 6.14 shows the singular configurations of the 3-RPR when $\phi = 0^\circ$. The initial and final positions are shown, and they are connected together with a straight line. This shows that in order for the end-effector to complete its required path, it must move through a singular configuration. To complete this motion, an $R_u P_v$ variable joint can be added in place of the passive revolute joint. This

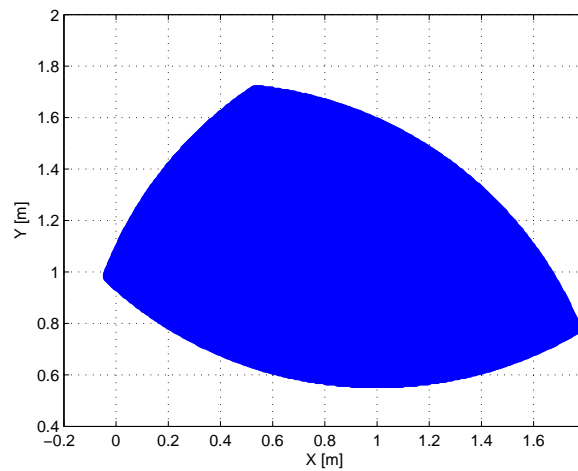


Figure 6.11: 3-RPR Reachable Workspace $\phi = 0^\circ$

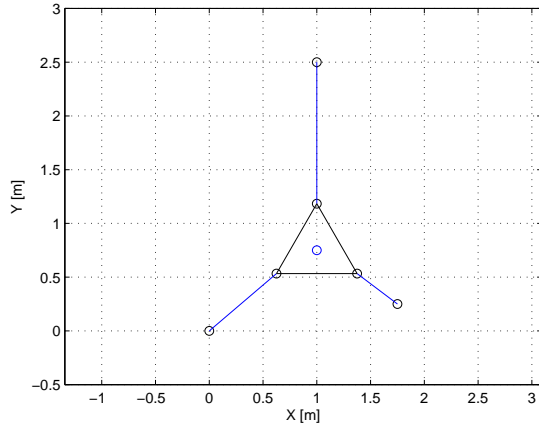


Figure 6.12: 3-RPR Initial Position

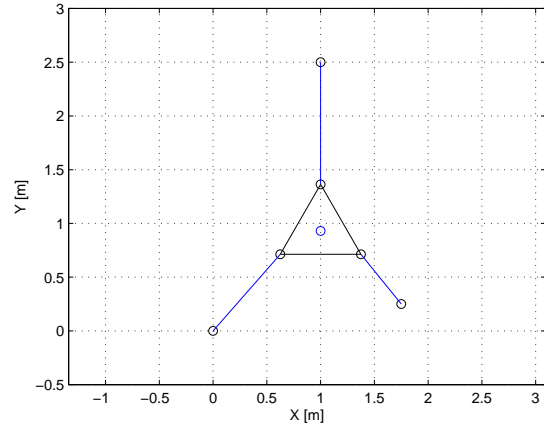
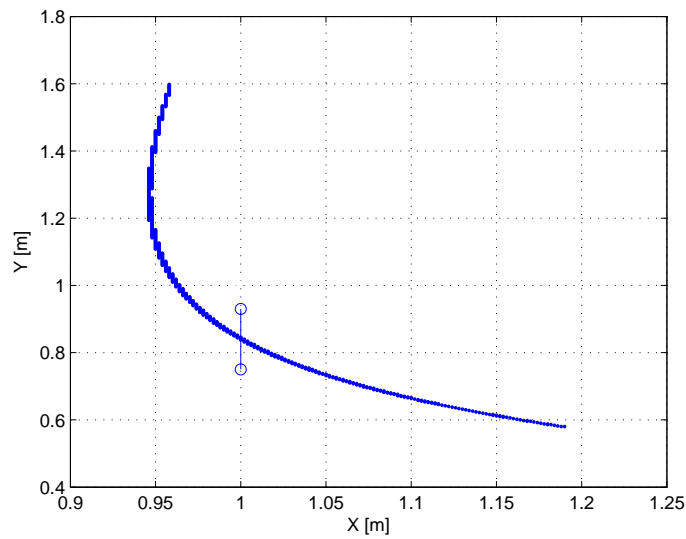


Figure 6.13: 3-RPR Final Position

passive solution effectively allows the end-effector to pass through the singularity curve shown in Fig. 6.14. To complete this task, an appropriate $R_u P_v$ variable joint must be designed, and this will be discussed in the next section.

Figure 6.14: Singular Configuration with $\phi = 0$

6.6 Joint Design for the 3-RPR

The R_uP_v variable joint designed in this section is for the example in Section 6.5. The joint is required to rotate from 45° to 90° and then translate a distance, l , of 0.18 m. This can be seen in the design configuration space shown in Fig. 5.14 where the values of ξ_1 , ξ_2 , and ξ_3 can be given in Eq. 6.8

$$\xi_1 = (0, 0, 45^\circ)^\top \quad (6.8)$$

$$\xi_2 = (0, 0.18, 90^\circ)^\top$$

$$\xi_3 = (0, 0, 90^\circ)^\top.$$

All units are in meters unless otherwise indicated. The synthesized R_2P_2 variable joint along with the joint parameters table is provided in Fig. 6.16 and Tab. 6.1. Similar to the joint in the previous chapter, the translational constraint points were aligned with the rotational constraint points. Aligning these points helps to simplify the joint design. The design shown in Fig. 6.16 contains only the minimum point contacts that are necessary for the required rotational to translational motion. A design that includes additional redundant points is shown in Fig. 6.17. The translational constraint points were extended to be lines to

Table 6.1: Joint Design Parameters for a R_2P_2 Variable Joint

Joint Design Parameter	l	w_1	w_2	r_1	r_2	r_3	α	β	δ_k	δ_{po}	θ_R
Value	0.05	0.14	0.14	0.15	0.15	0.15	180°	180°	δ	δ	-68°

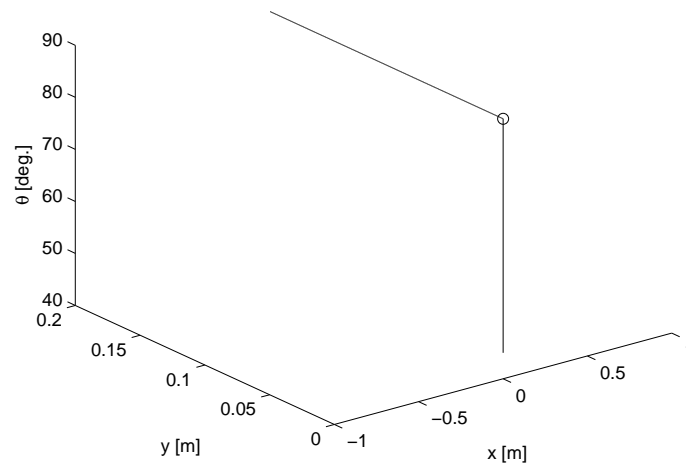
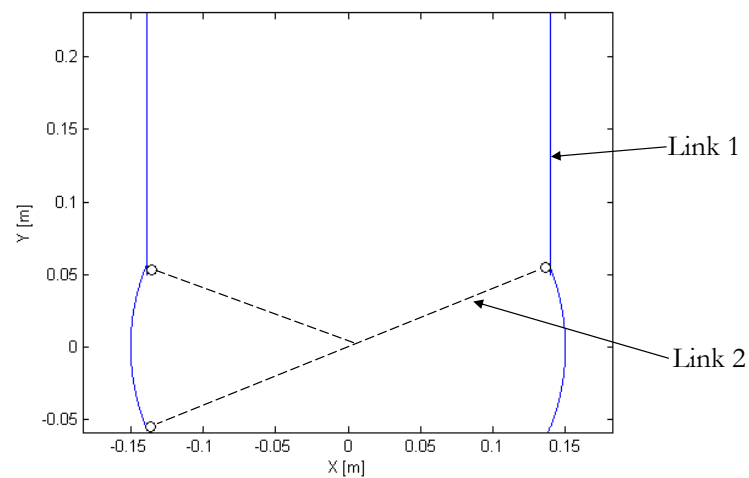


Figure 6.15: Design Configuration Space

provide added stability. Additional curvature was added to link 2 so that a surface contact is made during the rotational motion.

6.7 Summary

It was shown that a 3-RPR mechanism with variable topology can be used for singularity avoidance. The mechanism uses an R_2P_2 variable joint as one of the

Figure 6.16: Calculated R_2P_2 Joint

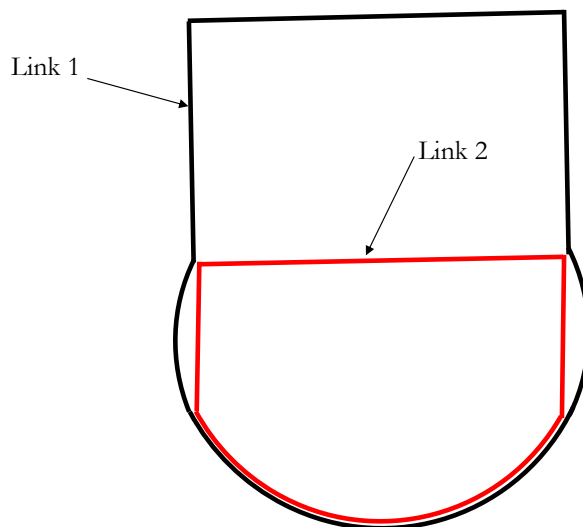


Figure 6.17: Final Joint Design for the R_2P_2 Variable Joint

passive joints attached to the end-effector. This allows for one of the legs in the mechanism to change from an $R\underline{P}R$ to an $R\underline{P}P$. It was shown by using Kennedy's theorem that this joint change eliminates the singularity.

CHAPTER 7

Summary and Conclusions

The final chapter provides a summary of the contributions made in this dissertation as well as some conclusions. The goal of this research was to provide a method that can be used for the profile synthesis of variable joints that change from a specific rotational motion to a specific translational motion. The synthesized variable joints can then be used in reconfigurable mechanisms. Using variable joints in a reconfigurable mechanism can help reduce costs and provide quick changeover for low volume manufacturing applications. These types of mechanisms are also used to provide added flexibility in the context of a constrained environment.

7.1 Higher Variable Joints

Higher variable joints were introduced fundamental components of planar, variable joints that change from a rotational motion to a translational motion. Higher variable joints are kinematically equivalent revolute and prismatic pairs but have different joint profiles. It was shown that second order effects, or surface curvature, of higher variable joints is critical to achieve a particular joint motion. Planar, higher variable joints were investigated for both rotational joints and translational joints. For rotational higher variable joints, the minimum number of

point contacts were found that can be used to constrain a circle to rotational motion. A similar procedure was also completed for translational higher variable joints. It was shown that there are three types of rotational higher variable joints and two types of translational higher variable joints. The resulting higher variable joints form the basis for the profile synthesis procedure.

7.2 Profile Synthesis of R_uP_v Variable Joints

Equations were provided that can be used for the profile synthesis of R_uP_v variable joints. General equations were developed based on a general joint profile that includes all R_uP_v variable joints. By changing different parameters in the equations, the profiles of the six different R_uP_v variable joints were determined. It was further shown how the profiles of R_uP_v variable joints can be created based on a design configuration space. Kinematic redundancies were then added to the joint design. An example was provided in which different adjustable pliers were created by placing multiple R_uP_v variable joints in series. In addition, it was shown that there are constraints on the direction of translation of R_uP_v variable joints due to the arcs used for rotational constraint. Finally, different combinations of separation angles were considered for R_1P_v variable joints.

7.3 Four Bar Mechanism with Variable Topology

A four-bar mechanism with variable topology of Type II was presented that can be used in an industrial manufacturing application. The variable joint that is used in the mechanism was developed using the methods from Chapter 4. It was shown that by using variable joints, a four-bar mechanism was created that is able

to perform a rigid body guidance task that is not possible to perform with a conventional four-bar mechanism. The mechanism drew upon classic four-bar mechanism theory in order to optimize the mechanism's transmission ratio, given the position constraints.

7.4 Singularity Avoidance in a 3-RPR Parallel Manipulator

It was shown how an R_uP_v variable joint can be used for singularity avoidance when a 3-RPR parallel manipulator (PM) is moved in the vertical direction. The advantage of this approach was that the end-effector of the 3-RPR mechanism can pass through a singular configuration without adding redundant actuation. This is accomplished by replacing one of the passive revolute joints on the end-effector with an R_uP_v variable joint that changes one of the legs of the mechanism to an RPP kinematic chain.

7.5 Conclusions

This sections outlines some of the conclusions that can be drawn from this research. Some of the conclusions are lessons that were learned during the research, and other conclusions can be considered ideas for future work. The conclusions can be outlined as follows:

1. Surface curvature is critical when determining the profiles of variable joints that change from a rotational motion to a translational motion. It is important to understand the minimum number of point contacts in order to determine an appropriate joint profile. Understanding the minimum number of points allows one to understand where kinematic redundancies are in the

design. Understanding where the kinematic redundancies are allows one to create a more robust joint.

2. Variable joints work well in cases in which the mechanisms's actuators can be used to actuate the variable joints during both joint motions. The advantage of this approach is that the number of actuators used in the mechanism is reduced which reduces the power supplies and coordination of the DOF. When one actuator is used for both joint motions there must be a way to determine which motion will be active. This can be accomplished by considering the dynamics of the mechanisms as well as the kinematic redundancies in the joint (i.e., mechanical stops).
3. Conventional kinematics theory can still be used when a variable joint is used in a mechanism. However, there are added constraints due the fact that two mechanisms are combined into one. Even though there are added constraints in the mechanism, the combination of two mechanisms into one mechanism may still be able to perform a task that is not possible to perform using each mechanism individually.
4. The design configuration space works well for planar joints. However, the design configuration space may be more difficult to use for spatial joints in which more than three parameters are required to describe the joint configuration. The design configuration space is not the only way to specify the design requirements. The design requirements could also be specified in

tabular or some other form, but configuration space is beneficial because it ensures no joint configurations are missed. In addition, tolerance analysis can be accomplished in configuration space using the works by Sacks et al. [38].

5. The methods presented in this dissertation can be expanded to include planar variable joints that change topology due to a change in direction as well as spatial joints. For instance, a spatial joint that changes direction of rotation can be thought of as combining two planar revolute joints that rotate around different axes. For spatial joints, it is also important to determine the minimum number of point contacts for a specific type of motion, and this is an area of future research.
6. Combining multiple R_uP_v variable joints in series creates added constraints that must be considered, and therefore the joint design is more difficult. However, the resulting variable joint has a broader range of possible configurations. The difficulty in connecting multiple R_uP_v variable joints in series is that every new joint motion impacts the downstream joint motion. For instance, the constraints on a R_1 joint motion effect the possibility of performing a future R_u or P_v type motion. One way to minimize this effect to use connect multiple R_uP_v variable joints of the same type.
7. Joint profile synthesis must be taken into consideration during the synthesis of Type II MVTs, and not after the mechanism design is completed. The reason for this is that even if the mechanism is feasible it may not be

possible synthesize a joint that can complete the required task. In addition, it is important to minimize the reaction forces that occur at the joint, and therefore it is important to consider the joint profile during the kinematic design stage.

8. New types of graphical symbols need to be developed as a standard way to represent variable joints that are used in Type II MVTs, and this is an area of future work. Potential options for R_uP_v variable joints have already been shown in this dissertation, but a more formal set of graphical symbols is needed.
9. Using a variable joint in a mechanism adds joint complexity, but the added joint complexity may lead a mechanism that provides a simple solution to a complex task. For instance, in this dissertation it was shown how the Type II MVT four-bar linkage was able to perform an operation that would not be possible using a conventional four-bar linkage.

7.6 Final Remarks

This dissertation provides a general procedure to synthesize the profiles of R_uP_v variable joints, and that is a powerful design tool. Currently, variable joints are rarely used in mechanism design. Yet, this dissertation provides two applications where R_uP_v variable joints can be used in a mechanism to solve a problem. In both examples, by using variable joints it is possible to utilize the actuators that are currently used in the mechanism. Using variable joint in a

mechanism does add mechanism complexity, but by building the complexity in the joints, fewer actuators are needed and the controls may become simpler.

REFERENCES

- [1] J. Liu and S. Sun. A brief survey on inflatable deployment space structures' research and development. In *Proceedings of the 2010 Reconfigurable Mechanisms and Robotics Conference*, pages 773–782, 2009.
- [2] G. Wei and J. Dai. Geometry and kinematic analysis of an origami-evolved mechanism based in artmimetics. *International Conference on Reconfigurable Mechanisms and Robotics*, pages 450–455, 2009.
- [3] J. Zhang, J. Yang, and B Li. Development of reconfigurable welding fixture system for automotive body. In *Proceedings of the 2009 Reconfigurable Mechanisms and Robotics Conference*, pages 702–708, 2009.
- [4] K. Wohlhart. Kinematotropic linkages. In J. Lenarcic and V. Parenti-Castelli, editors, *Recent Advances in Robot Kinematics*, pages 359–368. Kluwer Academic, Dordrecht, The Netherlands, 1996.
- [5] F. Reuleaux. *The Kinematics of Machinery*. Dover Publications, 1963.
- [6] A.B.W. Kennedy. *The Mechanics of Machinery*. MacMillan and Co, London, 1886.
- [7] L. Burmester. *Lehrbuch der Kinematik*. Verlag Von Arthur Felix, Leipzig, Germany, 1886.
- [8] R.S. Hartenberg and J. Denavit. *Kinematic Synthesis of Linkages*. McGraw-Hill Book Company, New York, 1964.
- [9] K.H. Hunt. *Kinematic Geometry of Mechanisms*. Oxford University Press, New York, 1978.

- [10] O. Bottema and B. Roth. *Theoretical Kinematics*. Dover Publications, Inc., New York, 1990.
- [11] F. Freudenstein and G.N. Sandor. Synthesis of path generating mechanism by means of a programmed digital computer. *ASME Journal of Engineering for Industry*, 81:159–168, 1959.
- [12] L. W. Tsai and A.P. Morgan. Solving the kinematics of the most general six and five degree-of-freedom manipulators by continuation methods. *Journal of Mechanisms, Transmissions, and Automation in Design*, 107(5), 1985.
- [13] C.W. Wampler and A.P. Morgan. Complete solution of the nine-point path synthesis problem for four-bar linkages. *Journal of Mechanical Design*, 114(1):153–159, 1992.
- [14] D.A. Ruth and J.M. McCarthy. Sphinxpc: An implementation of four position synthesis for planar and spherical linkages. In *Proceedings of the ASME Design Engineering Technical Conferences*, volume 1, pages 14–17, Sacramento, CA, September 1997.
- [15] J.S. Dai and J. Rees Jones. Mobility in metamorphic mechanisms of foldable/erectable kinds. *Journal of Mechanical Design*, 121:375–382, September 1999.
- [16] Larry Howell. *Compliant Mechanisms*. Wiley-Interscience, 2001.
- [17] H.S. Yan and N.T. Liu. Finite-state-machine representations for mechanisms and chains with variable topologies. In *Proceedings of the 26th ASME Mechanisms Conference*, Baltimore, Maryland, 2000. DETC2000/MECH-14054.
- [18] A.P. Murray, J.P. Schmiedeler, and B.M. Korte. Kinematic synthesis of planar, shape-changing rigid-body mechanisms. *Journal of Mechanical Design*, 130:1–10, March 2008.

- [19] Jian S. Dai and J. Rees Jones. Matrix representation of topological changes in metamorphic mechanisms. *Journal of Mechanical Design*, 127:837–840, July 2005.
- [20] H.-S. Yan and C.-H. Kuo. Topological representations and characteristics of variable kinematic joints. *ASME Journal of Mechanical Design*, 128:384–391, March 2006.
- [21] Z.H. Lan and R. Du. Representation of topological changes in metamorphic mechanisms with matrices of the same dimension. *Journal of Mechanical Design*, 130, July 2008.
- [22] B. Slaboch and P. Voglewede. Mechanism state matrices for planar reconfigurable mechanisms. *Journal of Mechanisms and Robotics, Transactions of the ASME*, 3(1), February 2011.
- [23] C. Galletti and P. Fanghella. Single-loop kinematotropic mechanisms. *Mechanism and Machine Theory*, 36(6):743–761, June 2001.
- [24] C. Galletti and P. Fanghella. Multiloop kinematotropic mechanisms. In *Proceedings of the ASME DETC*, Montreal, CA, September 2002.
- [25] J.M. Herve. Translational parallel manipulators with double planar limbs. *Mechanism and Machine Theory*, 41:433–455, 2006.
- [26] L. Z. Ma, A. Liu, H. Shen, and D. Yang. A method for structure synthesis of reconfigurable mechanism based on genetic optimization algorithm. In *Proceedings of the 2009 Reconfigurable Mechanisms and Robotics Conference*, pages 148–152, 2009.
- [27] T. Yang, A. Liu, L. Zhang, and J Yun. Comparative study of two methods for type synthesis of robot mechanisms. In *Proceedings of the 2009 Reconfigurable Mechanisms and Robotics Conference*, pages 205–214, 2009.

- [28] X. Kong and C. Huang. Type synthesis of parallel mechanisms with multiple operation modes. In *Proceedings of the 2009 Reconfigurable Mechanisms and Robotics Conference*, pages 141–146, 2009.
- [29] H.-S. Yan and C.-H. Kang. Configuration synthesis of mechanisms with variable topologies. *Mechanism and Machine Theory*, 44:896–911, 2009.
- [30] W. Wunderlich. Ein merkwürdiges zwolfstabgetriebe, österreichisches ingenieurarchiv. pages 224–228. Kluwer Academic, 1954.
- [31] K. Wohlhart. Degrees of shakiness. *Mechanism and Machine Theory*, 34(7):1103–1126, October 1999.
- [32] C.H. Kuo. Structural characteristics of mechanisms with variable topologies taking into account the configuration singularity. Master’s thesis, Department of Mechanical Engineering, National Cheng Kung University, Tainan, Taiwan, 2004.
- [33] W. Shieh, F. Sun, and D. Chen. On the topological representation and compatibility of variable topology mechanisms. In *Proceedings of the 2009 ASME Design Engineering Technical Conference*, Sand Diego, CA, September 2009. Paper Number: DETC2009-87205.
- [34] K. Zhang, Y. Fang, G. Wei, and J. Dai. Structural representation of reconfigurable linkages. In *Proceedings of the 2012 Reconfigurable Mechanisms and Robotics Conference*, pages 127–137, Tianjin, China, July 2012.
- [35] K.J. Waldron. A method of studying joint geometry. *Mechanism and Machine Theory*, 7(3):347–353, 1972.
- [36] L.-W. Tsai. *Mechanism Design: Enumeration of Kinematic Structures According to Function*. CRC Press LLC, Boca Raton, FL, 2001.
- [37] H.-S. Yan and C.-H. Kuo. Representations and identifications of structural

and motion state characteristics of mechanisms with variable topologies.

Transactions of the Canadian Society of Mechanical Engineering, 30:19–40, March 2006.

- [38] E. Sacks and L. Joskowicz. *The Configuration Space Method for Kinematic Design of Mechanism*. The MIT Press, London, England, 2010.
- [39] E. Rimon and J. Burdick. A configuration space analysis of bodies in contact - I. 1st order mobility. *Mechanism and Machine Theory*, 30(6):897–912, 1995.
- [40] E. Rimon and J. Burdick. A configuration space analysis of bodies in contact - II. 2nd order mobility. *Mechanism and Machine Theory*, 30(6):913–928, 1995.
- [41] J. Latombe. Robot motion planning. In *Robot Motion Planning*, pages x–xi, Norwell, MA, September 1991.
- [42] J.M. McCarthy. *Geometric Design of Linkages*, volume 11 of *Interdisciplinary Applied Mathematics*. Springer-Verlag, New York, 2000.
- [43] P.A. Voglewede. *Measuring Closeness to Singularities of Parallel Manipulators with Application to the Design of Redundant Actuation*. PhD thesis, Georgia Institute of Technology, March 2004.
- [44] C. Gosselin and J. Angeles. Singularity analysis of closed loop kinematic chains. *IEEE Transactions on Robotics and Automation*, 6(3):281–290, June 1990.
- [45] P.A. Voglewede and I. Ebert-Uphoff. Overarching framework for measuring closeness to singularities of parallel manipulators. *IEEE Transactions on Robotics*, 21(6):1037–1045, December 2005.
- [46] H.-S. Yan and C.-H. Kuo. Structural analysis and configuration synthesis of mechanisms with variable topologies. In *ASME/IFTOMM International Conference on Reconfigurable Mechanisms and Robots*, pages 23–31, London,

United Kingdom, 2009.

APPENDIX A

Analysis of Reconfigurable Mechanisms

This Appendix introduces mechanism state matrices as a new and improved way to represent the topological characteristics of reconfigurable mechanisms. The advantages of this approach are that each row corresponds to a unique state in the mechanism, the fixed and free links in the mechanism can be identified, and the DOF at each state are shown. A series of examples will be used to illustrate the proposed concept.

A.1 Introduction

Many researchers are currently working on ways to analyze and synthesize reconfigurable mechanisms. As part of this, there is a need for a concise matrix representation of the topological characteristics of reconfigurable mechanisms. The topological characteristics of any reconfigurable mechanism can be broken into five areas:

- (i) The connectivity of the links and joints
- (ii) The type of joint motion
- (iii) The kinematic orientation of the joints
- (iv) The fixed and free links
- (v) The degrees of freedom (DOF) of the mechanism.

Mechanism state matrices are a novel matrix representation that combines all five topological characteristics into a concise matrix representation. This chapter will develop mechanism state matrices and compare and contrast them to current

matrix representations which include conventional adjacency matrices [36], EU-matrix transformations¹ [15, 19], improved adjacency matrices [21], and directionality topology matrices [37].

Mechanism state matrices combine the upper triangular portion of the directionality topology matrix with the finite state representation [17]. Thus, each row of the mechanism state matrix corresponds to a distinct state of the mechanism. This is in contrast to conventional matrix representations in which each row corresponds to a distinct link in a mechanism. This new matrix representation is unique in that it allows for identification of the fixed links in a mechanism. In addition, the DOF of a mechanism at each state is clearly identified.

A.2 Current Matrix Representations

A number of researchers [19, 21, 37, 46] have introduced various methods of representing the topological characteristics of reconfigurable mechanisms using a matrix notation. While each of these matrix representations has its own advantages, none of these current matrix representations fully specify the five topological characteristics useful for analysis and synthesis of reconfigurable mechanisms.

A.2.1 Adjacency Matrices

Adjacency matrices are used to represent the topological structure of a mechanism where the links in a mechanism are labeled 1 through n . In an adjacency matrix, the row and column numbers correspond to the link numbers in

¹“EU” stands for an E-elementary matrix combined with a U-elementary matrix as outlined in [19].

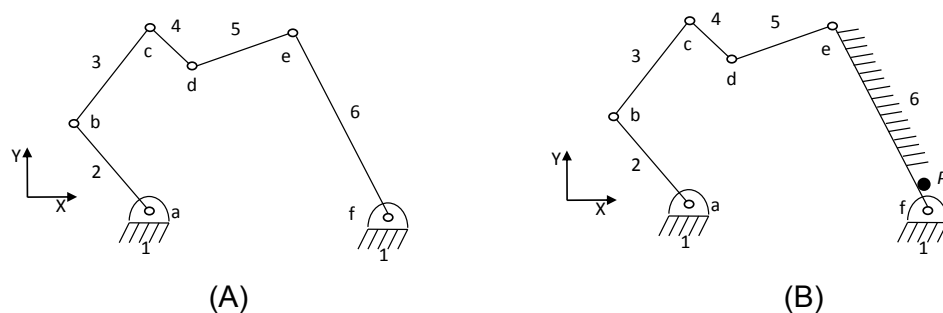


Figure A.1: (A) The Six-Bar Linkage in State 1 has Three DOF. (B) The Six-bar Linkage becomes a Five-bar Linkage in State 2 with Two DOF.

a mechanism. The definition of an adjacency matrix is given in [36] as

$$A(i, j) = \begin{cases} 1 & \text{if link } i \text{ is connected to link } j \text{ by a joint} \\ 0 & \text{otherwise (including } i = j), \end{cases} \quad (\text{A.1})$$

where $A(i, j)$ is the i^{th} row and j^{th} column of matrix A . For an n link mechanism an adjacency matrix is an $n \times n$ matrix. For example, matrix A_0 is the adjacency matrix for the six-bar linkage in Fig. A.1(A),

$$A_0 = \begin{bmatrix} 0 & 1 & 0 & 0 & 0 & 1 \\ 1 & 0 & 1 & 0 & 0 & 0 \\ 0 & 1 & 0 & 1 & 0 & 0 \\ 0 & 0 & 1 & 0 & 1 & 0 \\ 0 & 0 & 0 & 1 & 0 & 1 \\ 1 & 0 & 0 & 0 & 1 & 0 \end{bmatrix}. \quad (\text{A.2})$$

In this example, element $A_0(1, 2)$ is 1 because link 1 is attached to link 2 by a joint. Adjacency matrices are advantageous in that they provide information about the connectivity of the links and joints. However, adjacency matrices cannot be used to identify type of joints, the kinematic orientation of the joints, the fixed links, or the DOF of the mechanism.

A.2.2 EU-Matrix Transformations

In 2005 Dai and Jones [19] proposed an EU-elementary matrix operation to represent the state changes of metamorphic mechanisms. EU-elementary matrix operations are the first type of matrix operation that can be used to reduce the dimension of an adjacency matrix. An E-elementary matrix is combined with a U-elementary matrix to form an EU-elementary matrix operation. As shown in Fig. A.1(B), consider the case in which link 6 of the six-bar linkage becomes fixed as a result of a pin, P . The E-elementary matrix and the U-elementary matrix associated with the transformation from the six-bar linkage in state 1 (Fig. A.1(A)) to the six-bar linkage in state 2 (Fig. A.1(B)) are

$$E_6 = [I_5 \quad 0] = \begin{bmatrix} 1 & 0 & 0 & 0 & 0 & 0 \\ 0 & 1 & 0 & 0 & 0 & 0 \\ 0 & 0 & 1 & 0 & 0 & 0 \\ 0 & 0 & 0 & 1 & 0 & 0 \\ 0 & 0 & 0 & 0 & 1 & 0 \end{bmatrix} \quad (A.3)$$

$$U_{5,6} = \begin{bmatrix} 1 & 0 & 0 & 0 & 0 & 0 \\ 0 & 1 & 0 & 0 & 0 & 0 \\ 0 & 0 & 1 & 0 & 0 & 0 \\ 0 & 0 & 0 & 1 & 0 & 0 \\ 0 & 0 & 0 & 0 & 1 & 1 \\ 0 & 0 & 0 & 0 & 0 & 1 \end{bmatrix}.$$

The two matrices are used to perform the elementary matrix operation given in Eq. A.4 as

$$A_1 = (E_6 U_{5,6}) A_0 (E_6 U_{5,6})^T. \quad (A.4)$$

The matrix operation uses modulo-2 arithmetic and the results are given in Eq. A.5

$$A_1 = \begin{bmatrix} 0 & 1 & 0 & 0 & 1 \\ 1 & 0 & 1 & 0 & 0 \\ 0 & 1 & 0 & 1 & 0 \\ 0 & 0 & 1 & 0 & 1 \\ 1 & 0 & 0 & 1 & 0 \end{bmatrix}. \quad (\text{A.5})$$

The EU-matrix transformation effectively transformed A_0 to the adjacency matrix for the mechanism in Fig. A.1(B). Dai and Jones realized that, upon a change in the number of effective links, the dimension of an adjacency matrix changes as well as the order of the elements. In the previous example A_0 changed from a 6×6 matrix to A_1 , a 5×5 matrix. The EU-elementary matrix operation is useful in capturing this change. However, the EU-matrix transformation does not identify the type of joints, the kinematic orientation of the joints, the fixed links, or the DOF of the mechanism.

A.2.3 Improved Adjacency Matrix

In 2008 Lan and Du [21] proposed a “-1” element to indicate a fixed kinematic pair. In this way the dimension of the adjacency matrix remains the same after a topological change has occurred. In addition, information about the original state of the mechanism is not lost. For example, the improved adjacency matrix for the six-bar linkage in Fig. A.1(B) is given in A_2 as

$$A_2 = \begin{bmatrix} 0 & 1 & 0 & 0 & 0 & -1 \\ 1 & 0 & 1 & 0 & 0 & 0 \\ 0 & 1 & 0 & 1 & 0 & 0 \\ 0 & 0 & 1 & 0 & 1 & 0 \\ 0 & 0 & 0 & 1 & 0 & 1 \\ -1 & 0 & 0 & 0 & 1 & 0 \end{bmatrix}. \quad (\text{A.6})$$

This representation ensures that the dimension of the adjacency matrix

remains unchanged due to a change in the number of effective links. However, it does not identify the type of joints, the kinematic orientation of the joints, the fixed links, or the DOF of the mechanism.

A.2.4 Directionality Topology Matrices

The directionality topology matrix (M_{DT}) proposed by Yan and Kuo [37, 46] is one step closer to a complete representation of the topological characteristics of reconfigurable mechanisms. The directionality topology matrix in Eq. A.7 represents the topological change from the six-bar linkage in state 1 to the six-bar linkage in state 2.

$$M_{DT} = \begin{bmatrix} 1 & J_{Z,Z}^{R,R} & 0 & 0 & 0 & J_{Z,V}^{R,X} \\ a & 2 & J_{Z,Z}^{R,R} & 0 & 0 & 0 \\ 0 & b & 3 & J_{Z,Z}^{R,R} & 0 & 0 \\ 0 & 0 & c & 4 & J_{Z,Z}^{R,R} & 0 \\ 0 & 0 & 0 & d & 5 & J_{Z,Z}^{R,R} \\ f & 0 & 0 & 0 & e & 6 \end{bmatrix} \quad (\text{A.7})$$

For $i = j$, $M_{DT}(i, j)$ denotes the label of link i . For $i > j$, $M_{DT}(i, j)$ denotes the label of the kinematic pair connecting links i and j , and for $j > i$, $M_{DT}(i, j)$ contains the joint code for links i and j . Joint code is in the form of J_{μ}^{λ} where λ and μ represent the type and orientation of a kinematic pair, respectively.

Figure A.2 contains the schematic diagram and the joint code for common kinematic pairs. Fixed pair notation is given by J_V^X , where V represents an arbitrary kinematic orientation and X represents a fixed joint. Reconfigurable mechanisms are unique in that they have the ability to transition from one state with a certain configuration to another state with a different configuration. The

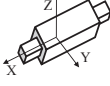
Pair (Joint) Type	Schematic Diagram	DOF	Joint Code	Representative Orientations
Revolute		1	J_X^R	Direction of rotation axis.
Prismatic		1	J_X^P	Direction of translation motion.
Fixed	N/A	0	J_V^X	N/A

Figure A.2: Joint Code of Common Kinematic Pairs

joint code representing these changes can be expressed in a joint sequence, $J(\lambda, \mu)$,

$$J_{\mu_1, \mu_2, \dots, \mu_n}^{\lambda_1, \lambda_2, \dots, \lambda_n} \quad (\text{A.8})$$

in which λ_n and μ_n correspond to the joint code for the n^{th} state of the mechanism.

Directionality topology matrices identify the connectivity of the links and joints, the type of joints, and the kinematic orientation of the joint. In addition, joint sequences allow for multiple states to be conveniently represented in a single matrix. Mechanism state matrices build upon directionality topology matrices by identifying the fixed links, as well as providing the information about the DOF of the mechanism. In addition, each row of the matrix will correspond to a distinct state in a mechanism.

A.3 Mechanism State Matrices

Recall that the topological characteristics of reconfigurable mechanisms can be broken into five areas:

- (i) The connectivity of the links and joints
- (ii) The type of joint motion

Table A.1: Topological Characteristics

Matrix Representations	(i)	(ii)	(iii)	(iv)	(v)
Adjacency Matrix	✓				
EU-Matrix Operations	✓				
Improved Adjacency Matrix	✓				
Directionality Topology Matrix	✓	✓	✓		
Mechanism State Matrix	✓	✓	✓	✓	
Augmented Mechanism State Matrix	✓	✓	✓	✓	✓

(iii) The kinematic orientation of the joints

(iv) The fixed and free links

(v) The degrees of freedom (DOF) of the mechanism.

As shown in Tab. A.1, current matrix representations fail to identify all five topological characteristics. The goal of mechanism state matrices is to incorporate all five topological characteristics into a single matrix representation.

A.3.1 Matrix Notation

Mechanism state matrices provide a new way to capture the topological characteristics of a reconfigurable mechanism as it changes from one state to another. This representation combines the desirable characteristics from current matrix representations into a more compact form. For example, mechanism state matrices incorporate EU-matrix transformations into its inherent structure. In addition, fixed joint notation remains consistent with improved adjacency matrices. Lastly, joint code notation used in directionality topology matrices is retained in mechanism state matrices.

This novel matrix representation is fundamentally different than current matrix representations in multiple ways. First, each row of a mechanism state

$$M_{SM(m,n)} = \left[\begin{array}{cccc}
\begin{matrix} \lambda_{1(i,j)} & \lambda_{2(i,j)} & \dots & \lambda_{r(i,j)} \\ \kappa(i,j) \gamma_{1(i,j) \mu_{1(i,j)}} & \gamma_{2(i,j) \mu_{2(i,j)}} & \dots & \gamma_{r(i,j) \mu_{r(i,j)}} \end{matrix} & \begin{matrix} \lambda_{1(i,j)} & \lambda_{2(i,j)} & \dots & \lambda_{r(i,j)} \\ \kappa(i,j) \gamma_{1(i,j) \mu_{1(i,j)}} & \gamma_{2(i,j) \mu_{2(i,j)}} & \dots & \gamma_{r(i,j) \mu_{r(i,j)}} \end{matrix} & \dots & \dots & \kappa(1,n) \\
\begin{matrix} \lambda_{1(i,j)} & \lambda_{2(i,j)} & \dots & \lambda_{r(i,j)} \\ \kappa(i,j) \gamma_{1(i,j) \mu_{1(i,j)}} & \gamma_{2(i,j) \mu_{2(i,j)}} & \dots & \gamma_{r(i,j) \mu_{r(i,j)}} \end{matrix} & \begin{matrix} \lambda_{1(i,j)} & \lambda_{2(i,j)} & \dots & \lambda_{r(i,j)} \\ \kappa(i,j) \gamma_{1(i,j) \mu_{1(i,j)}} & \gamma_{2(i,j) \mu_{2(i,j)}} & \dots & \gamma_{r(i,j) \mu_{r(i,j)}} \end{matrix} & \dots & \dots & \dots \\
\vdots & \vdots & \ddots & \vdots & \vdots & \vdots & \vdots \\
\vdots & \vdots & \vdots & \vdots & \vdots & \vdots & \vdots \\
\begin{matrix} \lambda_{1(m,1)} & \lambda_{2(m,1)} & \dots & \lambda_{r(m,1)} \\ \kappa(m,1) \gamma_{1(m,1) \mu_{1(m,1)}} & \gamma_{2(m,1) \mu_{2(m,1)}} & \dots & \gamma_{r(m,1) \mu_{r(m,1)}} \end{matrix} & \dots & \dots & \dots & \kappa(m,n)
\end{array} \right]. \quad (\text{A.9})$$

matrix corresponds to a unique *state* of the mechanism. This is in contrast to current matrix representations in which each row corresponds to a unique *link* in a mechanism. Second, each link in a mechanism is designated as either a *free* link or a *fixed* link. Free links are denoted by β , and fixed links are denoted by α .

Mechanism state matrices will now be rigorously defined, and then a simple example will be used to elucidate the theory. The following list outlines the guidelines used for forming mechanism state matrices.

1. The mechanism state matrix is an $m \times n$ matrix.
2. For an n link mechanism, the links are labeled 1 to n .
3. The m rows of the matrix correspond to the m states of the mechanism.
4. The n columns of the matrix correspond to the n links of the mechanism.
5. Mechanism state matrices are read from left to right.
6. Once the connectivity of two links is established, it is not repeated.

The general form of the mechanism state matrix is given in Eq. A.9.

$M_{SM}(i, j)$ contains the link code for the j^{th} link at the i^{th} state. Link code has the general form of

$$\kappa(i,j) \gamma_{1(i,j) \mu_{1(i,j)}}^{\lambda_{1(i,j)}} \gamma_{2(i,j) \mu_{2(i,j)}}^{\lambda_{2(i,j)}} \dots \gamma_{r(i,j) \mu_{r(i,j)}}^{\lambda_{r(i,j)}}. \quad (\text{A.10})$$

For the j^{th} link at the i^{th} state $\kappa(i, j)$ is defined as

$$\kappa(i, j) = \begin{cases} \alpha & \text{if link } j \text{ is a fixed link} \\ \beta & \text{if link } j \text{ is not a fixed link.} \end{cases} \quad (\text{A.11})$$

The remaining variables are defined as follows:

1. x : an integer from 1 to r
2. r : the number of links connected to link j for $\gamma_{x(i,j)} > j$
3. $\gamma_{x(i,j)}$: a link number (1 to n) corresponding to a link connected to link j by a joint, where $\gamma_{x+1(i,j)} > \gamma_{x(i,j)} > j$
4. $\lambda_{x(i,j)}$: the type of kinematic pair connecting link j to link $\gamma_{x(i,j)}$
5. $\mu_{x(i,j)}$: the orientation of the kinematic pair connecting link j to link $\gamma_{x(i,j)}$.

It should be noted that $\begin{matrix} \lambda_{x(i,j)} \\ \mu_{x(i,j)} \end{matrix}$ is identical to the joint code used for directionality topology matrices [37]. The notation for the type and orientation of common kinematic pairs can be found in Fig. A.2.

A.3.2 Representative Example

The transformation from the mechanism in Fig. A.1(A) to the mechanism in Fig. A.1(B) will be used to illustrate how mechanism state matrices can be used to represent the topological characteristics of reconfigurable mechanisms. In this example, the values associated with the link code for $M_{SM}(1, 1)$ are as follows:

$$\begin{aligned} \kappa(1, 1) &= \alpha \\ \gamma_{1(1,1)} &= 2, & \gamma_{2(1,1)} &= 6 \\ \lambda_{1(1,1)} &= R, & \lambda_{2(1,1)} &= R \\ \mu_{1(1,1)} &= Z, & \mu_{2(1,1)} &= Z. \end{aligned}$$

The values for the link code can be found for every element of M_{SM} . Substituting the link code values into the generalized form of the mechanism state matrix yields the matrix given in Eq. A.12

$$M_{SM} = \begin{bmatrix} \alpha 2_Z^R, 6_Z^R & \beta 3_Z^R & \beta 4_Z^R & \beta 5_Z^R & \beta 6_Z^R & \beta \\ \alpha 2_Z^R, 6_V^X & \beta 3_Z^R & \beta 4_Z^R & \beta 5_Z^R & \beta 6_Z^R & \alpha \end{bmatrix}. \quad (\text{A.12})$$

Notice that each row of the mechanism state matrix corresponds to a distinct state in the mechanism. That is, the first row corresponds to the six-bar linkage in state 1 and the second row corresponds to the six-bar linkage in state 2. There are 6 columns corresponding to the 6 links in the mechanism.

Link code is used to describe each link at the corresponding state. For instance, consider $M_{SM}(1, 1)$. α specifies that link 1 is a fixed link. The notation $2_Z^R, 6_Z^R$ specifies that link 1 is connected to link 2 through a revolute joint, and link 1 is also connected to link 6 through a revolute joint. The direction of the rotation axis is specified as the Z -axis in both cases. It is important to reiterate that mechanism state matrices are read left to right, and that once a connectivity is established it is not repeated. For example, link 1 is specified to be connected to link 2. Thus, $M_{SM}(1, 2)$ is given as $\beta 3_Z^R$ and not $\beta 1_Z^R, 3_Z^R$ because $M_{SM}(1, 1)$ already specified that link 1 is connected to link 2.

In state 2 the mechanism changes in two ways. Link 6 becomes a fixed link, and the joint connecting links 1 and 6 becomes a fixed joint. By looking at $M_{SM}(2, 1)$ it is clear that the joint between links 1 and 6 has become fixed. This is given by the joint code 6_V^X . Likewise, one can easily determine that link 6 has become a fixed link. This is given by α in $M_{SM}(2, 6)$.

A.4 Augmented Mechanism State Matrices

A defining characteristic of many reconfigurable mechanisms is that the DOF of the mechanism changes as the mechanism moves from one state to another. Knowledge of the DOF of a mechanism is important for both the analysis and synthesis of reconfigurable mechanisms. To capture this important information the DOF matrix will be defined as

$$D = \begin{bmatrix} S_1 \\ S_2 \\ \vdots \\ S_m \end{bmatrix}, \quad (\text{A.13})$$

where S_m corresponds to the DOF at state m . The DOF matrix can then be combined with the mechanism state matrix to form an augmented mechanism state matrix. The augmented mechanism state matrix, M_{ASM} , is defined in Eq. A.14 as

$$M_{ASM} = (M_{SM}|D) \quad (\text{A.14})$$

The general form is given in Eq. A.15

$$M_{ASM(m,n+1)} = \begin{bmatrix} \begin{matrix} \lambda_{1(i,j)} & \lambda_{2(i,j)} & \dots & \lambda_{r(i,j)} \\ \kappa_{(i,j)} \gamma_{1(i,j)} \mu_{1(i,j)} & \gamma_{2(i,j)} \mu_{2(i,j)} & \dots & \gamma_{r(i,j)} \mu_{r(i,j)} \end{matrix} & \begin{matrix} \lambda_{1(i,j)} & \lambda_{2(i,j)} & \dots & \lambda_{r(i,j)} \\ \kappa_{(i,j)} \gamma_{1(i,j)} \mu_{1(i,j)} & \gamma_{2(i,j)} \mu_{2(i,j)} & \dots & \gamma_{r(i,j)} \mu_{r(i,j)} \end{matrix} & \dots & \dots & \kappa_{(1,n)} \\ \begin{matrix} \lambda_{1(i,j)} & \lambda_{2(i,j)} & \dots & \lambda_{r(i,j)} \\ \kappa_{(i,j)} \gamma_{1(i,j)} \mu_{1(i,j)} & \gamma_{2(i,j)} \mu_{2(i,j)} & \dots & \gamma_{r(i,j)} \mu_{r(i,j)} \end{matrix} & \begin{matrix} \lambda_{1(i,j)} & \lambda_{2(i,j)} & \dots & \lambda_{r(i,j)} \\ \kappa_{(i,j)} \gamma_{1(i,j)} \mu_{1(i,j)} & \gamma_{2(i,j)} \mu_{2(i,j)} & \dots & \gamma_{r(i,j)} \mu_{r(i,j)} \end{matrix} & \dots & \dots & \dots \\ \vdots & \vdots & \ddots & \vdots & \vdots \\ \vdots & \vdots & \ddots & \vdots & \vdots \\ \begin{matrix} \lambda_{1(m,1)} & \lambda_{2(m,1)} & \dots & \lambda_{r(m,1)} \\ \kappa_{(m,1)} \gamma_{1(m,1)} \mu_{1(m,1)} & \gamma_{2(m,1)} \mu_{2(m,1)} & \dots & \gamma_{r(m,1)} \mu_{r(m,1)} \end{matrix} & \dots & \dots & \dots & \kappa_{(m,n)} \end{matrix} \begin{matrix} S_1 \\ S_2 \\ \vdots \\ \vdots \\ S_m \end{matrix} \quad (\text{A.15})$$

where all variables are as previously defined. For the six-bar linkage example, the mechanism changes from a 3 DOF mechanism in state 1 to a 2 DOF mechanism in state 2. In this case, the DOF matrix would be

$$D = \begin{bmatrix} 3 \\ 2 \end{bmatrix}. \quad (\text{A.16})$$

The corresponding augmented mechanism state matrix is given in Eq. A.17

$$M_{ASM} = \left[\begin{array}{cccccc|c} \alpha 2_Z^R, 6_Z^R & \beta 3_Z^R & \beta 4_Z^R & \beta 5_Z^R & \beta 6_Z^R & \beta & 3 \\ \alpha 2_Z^R, 6_V^X & \beta 3_Z^R & \beta 4_Z^R & \beta 5_Z^R & \beta 6_Z^R & \alpha & 2 \end{array} \right]. \quad (\text{A.17})$$

Augmented mechanism state matrices fully specify all five topological characteristics of reconfigurable mechanisms. They are a convenient way to capture the changes in the DOF of a mechanism as it moves from one state to the next.

A.5 Examples

In this section three examples will be provided to illustrate how mechanism state matrices can be a useful analysis tool for reconfigurable mechanisms. The first example will focus on a 3RRR mechanism that moves through three states. In the second example, a planar metamorphic mechanism will be analyzed [21]. The last example will show how mechanism state matrices work well for topologically identical mechanisms with different configurations.

A.5.1 3RRR Mechanism

Consider the 3RRR² mechanisms in Figures A.3(A), A.3(B), and A.3(C). For this example it is assumed that the mechanism transforms from state 1 in Fig. A.3(A) to state 2 in Fig. A.3(B) to state 3 in Fig. A.3(C). In state 1 link 1 is the only fixed link. In state 2 both links 8 and 1 are fixed links, and in state 3 links 7 and 1 are designated as fixed links. The mechanism state matrix for the three states is given in Eq. A.18 as

²3RRR denotes a manipulator with three kinematic chains of the type revolute-revolute-revolute.

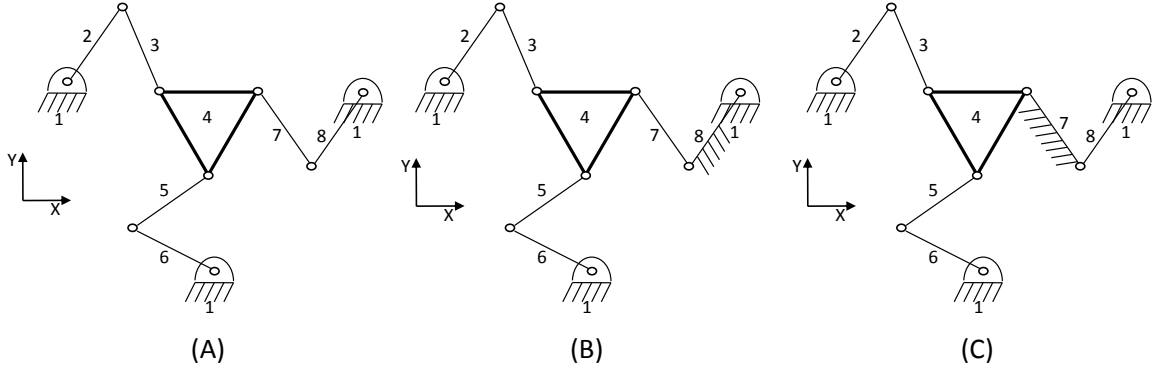


Figure A.3: (A) 3RPR Linkage with Three DOF. (B) 3RPR Linkage with Two DOF. (C) 3RPR Linkage with One DOF.

$$M_{SM} = \begin{bmatrix} \alpha 2_Z^R, 6_Z^R, 8_Z^R & \beta 3_Z^R & \beta 4_Z^R & \beta 5_Z^R, 7_Z^R & \beta 6_Z^R & \beta & \beta 8_Z^R & \beta \\ \alpha 2_Z^R, 6_Z^R, 8_V^X & \beta 3_Z^R & \beta 4_Z^R & \beta 5_Z^R, 7_Z^R & \beta 6_Z^R & \beta & \beta 8_Z^R & \alpha \\ \alpha 2_Z^R, 6_Z^R, 8_V^X & \beta 3_Z^R & \beta 4_Z^R & \beta 5_Z^R, 7_Z^R & \beta 6_Z^R & \beta & \alpha 8_V^X & \alpha \end{bmatrix}. \quad (\text{A.18})$$

The corresponding augmented mechanism state matrix is given in Eq. A.19

as

$$M_{ASM} = \left[\begin{array}{cccccccc|c} \alpha 2_Z^R, 6_Z^R, 8_Z^R & \beta 3_Z^R & \beta 4_Z^R & \beta 5_Z^R, 7_Z^R & \beta 6_Z^R & \beta & \beta 8_Z^R & \beta & 3 \\ \alpha 2_Z^R, 6_Z^R, 8_V^X & \beta 3_Z^R & \beta 4_Z^R & \beta 5_Z^R, 7_Z^R & \beta 6_Z^R & \beta & \beta 8_Z^R & \alpha & 2 \\ \alpha 2_Z^R, 6_Z^R, 8_V^X & \beta 3_Z^R & \beta 4_Z^R & \beta 5_Z^R, 7_Z^R & \beta 6_Z^R & \beta & \alpha 8_V^X & \alpha & 1 \end{array} \right]. \quad (\text{A.19})$$

The augmented mechanism state matrix identifies how the DOF of this mechanism changes as it moves from one state to another. Additionally, it is easy to track how a link changes as the mechanism changes states. For instance, link 8 changes from a movable link in state 1 to a fixed link in states 2 and 3.

A.5.2 Planar Metamorphic Mechanism

The second example will be that of the planar metamorphic mechanism analyzed in [21] and shown in Figure A.4. This is a five-link mechanism that oscillates between pins P_1 and P_2 . The spring embedded in link 2 pushes link 3

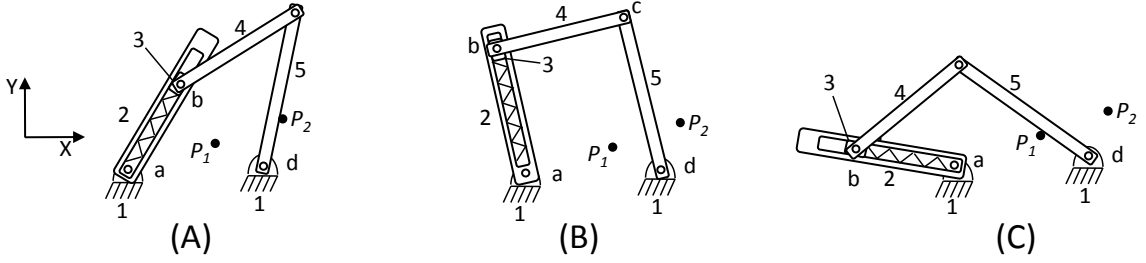


Figure A.4: The Mechanisms Oscillates Between Pins P_1 and P_2 .

along the slot in link 2. In every state the mechanism is a five-bar linkage with one DOF. However, the state of the mechanism changes as it oscillates between pins P_1 and P_2 . The mechanism state matrix is given in Eq. A.20 as

$$M_{SM} = \begin{bmatrix} \alpha 2_Z^R, 5_V^X & \beta 3_V^P & \beta 4_Z^R & \beta 5_Z^R & \alpha \\ \alpha 2_Z^R, 5_Z^R & \beta 3_V^X & \alpha 4_Z^R & \beta 5_Z^R & \beta \\ \alpha 2_Z^R, 5_V^X & \beta 3_V^P & \beta 4_Z^R & \beta 5_Z^R & \alpha \end{bmatrix}. \quad (\text{A.20})$$

The augmented mechanism state matrix for this example is given in Eq. A.21 as

$$M_{ASM} = \left[\begin{array}{ccccc|c} \alpha 2_Z^R, 5_V^X & \beta 3_V^P & \beta 4_Z^R & \beta 5_Z^R & \alpha & 1 \\ \alpha 2_Z^R, 5_Z^R & \beta 3_V^X & \alpha 4_Z^R & \beta 5_Z^R & \beta & 1 \\ \alpha 2_Z^R, 5_V^X & \beta 3_V^P & \beta 4_Z^R & \beta 5_Z^R & \alpha & 1 \end{array} \right]. \quad (\text{A.21})$$

In this case the DOF does not change as the mechanism changes states. However, the augmented mechanism state matrix shows how the links and joints change as the mechanism moves from one state to another.

A.5.3 2R-2P Mechanism

Mechanism state matrices can be used to identify topologically identical mechanisms with different configurations. Consider the 2R-2P mechanisms shown in Figures A.5 and A.6. These are topologically identical mechanisms with different configurations. The difference between them is evident by forming the augmented mechanism state matrices. The augmented mechanism state matrix for

the 2R-2P mechanism in Fig. A.6 is given by

$$M_{ASM} = \left[\begin{array}{ccc|c} \alpha 2_Z^R, 4_X^P & \beta 3_Z^R & \beta 4_Y^P & \beta \\ \hline & & & 1 \end{array} \right], \quad (\text{A.22})$$

and the augmented mechanism state matrix for the 2R-2P mechanism in Fig. A.6 is given as

$$M_{ASM} = \left[\begin{array}{ccc|c} \alpha 2_V^X, 4_X^P & \alpha 3_V^X & \alpha 4_X^P & \beta \\ \hline & & & 1 \end{array} \right]. \quad (\text{A.23})$$

Equation A.22 shows that either links 2, 3, or 4 could be an input link. This is not the case for the 2R-2P mechanism with parallel prismatic joints. As shown in Eq. A.23 only link 4 can be an input link. The other three links are fixed. It should be noted that the 2R-2P mechanism with parallel prismatic joints is a special case in which the configuration of the mechanism causes three of the four links to be fixed.

A.6 Review of Mechanism State Matrices

This Appendix introduced mechanism state matrices as a novel way to represent the topological characteristics of reconfigurable mechanisms. Mechanism state matrices are unique in that each row of the matrix corresponds to a distinct state in the mechanism. In addition, this is the first approach that identifies fixed and free links. Finally, the DOF at each state in the mechanism can be added to

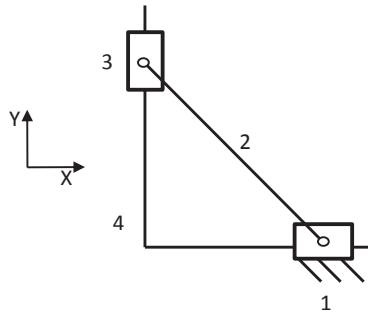


Figure A.5: 2R-2P Mechanism with Perpendicular Prismatic Joints

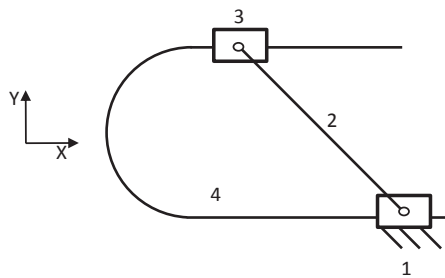


Figure A.6: 2R-2P Mechanism with Parallel Prismatic Joints

the mechanism state matrix to form the augmented mechanism state matrix.

APPENDIX B

Lower Pairs

A *revolute joint*, R , permits two paired elements to rotate with respect to one another about an axis that is defined by the geometry of the joint. Therefore, the revolute joint is a one degree-of-freedom (dof) joint.

A *prismatic joint*, P , allows two paired elements to slide with respect to each other along an axis defined by the geometry of the joint. Similar to a revolute joint the prismatic joint is a one-dof joint. It imposes five constraints on the paired elements. The prismatic joint is also called a *sliding pair*.

A *cylindric joint*, C , permits a rotation about an independent translation along an axis defined by the geometry of the joint. Therefore, the cylindric joint is a two dof joint.

A *helical joint*, H , allows two paired elements to rotate about and translate along an axis defined by the geometry of the joint. However, the translation is related to the rotation by the pitch of the joint. Hence, the helical joint is a one-dof joint.

A *spherical joint*, S , allows one element to rotate freely with respect to the other about the center of a sphere. It is a ball-and-socket joint that permits no translations between the paired elements. Hence, the

spherical joint is a three-dof joint.

A *plane pair*, E , permits two translational degrees of freedom on a plane and a rotation degree of freedom about an axis that is normal to the plane of contact. Hence, the plane pair is a three-dof joint.